THE IMMUNOMETABOLIC RESPONSES SALMONELLA ENTERITIDIS AND SALMONELLA HEIDELBERG INDUCE IN CHICKEN MACROPHAGES

by

Famatta Perry

A thesis submitted to the Faculty of the University of Delaware in partial fulfillment of the requirements for the degree of Master of Science in Biological Sciences

Summer 2019

THE IMMUNOMETABOLIC RESPONSES SALMONELLA ENTERITIDIS AND SALMONELLA HEIDELBERG INDUCE IN CHICKEN MACROPHAGES

by

Famatta Perry

Approved: _____
Ryan J. Arsenault, Ph.D.
Professor in charge of thesis on behalf of the Advisory Committee

Approved: _____
Velia M. Fowler, Ph.D.
Chair of the Department of Biological Sciences

Approved: _____
John Pelesko, Ph.D.
Interim Dean of the College of Arts and Sciences

Approved: _____
Douglas J. Doren, Ph.D.
Interim Vice Provost for Graduate and Professional Education and Dean of the Graduate College

ACKNOWLEDGMENTS

First, I want to thank my advisor Dr. Ryan Arsenault for the great opportunity to join his lab and for his time and patience. Dr. Arsenault, my deepest and sincerest gratitude for your unwavering support, guidance, teaching and mentorship. Your astounding work ethics, love for research, knowledge and all your other great qualities have been a source of encouragement to further my education and constantly challenge myself. Your dedication to your students and passion for research is beyond measure. You are the best Sensei I could ever have. If academia had a Superman, you would be him, but you are way smarter. Words cannot express how grateful I am to you for everything.

I also want to thank my committee members, Dr. Aimee Jaramillo-Lambert and Dr. Randall Duncan for their constant guidance and encouragement over the last two and a half years. I have learned and grown so much because of your expectations. I want you to know every bit of your time and effort has been very much appreciated.

In Dr. Arsenault's lab, I had the opportunity to meet great friends and colleagues. I want to thank Casey Johnson, Iyana Admasu and Bridget Aylward for their physical, mental and emotional support. Casey, thank you for all your help with this project, from running the rapamycin arrays to helping me figure out all the nitpicky details of every experiment. Thank you for being you (awesome)! And thank

you for always challenging me to think critically. Iyana, thank you for opening your home to me when I needed it the most. Most of all, thank you for your friendship and support.

I want to thank the University of Delaware, faculty and Staff for the incredible opportunity to earn this master's degree. I would like to thank the Department of Biological Sciences, and recognize Betty Cowgill for all her hard work, kindness and patience. Betty, thank you for making this journey less stressful. Special thanks to the Department of Animal and Food Sciences for their hospitality and treating me as one of their own.

I also want to thank those who have contributed to my financial and academic well-being from other departments and institutions. Dr. Michael Vaughan of the College of Engineering, Dr. Stephen Cox and Veniece Keene of Drexel University. Dr. Mazen Shahin and Dr. Murali Temburni of Delaware State University. I would like to acknowledge the NSF Bridge to the Doctorate Fellowship program and the Department of Biological Science for financial support over the course of this master's.

To my family and friends, thank you for all the love, kindness and support. There are no words to show how much I appreciate you all. Thank you for the food, vacation spots, the rescue missions and all the other thousands of things I make you do every week. Thank you Juewuo Reeves for being my rock.

And lastly, I want to thank me. Famatta, you are doing great and you will continue to do great. Thank you for earning this degree. You are almost there, don't push yourself too hard. Graduate school can get hard and I promise it will all get better. It might feel a little worse going forward, just remember if it was easy everyone would do it. Never give up!

To everyone, I humbly express my deepest gratitude and appreciation.

****I dedicate this Thesis to my mother Zapporah Wiefue.**

IN LOVING MEMORY OF

ELIZABETH KARGEOR AND ROOSEVELT FREEMAN.

TABLE OF CONTENTS

LIST OF TABLES ix
LIST OF FIGURES x
ABSTRACT xii

Chapter

1 INTRODUCTION 1

1.1 *Salmonella* 1

1.1.1 Symptoms and treatments 3
1.1.2 Economic burden 6
1.1.3 Mechanism and Pathogenesis 7

1.2 Importance of macrophages in understanding of *Salmonella* Infections 11
1.3 Immunometabolism 13
1.4 Kinome peptide array 14

2 HYPOTHESIS AND AIMS 17

3 MATERIALS AND METHODS 18

3.1 Cell Line and Maintenance 18
3.2 Bacteria Strains 19
3.3 Infection of Cells with *Salmonella* 20
3.4 Gentamicin Protection Assay 20
3.5 Kinome Peptide Array analysis 21
3.6 Generation and Analysis of the Kinome Peptide Array Data 22
3.7 Seahorse XFp Metabolic Assay 23
3.8 Western Blot 25
3.9 Flow Cytometry 27
3.10 Statistics 28

4 RESULTS 29

4.1 *Salmonella* alters host (HD11 cells) immunometabolism 29

4.1.1 Kinome Peptide Array *S.* Enteritidis 30 minutes post infection.. 31
4.1.2 Kinome Peptide Array Analysis *S.* Heidelberg 30 minutes Post Infection 39

4.1.2.1 S. Heidelberg infection at 30 minutes in HD11 cells does not induce the phosphorylation of three major glycolytic enzymes 40

4.1.3 Kinome Peptide Array Analysis *S*. Enteritidis 2 hours post infection. 43
4.1.4 Kinome Peptide Array Analysis *S*. Heidelberg 2 hours Post Infection. 46
4.1.5 Kinome Peptide Array Analysis *S*. Enteritidis 6 Hours Post Infection. 47
4.1.6 Kinome Peptide Array Analysis *S*. Heidelberg 6 hours Post Infection. 51

4.2 *S*. Enteritidis and *S*. Heidelberg induce differential metabolic states. 52

4.2.1 *S*. Enteritidis infection induces an early increase in glucose metabolism 53
4.2.2 Early *S*. Heidelberg infection reduces glucose metabolism. 54
4.2.3 *Salmonella* infections induce increased oxygen metabolism in HD11 cells 56

4.3 Rapamycin inhibits mTOR and MHY1485 indirectly activates mTOR in HD11 cells 57
4.4 The action of mTOR in *Salmonella* infected cells is not glycolysis dependent. 59
4.5 *S*. Enteritidis is more invasive than *S*. Heidelberg. 60
4.6 Validation of Kinome peptide array via western blot. 62
4.7 Early *S*. Enteritidis Infection Induces Increased Cell Death 63

5 DISCUSSION 66

5.1 Overview of the kinome peptide array data of HD11 cells 67

5.1.1 *S*. Enteritidis at 30 minutes post infection alters host AMPK-mTORC1 signaling cascade 68
5.1.2 *S*. Enteritidis at 2 hours post infection alters host AMPK-mTORC1 signaling cascade 70
5.1.3 *S*. Enteritidis at 6 hours post infection alters host AMPK-mTORC1 signaling cascade 72
5.1.4 *S*. Heidelberg at 30 minutes post infection alters host AMPK-mTORC1 signaling cascade 73

5.1.4.1 *S*. Heidelberg Relies on the Pentose Phosphate Shunt for Initial Invasion 75

5.1.5 *S.* Heidelberg at 2 hours post infection alters host AMPK-mTORC1 signaling cascade 77
5.1.6 *S.* Heidelberg at 6 hours post infection alters host AMPK-mTORC1 signaling cascade 78

5.2 TNF-alpha induced cell death validation via flow cytometry 79
5.3 The metabolic states of HD11 cells during *Salmonella* infection 82
5.4 The gentamicin protection assays are reflective of the inflammatory profile of HD11 during *Salmonella* infections. 87
5.5 Presence of mTOR S2448 in *Salmonella* Infected HD11 Cells 90

6 CONCLUSION 92

7 FUTURE DIRECTIONS 95

REFERENCES 96

Appendix

CHANGES IN IMMUNOMETABOLIC PEPTIDES AT THE DIFFERENT SITES ESSENTIAL TO THIS STUDY 110

LIST OF TABLES

Table 1: **Highly significant immunometabolic pathways** 31

Table 2: **Changes in immunometabolic peptides of S. Enteritidis and S. Heidelberg infected HD11.**..... 34

Table 3: **Phosphorylation status of some important peptides in the S. Enteritidis 30 minutes post infection**. 69

Table 4: **Phosphorylation status of some important peptides in the S. Enteritidis 2 hours post infection**. 71

Table 5: **Phosphorylation status of some important peptides in the S. Enteritidis 6 hours post infection**. 73

Table 6: **Phosphorylation status of some important peptides in the S. Heidelberg 30 minutes post infection**..... 75

Table 7: **Phosphorylation status of some important peptides in the S. Heidelberg 2 hours post infection**. 78

Table 8: **Phosphorylation status of some important peptides in the S. Heidelberg 6 hours post infection**. 79

Table 9: **Average percentage of live cells compared to apoptotic/dead cells in a S. Enteritidis or S. Heidelberg infection at 30 minutes post infection**. 81

LIST OF FIGURES

Figure **1:** **Proteins common to metabolic and immune pathway..** 29

Figure **2:** **Changes in AMPK signaling peptides at 30 minutes Salmonella infections.**..... 38

Figure **3:** **Missing glycolytic enzymes in 30 minutes S. Heidelberg infection.**.. 42

Figure **4:** **Changes in AMPK signaling peptides at 2 hours Salmonella infections.**..... 45

Figure **5:** **Changes in AMPK signaling peptides at 6 hours Salmonella infections.**..... 50

Figure **6:** **Metabolic differences between S. Enteritidis and S. Heidelberg infected HD11 cells..** 53

Figure **7:** **Difference in glucose metabolism in S. Enteritidis infected HD11 cells and uninfected HD11 cells..** 54

Figure **8:** **Difference in glucose metabolism in S. Heidelberg infected HD11 cells and uninfected HD11 cells..** 55

Figure **9:** **Difference in glucose metabolism between S. Enteritidis infected, S. Heidelberg infected and uninfected HD11 cells.**..... 56

Figure **10:** **Difference in oxygen consumption in S. Enteritidis infected, S. Heidelberg infected HD11 cells and uninfected HD11 cells..** 57

Figure **11:** **Dephosphorylation of mTOR due to rapamycin.** 58

Figure **12:** **Increase cell growth due to MHY1485 activity.**..... 59

Figure **13:** **Difference in glucose metabolism between S. Enteritidis infected HD11 cells treated with MHY1485 and rapamycin treatment..** 60

Figure **14:** **Invasiveness of S. Enteritidis and S. Heidelberg in HD11 macrophages at 30 minutes post infection..** 61

Figure **15:** **Invasiveness of S. Enteritidis (SE) and S. Heidelberg (SH) in HD11 macrophages at 2 hours post infection..** 62

Figure **16:** **Western blot analysis of mTOR S2448 in HD11 macrophages.**..... 63

Figure **17: Flow cytometry of S. Heidelberg and S. Enteritidis infected HD11 30 minutes post infection.**. 65

ABSTRACT

Salmonella is a burden to the agriculture and health sectors as a result of the high number of illnesses, food contamination, and recalls. *Salmonella* Enteritidis (*S*. Enteritidis) is one of the most prevalent serotypes isolated from poultry. *Salmonella* Heidelberg (*S*. Heidelberg), which is becoming more prevalent than *S*. Enteritidis, is one of the five most isolated serotypes. Many animals including poultry are carriers of *Salmonella* but do not show any symptoms. Thus, it is more difficult for producers to avoid the processing and the distribution of contaminated products especially due to the restriction of antibiotic use in food animals. *Salmonella* invades host cells and exploits host mechanisms for its own benefits. For example, *Salmonellae* are capable of surviving in macrophages whose role is to kill pathogenic bacteria. Understanding the mechanism by which *Salmonella* infects and creates a suitable niche in hosts will reveal a potential target for the treatment and prevention of *Salmonella* contamination without the use of antibiotics. Although *S*. Enteritidis and *S*. Heidelberg are almost genetically identical, they both are capable of inducing different immune and metabolic responses in host cells to successfully establish an infection. Kinome peptide array data and available literature showed significant changes in the phosphorylation states of mTOR and AMPK peptides in chickens during *Salmonella* infections. Therefore, focusing on the AMPK-mTOR signaling cascade, we demonstrated that *S*. Enteritidis and *S*. Heidelberg infections induced differential kinase activities in metabolic and immune related peptides of HD11 chicken

macrophages. Metabolic flux assays measuring extracellular acidification rate (ECAR) and oxygen consumption rate (OCR) demonstrated that, i) *S*. Enteritidis at 30 minutes post infection increased glucose metabolism ii) *S*. Heidelberg at 30 minutes post infection decreased glucose metabolism iii) Both *Salmonella* infections induce increased oxygen metabolism. Gentamicin protection assays performed at 30 minutes and 2 hours post infection revealed that *S*. Enteritidis bacteria are more invasive than *S*. Heidelberg. Furthermore, flow cytometry results showed increased apoptotic/dead cell population in *S*. Enteritidis infections compared to *S*. Heidelberg. These results show different immunometabolic responses of HD11 macrophages to *S*. Enteritidis and *S*. Heidelberg infections.

Chapter 1

INTRODUCTION

1.1 *Salmonella*

In 2013, *Salmonella* contamination caused about 3.7 billion dollars in economic losses in the United States (US) alone (16). According to the CDC, *Salmonella* infections cause approximately 1.2 million illnesses associated with 23,000 hospitalizations and 450 deaths per year in the US (17). *Salmonellae* are rod shaped gram negative facultative anaerobes (1) and are the number one cause of foodborne gastroenteritis (2, 3). *Salmonellae* are motile bacilli usually 2-5 microns long and 0.5-1.5 microns wide and belong to the Enterobacteriaceae family (1–3). *Salmonellae* are composed of two known species *Bongori* and *Enterica* (1,4).The species *Salmonella enterica* is a highly diverse bacterial species consisting of six subtypes and over 2,500 serovars (1,4,5), with genomes ranging from 4460 to 4857 Kb and slight differences in the genetic makeup (1,6). *Salmonella enterica* is known to infect vast numbers of warm-blooded animals (5) unlike *Bongori* which is known to infect a broad range of cold-blooded animals (7, 8).

Of the six subtypes of *Salmonella enterica*, the subtype *enterica* is comprised of serovars that cause typhoid fever and others that are non-typhoidal (5). Typhoidal *Salmonella* including Typhi and Paratyphi are serovars that infect only human hosts

and can cause enteric diseases (7, 9). *Salmonella enterica* subspecies *enterica* serovar *Enteritidis (S.* Enteritidis) and *Salmonella enterica* subspecies *enterica* serovar *(S.* Heidelberg) are two different serovars under the subspecies (10, 11).

The most common symptom of foodborne infections is gastroenteritis associated with diarrhea. Among the foodborne disease causing agents that result in gastroenteritis, zoonotic *Salmonella* subspecies, primarily nontyphoidal *Salmonella* is the leading bacterial cause of contaminated food associated gastroenteritis (18). A majority of the global estimate of 93.8 million cases of gastroenteritis (17) associated with diarrhea are due to these three serovars of *Salmonella enterica*; *Salmonella enterica* subspecies *enterica* Typhimurium, *S*. Enteritidis and *S*. Heidelberg (9, 19). *Salmonella* infections are also known to be invasive on a systemic scale. Many studies done in third world countries have shown that *Salmonella* infections in immunocompromised or nutrient deficient patients leads to infection in the bloodstream (4,20), resulting in more severe conditions. The complexity of such illnesses may lead to an increase in death for these different conditions. The primary mode of transmission of *Salmonella* amongst humans is by ingestion of contaminated foods (3, 17). However, other ways *Salmonella* can be transmitted is by interaction with infected people, pets or animals (e.g. guinea pigs) and drinking contaminated water (9, 15, 17). Among farm animals, sources of *Salmonella* include soil, bedding, feed, litter and pests found on site (1).

Although *S*. Enteritidis and *S*. Heidelberg are highly similar and found in the same subspecies, research shows that they induce different immune responses in poultry host (102). Despite their similarity, *S*. Enteritidis and *S*. Heidelberg showed vast differences in the numbers and characteristics of flagellar (H) and somatic (O) antigens on each of their surfaces (100, 101) and perhaps may be responsible for the different responses in the host (102). Non-typhoidal *Salmonella* including Enteritidis and Heidelberg cause gastroenteritis referred to as non-typhoidal salmonellosis (9, 12). *S.* Enteritidis and *S.* Heidelberg are two of the five most prevalent *Salmonella* infections resulting in contaminated food products and diseases (13, 14). *Salmonella* infections and contaminations are increasing concerns to the food industry (13, 15).

1.1.1 Symptoms and treatments

Salmonellae that can be transmitted from animals and humans or plants are referred to as non-specific serovars (non-restricted) (1, 4, 5) and these serovars are the non typhoidal *Salmonellosis* (NTS) agents. Unlike *Salmonellae* that cause typhoid fevers, NTS bacteria are usually self-limiting (5) meaning most cases do not require treatment or hospitalization. However, reported cases of NTS poisoning include acute gastroenteritis and watery diarrhea that begins approximately 6-12 hours after ingestion or contraction of bacteria in humans (4, 5). Other common symptoms may include nausea, vomiting, abdominal pain and fever (5). NTS symptoms usually last 4 to 10 days (17). NTS can become invasive in humans. This happens when the pathogen is contracted by an individual that is immunocompromised (20) or has an

undeveloped /weak immune system as in the case of children and elderly people (5,12,20). Invasive NTS (iNTS) have enteric fever symptoms. Similar to typhoidal *Salmonella*, patients suffer from high fever, respiratory complications and hepatosplenomegaly (5). NTS are known to cause more severe conditions like aseptic arthritis and Reiter's syndrome (1). Some common treatments for *Salmonella* infections are fluoroquinone (NTS; 5–7 days), chloramphenicol, and amoxicillin (21). Unless severe, antibiotics are not recommended for NTS poisoning due to increase susceptibility to gastrointestinal disorders (1, 4). For human restricted typhoid causing-*Salmonella*, vaccines and other effective treatments have been developed (4, 22), thus a decrease in the death toll, compared to NTS.

One key clinical manifestation that distinguishes typhoidal Salmonellosis from NTS is that typhoidal *Salmonellae* do not induce an excessive inflammatory response upon initial infection of the gastrointestinal tract (21, 22). Typhoidal *Salmonellae* infections are capable of inducing both humoral and innate immune responses (4, 5, 22). Immunological studies show that patients with IL-12 and IL-23 deficiencies are highly susceptible to NTS *Salmonella* because these patients cannot respond to microbial invasion by stimulating an innate immune response (22, 23).

S. Enteritidis and *S*. Heidelberg are among the serovars with the highest recovery rates and two of the three serovars commonly related to NTS (1, 24). Although non-pathogenic to chickens, *S*. Enteritidis was recognized as the most prevalent *Salmonella* isolate in poultry some decades ago (1) and is one of the major

serovars in poultry now (17, 25). Eggs are known to be the number one vehicle of *S*. Enteritidis infection in humans (17, 26) although this was not always the case (131). Researchers attribute the spread and prevalence of *S*. Enteritidis to the eradication of two serovars of *Salmonella* that are pathogenic to chickens. These two serovars are *S*. Gallinarum and *S*. Pullorum. The eradication of *S*. Gallinarium and *S*. Pollorum is suggested to influence the increased prevalence of *S*. Enteritidis due to a trend that showed an increase in *S*. Enteritidis during the absence of those two serovars (1). Also, *S*. Gallinarum and *S*. Enteritidis have similar extracellular structures like lipopolysaccharides (1, 27), thus scientists suggest that *S*. Enteritidis was able to infect chickens *incognito* during *S*. Gallinarum eradication (1) due to their similarity in structure. However, *S*. Enteritidis may be non-pathogenic to chickens because it lacks important genetic features of *S*. Gallinarum (136). Over the years, *S*. Enteritidis has maintained a high prevalence on farms and in poultry, beef, and pork due to carriers such as rodents and other farm pests (4, 28). In addition to its high prevalence, 88% of *S*. Enteritidis were reported to be resistant to at least one of the commonly used antibiotics including ampicillin, nalidixic acid, and tetracycline (1, 4).

Just like *S*. Enteritidis, *S*. Heidelberg has been a major concern for many decades because it is infectious to humans (132) and recently, there has been an increase in its prevalence (130). In 2011, multidrug-resistant *S*. Heidelberg were associated with disease outbreak via strains isolated from turkey products (4, 29). Again, in 2014, *S*. Heidelberg was involved in another outbreak where well over half

of the isolates were resistant to three or more drugs (4, 17). It was discovered that strains of *S*. Heidelberg are resistant to more than five of the most commonly used antibiotics and is highly invasive compared to other strains (17). Moreover, similar to *S*. Enteritidis and many food related NTS serovars, *S*. Heidelberg has reservoirs on farms and has been isolated from poultry, pig, horse, cattle and plants (4,28) hence becoming one of the most isolated serovars leading to illnesses, hospitalizations and even death (12,20,29).

1.1.2 Economic burden

Over the years, the hazard *Salmonella* poses on the health of people and the agriculture sector has increased drastically (17). *Salmonella* is associated with one of the highest economic cost burdens in the US due to foodborne pathogens (3, 30). Next to leafy greens, fruits and vegetables, poultry products and eggs are attributed as one of the major causes of Salmonellosis due to poultry being a reservoir of *Salmonella* bacteria, contributing to *Salmonella* outbreaks (4, 9, 15, 17). This prevalence may be due to the strict regulations of antibiotic use in poultry products in fear of antibiotic resistance and consumer preferences and concerns (31, 32). Most farm animals including chickens are carriers of *Salmonella* infections but do not display any symptoms (33). This makes it harder for farmers or breeders to recognize infected farm animals or detect contaminated meat products (28, 34) and these contaminated products may reach the end consumer. This, in many cases, leads to costly *Salmonella* outbreaks resulting in illnesses, hospitalizations and loss of lives.

1.1.3 Mechanism and Pathogenesis

Salmonella is a facultative intracellular invader of the gut of humans, animals and sometimes insects (1, 2, 9, 35) through a fecal oral route (5). *Salmonella* may lack some cytochrome complexes (36, 37); bacteria electron transport chain oxidases that transfer electrons to oxygen to make water or hydrogen peroxide. However, it contains catalase that breaks down water and hydrogen peroxide (1). The presence of catalase and the electron transport chain end products indicate that *Salmonellae* employ unique mechanisms to carry out aerobic respiration. The gastrointestinal tract has a highly anaerobic environment (38), however, this is not a challenge for *Salmonella*. Apart from being able to utilize oxygen for respiration (37), most *Salmonella* bacteria are lactose fermenters and hydrogen sulfide producers (1). *Salmonella* invades the gut lumen and promotes its survival by triggering a series of immune and metabolic processes (2). When *Salmonella* invades the gut lumen, it first encounters commensal bacteria, a mucus layer and an epithelial cell layer. *Salmonella* competes with the commensal bacteria for nutrients in the mucus (39). *Salmonella* also causes inflammation by infecting epithelial and some immune cells in the intestinal epithelial layer of the gut (7, 40). This inflammation results in the release of pro-inflammatory factors like reactive oxygen species into the lumen (35, 41). Reactive oxygen species kill commensal bacteria and converts thiosulfate, a byproduct of hydrogen sulfide to tetrathionate (40). *Salmonella* utilizes tetrathionate as an electron acceptor for anaerobic respiration (35, 40, 41). When *Salmonella* manages to outgrow the commensal bacteria (42), they can infect more immune and epithelial cells thus

disrupting the epithelial cell barrier that separates the lumen from the lamina propria and blood vessels (5, 9, 35). *Salmonella* is skilled at using the host innate immune response for its own benefit, for example, nitric oxide produced as a pro-inflammatory factor to fight off infection is used by *Salmonella* to promote its own growth (40, 97).

The bacteria uses the system of invasion known as the type III secretion system (T3SS) (43) which produces bacteriocins that are injected into the host cell via a needle like projection off the bacteria cell wall (44). This T3SS injects bacterial proteins that activate endocytosis of the bacteria and make changes to the host cell for the bacteria's own benefits (44). Some of these changes include altering host kinase activities in certain immune, metabolic or inflammatory pathways (2, 42,45) that may be beneficial for the bacteria. The discovery and in-depth study of the T3SS effector proteins has greatly advanced our knowledge and understanding of the different mechanisms bacteria induce to avoid or subvert immune responses in host cells (44). For example, *Salmonella* secretes SopE into host cells (103, 104), this leads to disruption of Rho GTPases and the activation of caspase-1, an immune stimulator to produce proinflammatory cytokines in epithelial cells, thus causing inflammation that benefits the bacteria (103, 104). One way *Salmonella* benefits from inflammation is that inflammation kills commensal bacteria that produce butyrate (105, 106). With a decrease in butyrate, the epithelial cells increase lactate fermentation, which *Salmonella* utilizes as a nutrient (105).

The immune status of the host, the interplay between the innate immune function of the host and pathogen virulence mechanisms, and dose of inoculation are factors that dictate the outcome of *Salmonella* infections (1, 22, 41). As extensive as the research has been, our understanding of the interactions between host and pathogen remains lacking. *Salmonella* hijacks host cells and manipulates the innate programs of the cells for its benefit (44). Toll-like receptors (TLRs) are pattern recognition receptors important in the activation of immune cells to fight against microbes and pathogens (46). A study done by Arpaia, *et al.,* showed that specific TLRs knockouts resulted in the increased virulence and invasiveness of *Salmonella* (22). The results from the research indicates that changing the complement of host enzymes plays an important role in disease prevalence during *Salmonella* infections. Besides manipulating host cells, *Salmonella* is capable of evolving to resist antibiotics. Antibiotic resistant *Salmonella* is more difficult to treat and can lead to prolonged illness in humans. Antibiotic resistance in *Salmonella* is due to a combination of different mechanisms involving plasmids, integrons and transposons (4, 44). Many genes contribute to the antibiotic resistance of *Salmonella* (31, 44). These genes are known as the *Salmonella* Genomic Islands (SGI) (43, 44). Genes included in the SGI are *tetA*, *aminoglycoside acetyltransferases* (*aac*), *Aminoglycoside N6'-acetyltransferase* (*aad*), *integrase* (*int1*), *Acr*, *sul1* and more (4). These genes provide antibiotic resistance by inactivation, mutation or hydrolysis of targeted bacterial enzymes, insensitivity of bacterial enzymes/components to antibiotics, activation of antimicrobial flux pumps and modification of bacterial cell wall (1, 4, 44). For

example, certain *S*. Enteritidis and *S*. Heidelberg strains have shown sulfonamide resistance due to the presence of the *sul* gene that cause the increase in insensitivity to dihydropteroate synthase (4). These mechanisms are a major concern for public health (31,32) because they result in the resistance to antibiotics like Ceftriaxone, used to treat *Salmonella* infections in children and fluoroquinolones, used to treat *Salmonella* infections in adults (1,4).

Despite the slow growth in prevention of *Salmonella* infections, farmers, producers and breeders have developed customized preventive measures to control the spread of *Salmonella* and *Salmonella* contamination. Some of the measures include separation or isolation of animals, improving pest control, cleaning and hygiene, waste management and more (28). Some potential interventions used to target *Salmonella* infections include prebiotic, plant derived-compounds, organic acids and direct fed microbials (28, 47). Although the consistent efforts to implement these measures have caused a decrease in *Salmonella* contamination, these bacteria are still considered as operational and economic burdens by many producers (3, 48, 49). This raises the question, how do we effectively control and prevent *Salmonella* infections in livestock without the use of antibiotics? First, we must understand the mechanism of *Salmonella* infections in these animals. For example, chickens are asymptomatic to some *Salmonella* bacteria; however, research has shown that there are changes in the metabolic and immune states of infected chickens' gastrointestinal cells (2, 45). These changes in response are indicative of an attempt to clear infection, thus an immune

response. Therefore, identifying targets to intensify or supplement observed immune responses in host cells would be ideal for the treatment of *Salmonella* infections in chickens.

Although the different intracellular effects of *Salmonella* is not fully understood, there is considerably more information about the genomics of *Salmonella* species, their different strains and subtypes as compared to information on the changes it induces in host from a proteomics standpoint. Understanding the functional changes *Salmonella* induces in host systems would lead to a better understanding of the disease and how to combat it. It is also important to understand that the subtypes of *Salmonella* show differences in prevalence and invasiveness in poultry and other domestic animals (130). Therefore, it is critical that we understand the different influences of these serotypes on the activation of proteins. Cellular signaling pathways can provide some of this information for a better understanding of the systemic changes during infections in chickens to prevent the spread of *Salmonella* on farms and among domestic animals.

1.2 Importance of macrophages in understanding of *Salmonella* Infections

Macrophages are important components of the innate immune system that plays a vital role in responding to bacteria invasion (50). Macrophages play a central role in the innate immune defense of the host by recognizing and killing pathogens (50, 51). One reason macrophages were chosen for this research is the recognition that

macrophages serve as host to *Salmonella* (52). *Salmonella* can survive and replicate in a cell that targets it for destruction. Another reason macrophages were studied is that they are present in many distinct tissues of the host, including the gut (38, 52). Macrophages are known to exist in two main states, the inflammatory state (M1) and the anti-inflammatory state (M2) (53, 54). Researchers have shown that the M1 state is closely associated with the up-regulation and activation of glycolytic proteins, reactive oxygen species (ROS) and inflammatory cytokines (Tumor necrosis factor (TNF)-alpha, interleukins) while the M2 cells undergo fatty acid oxidation, immune suppression (increase TGF-beta and IL-10) and cell repair (51,54). Using the information available about macrophages, their control of pathogens and their response to intracellular invasion, we aimed to expand our understanding of the metabolic changes overtime that render these immune heroes susceptible to *Salmonella* infections.

Most *in vitro* macrophage studies are conducted in mammalian cell lines, however, an avian macrophage cell line has been used by poultry researchers to study immune responses to *Salmonella* infections and other pathogens (45,84,86). The avian macrophage cell line known as HD11 chicken macrophage like cells are avian myelocytomatosis type MC29 virus transformed chicken hematopoietic cells that displayed macrophage surface antigen and phagocytic capacities (85,86). Similar to macrophages *in vivo*, HD11 cells have been shown to phagocytize bacteria (85-87).

For example, a study performed by Wisner et al. also showed that HD11 cells can phagocytize different strains of *Salmonella* (87).

1.3 Immunometabolism

Immunometabolism is an emerging field recognized some 10 years ago (55, 60). This field centers on investigating the cross talk between the immune system and metabolism, that is, looking at these two systems as one. The relevance of immunometabolism is supported by research showing the involvement of immune cells in many non-immune functions like neurodegeneration, cardiovascular diseases, metabolism, metabolic diseases, etc (61). There are two perspectives of immunometabolism study. The first perspective of immunometabolism is the role of the immune system in organ metabolism and metabolic diseases (55, 60), that is, how dysfunctions in the immune system like in the case of diabetes can impact whole system metabolism. The second perspective is the role of metabolic processes that occur within immune cells and how they affect overall immunity (55, 60), that is, the energetic status of immune cells during infections indicate their inflammatory state. For instance, many studies have shown that increase in glucose metabolism is an indication of inflammation (54). This research focuses mainly on the second aspect of immunometabolism to determine the distinct metabolic processes activated during *Salmonella* infections in macrophages.

1.4 Kinome peptide array

Our laboratory employs kinome peptide array analysis as our primary method of determining changes in cellular processes. This technique measures the activity of enzymes responsible for the post-translational modification of peptides known as phosphorylation (55, 56). Phosphorylation is a post-translational modification carried out by kinases, enzymes that add a phosphate (PO_4) group to other enzymes and proteins using the gamma phosphate from an adenosine triphosphate (ATP) molecule. Kinome peptide arrays allow the visualization of peptides phosphorylated by kinases in a biological sample to infer changes in protein functions affecting cellular processes and pathways (57, 58). Phosphorylation based signaling cascades are critical for the coordination of many cellular events (98, 133). During the initiation of signal transduction, phosphorylation can act as a molecular switch to activate or deactivate proteins, a mediator of temporary protein-protein interaction and a tool in producing and recycling energy (98). Since, many signaling processes within a cell are dependent on phosphorylation by kinases, recognizing specific kinase target sequences and the specific serine, threonine or tyrosine residues within that sequence subject to phosphorylation allows us to determine the change in functionality of the protein and thus the change in cell response. Sites with phosphorylatable amino acid residues recognized by kinases are referred to as phosphosites. Addition of phosphate groups by kinases can result in the activation or deactivation of proteins that control different signals in a cell (55, 59, 98). Thus, these sites can be considered activity inducing or inhibition sites.

The kinome peptide array technique uses the sequences of kinase-target peptide that have been immobilized and printed on a glass array (55). The study of these kinases including their complement of the genome and activity within a biological sample is referred to as kinomics (163). Unlike other -omics, kinomics considers genes/proteins that actively alter phenotype. In contrast, transcriptomics studies the sum of all RNA transcripts in a cell at a given time, however, the expression of RNA does not signify its translation into protein or the activity of these predicted proteins in the cells.

Although the kinome peptide array was originally designed for research on mice (57), work done by Arsenault and colleagues resulted in the development of a chicken-specific kinome peptide array, therefore it does not rely on cross reactivity between species (55, 57). Another advantage of the kinome peptide array technique, other than species specificity, is its process-specificity (58). Through the selection of peptides involved in specific cellular and systemic processes, the kinome peptide array can be designed to investigate specific biological functions (55). For example, the immunometabolic signaling processes analyzed throughout this project. The kinome peptide array used for this project was designed by printing carbohydrate, fatty acid, stress, innate and adaptive immune related peptide sequences on the glass array (55–57).

This project also focuses on the intracellular responses of poultry hosts to *Salmonella* infections at different time points *in vitro*. Understanding the metabolic

changes the bacteria induces in the host and subsequent host immune response highlights key mechanisms of infection in the immune system. This understanding may serve as a basis for potential treatment of different serovars of *Salmonella* infections in poultry. This understanding would also contribute to the research on treatments for *Salmonella* in other animals, *Salmonella* induced gastroenteritis in humans and the prevention of foodborne disease.

Chapter 2

HYPOTHESIS AND AIMS

Before the analysis of the kinome peptide array data, we hypothesized that *S*. Enteritidis and *S*. Heidelberg would induce a change in immunometabolic signaling of host macrophages because macrophages undergo a change in metabolic profile during an immune response. After the analysis of the kinome peptide array data and review of the literature, we specifically hypothesized that *S*. Enteritidis and *S*. Heidelberg induce different immune and metabolic responses via the AMPK-mTOR cascade that control cells energetic status for successful invasion and infection of hosts. This hypothesis was tested in the following aims: Aim 1: To determine and validate the changes in the immunometabolic profile of HD11 macrophages due to the two serotypes of *Salmonella* infections. That is, identify distinct metabolic and immune characteristics of the two serovars in the results of kinome and validation assays. Aim 2: Determine the role of mTOR complex 1 in *Salmonella* infection and invasion of HD11 macrophages. Together, the completion of these aims will lead to a clearer mechanism of the invasion of *S*. Enteritidis and *S*. Heidelberg respectively. Completion of these aims will also show if mTOR complex 1 is a potential target for the treatment of *Salmonella* infections.

Chapter 3

MATERIALS AND METHODS

3.1 Cell Line and Maintenance

HD11 cells are referred to as chicken macrophage-like cells because they are an immortalized cell line derived from bone marrow and transformed with the avian myelocytomatosis type MC29 virus (45). The HD11 cells were obtained from the laboratory of Dr. Mark Parcells, University of Delaware. The cells were maintained in cell culture media containing Iscove's Modified Dulbecco's Media (IMDM) (GE Life Sciences, Logan, UT) with 10% fetal bovine serum (Midsci, Valley Park, MO), 1% 1.5 mM L-glutamine (containing penicillin and streptomycin) (Gibco, Grand Island, NY) at 37℃, with 5% CO_2 and 95% humidity. To passage HD11 cells, media was removed from the flask and discarded. 5 ml of 0.05% trypsin (MP Biomedicals, Solon, OH) was added to tubes and incubated for 5 minutes at 37 ℃. After 5 minutes, trypsinized cells were transferred to a centrifuge tube. The flask was washed with 5 ml of culture media and added to the tube with trypsinized cells. The cell suspension was centrifuged for 5 minutes at 300 x g. After centrifugation, supernatant was removed and the pellet was resuspended in 1 to 3 ml of culture media. When required, cells were counted using a hemocytometer, diluting the cell suspension 1:10 in trypan blue (Sigma-Aldrich, St. Louis, MO). 10 µl was loaded onto a hemocytometer, 16 squares covering 1 cubic millimeter were counted. The number of cells derived from the cell count was multiplied by (10x1000/ml), then multiplied by a dilution factor of 10 to

determine the number of cells per mL. The number of cells per well was determined by dividing the number of cells per mL (desired number of cells/number of cells per mL) x1000 to yield the final amount to be added to the well in µl. The appropriate amount of cell suspension was added to the flask, (20 ml of culture media for a T75 flask and 5 ml for a T25 flask). After plating, HD11 cells, were incubated at 37 ℃.

3.2 Bacteria Strains

Serotyped *S.* Enteritidis and serotyped *S.* Heidelberg from infected chickens were obtained from US Department of Agriculture- Agriculture Research Service. Freezer stocks of these two strains were cultured for macrophage infection. It is important to note that both *S*. Enteritidis and *S*. Heidelberg are resistant to nalidixic acid and novobiocin. 100 µl of *Salmonella* stocks stored in tryptic soy broth (TSB [Becton, Dickinson and Company, Sparks, MD]) and glycerol (Sigma-Aldrich, St. Louis, MO) at -80℃ were cultured in a shaker at 37℃ in an Erlenmeyer flask containing 30 mL of TSB with antibiotics (25 µg/mL novobiocin and 20 µg/mL nalidixic acid [Sigma-Aldrich, St. Louis, MO]) overnight. 100 µl of the overnight cultures were then added to a separate Erlenmeyer flask and cultured under the same conditions for 4 hours. Only the 4 hour cultures were used for infections. The optical density of the 4 hour cultures were determined using a spectrophotometer. The measurement derived from a spectrophotometer was converted to bacteria count using the Agilent OD600 online calculator (website) for *E. Coli*. To calculate the desired

number of bacteria required for each assay, (n/OD600) x1000, if n=desired number of bacteria and OD600=bacteria OD conversion.

3.3 Infection of Cells with *Salmonella*

Using cell counts from a hemocytometer, an appropriate volume of cell suspension to obtain $1x10^6$ cells were plated in 24 well plates for approximately 2 hours to adhere to the wells. These cells were then infected for 1 hour with a multiplicity of infection (MOI) of 1:100 for each serovar in 3 well replicates plus control. Infected cells were treated with 100 µg/mL of gentamicin (Sigma-Aldrich, St. Louis, MO) for 30 minutes or 1 hour post infection and incubated for 1 hour or 5 hours to yield 1.5 hours, 3 hours and 7 hours infections. Gentamicin is an antibiotic, targeting mostly gram positive bacteria (62). However, studies have shown that treatment with gentamicin after *Salmonella* infection kills extracellular bacteria (62). Therefore, treatment with gentamicin ensures that only changes due to intracellular *Salmonella* are being measured. The infected cells and control cells were used for experiments using different techniques as described below.

3.4 Gentamicin Protection Assay

After infection and treatment with gentamicin, the cells were lysed in 0.01 M of phosphate buffered saline (PBS) (Sigma-Aldrich, St. Louis, MO) containing 1% triton X100 (Sigma-Aldrich, St. Louis, MO). After lysis, 100 µl from each well was added to 15 mL centrifuge tubes containing 9.9 ml of 0.01M PBS (10^2) and mixed

gently. 1000 µl of each 10^2 mix was added to a separate 15 mL centrifuge tube containing 9 ml of PBS (10^3) and mixed gently. 1000 µl of 10^3 was added to a centrifuge tube containing 9 mL of PBS, mixed gently and plated in tryptic soy agar plates containing antibiotic (25 µg/mL novobiocin and 20 µg/mL nalidixic acid). After 12-18 hours incubation in 37 ℃, the bacteria colonies formed on the plates were counted and recorded.

3.5 Kinome Peptide Array analysis

After infection, cells were lysed in 100 µl of specially made lysis buffer containing protease inhibitors (1 g/mL aprotinin and 1 ug/mL leupeptin) along with other Sigma-Aldrich, St Louis, MO products (20 mM Tris-HCl, pH 7.5, 150 mM NaCl, 1 mM EDTA, 1 mM EGTA, 1% Triton, 2.5 mM sodium pyrophosphate, 1 mM Sodium Orthovanadate, 1 mM Sodium Fluoride, 1 mM phenylmethylsulfonyl fluoride [PMSF]). After the lysis step, the cells sat on ice or at 4℃ for 10 min. Next the lysates were centrifuged for 10 min at 14,000 x g. 70 µl of the supernatant was mixed with 10 µl of activation mixture containing 500 µM of ATP with 50% glycerol (New England BioLabs, Ipswich, MA), 60mM Magnesium Chloride, 0.05% [vol/vol] Brij L23, and 0.25 mg/ml bovine serum albumin [BSA] (all from Sigma-Aldrich, St Louis, MO). 80 µl of each sample was applied to a glass peptide array (JPT Peptide Technologies, Berlin, Germany) with lifted edge glass slips to cover the samples. Measures were taken to ensure there were no bubbles present under coverslips after application of lysate. The arrays were incubated in a humidity chamber; a sealed container placed in

a 5% CO_2 incubator at 37°C for 2 hours. After incubation, the array was submerged in 0.01M PBS with 1% triton to remove the coverslip. After the removal of the coverslip, the slides were washed twice with agitation in 2M NaCl containing 1% triton and then rinsed in double deionized water, in 50 mL centrifuge tubes. After the rinses, slides were submerged in phospho-specific fluorescent ProQ Diamond Phosphoprotein Stain (Life Technologies, Carlsbad, CA) for 1 hour. After 1 hour of phospho-specific stain incubation, slides were washed 3 times for 10 minutes each with destaining solution containing 20% acetonitrile (EMD Millipore Chemicals, Billerica, MA) and 50 mM sodium acetate (Sigma-Aldrich, St. Louis, MO) at pH 4.0. Phospho-staining and destaining was carried out on a shaker for 10 min with protection from light. The wash process was repeated with double deionized water after destaining. The glass arrays were spun at 300 x g in 50 mL centrifuge tube (with Kim wipes stuffed at the bottom) to remove moisture. After drying, arrays were scanned in a Tecan PowerScanner microarray scanner (Tecan Systems, San Jose, CA) at 532 to 560 nm with a 580-nm filter to detect dye fluorescence.

3.6 Generation and Analysis of the Kinome Peptide Array Data

The images of the scanned array were gridded manually to fit the phospho-specific spots and extract signal intensity using GenePix Pro software (version 7.2.29 1, Molecular Devices, CA). Microsoft Excel 2016 (Redmond, WA) files containing kinomic data were generated and further analyzed using the online normalization and analysis tool known as PIIKA2 (91). The kinome peptide array data generated from

PIIKA2 was analyzed by using other online databases like STRING (90), KEGG color and search pathway (92), Uniprot (93-95) and phosphoSitePlus (89). Before analysis with online databases like STRING and KEGG, the data generated by PIIKA2 was sorted. The data was separated into 3 groups, namely; 30 minutes, 2 hours and 6 hours. The p-value and fold changes generated by PIIKA2 were used to sort the peptides based on significance. The data was further sorted by discarding any peptide with a p-value above 0.05 and grouping all the peptides of the same strain with a negative fold change together by serovars. The sorted list of peptides were placed into STRING. STRING showed a visual representation of the interactions between the proteins and also generates, in descending order, a list of biological signaling pathways in which the proteins function (Table 1).

3.7 Seahorse XFp Metabolic Assay

The Seahorse XFp Analyzer (Agilent technologies, Santa Clara, CA) is technology that measures functional metabolic data such as extracellular acidification rate (ECAR) and oxygen consumption rate (OCR) (agilent.com, seahorse XFp manual). The seahorse XFp analyzer was used to perform metabolic analysis of HD11 cells before and after infection (with *S*. Enteritidis or *S*. Heidelberg) or treatment (with rapamycin [Sigma-Aldrich, St Louis, MO] or MHY1485 [MilliporeSigma, Burlington, MA]). Data from the metabolic analysis was used to validate the results of the peptide array analysis.

Cells were prepared for plating in a seahorse mini culture plate by adding 5 mL

of trypsin to each T75 flask of cells. The cell-trypsin suspension was transferred to a 15 mL or 50 mL centrifuge tube (depending on the number of flasks). The flask(s) were washed with 5 mL of IMDM media. The washes were transferred into the cell-trypsin suspension tubes and centrifuged at 300 x g for 5 minutes. After centrifugation, the supernatant was discarded and the pellet was collected. The pellet was then resuspended in 2-5 mL of IMDM media. The cells were counted using a manual hemocytometer to determine the volume of suspension needed for 50,000 cells to be plated. The desired volume of cells (50 µl of IMDM-cell mixture) was added to the wells of the mini culture plate (excluding wells A and H). The wells on the side of the plate was moated with 400 µl of double deionized water. After the plating process, the plates were incubated in 5% CO_2 for at least 2 hours.

Before the day of experiment, overnight inoculants of *S*. Enteritidis and *S*. Heidelberg were prepared. On the day of experiment, 4 hour inoculants were prepared by adding 100 µl of *S*. Enteritidis and *S*. Heidelberg overnight cultures to flasks containing 30 mL of TSB and antibiotics. Also, it is strongly advised to calibrate the seahorse machine before each run, therefore calibration plates were prepared at least 8 hours before each experiment. The calibration plates were prepared by adding 400 µl of double deionized water to the moat wells and 200 µl of Agilent Seahorse calibrant to the 8 wells that hold the cartridge. The cartridge was placed into the wells and incubated at 37°C in a non-CO_2 incubator.

After allotted time for mini culture plates incubation at 37°C with CO_2 , 200 µl

of seahorse media (XF DMEM medium, pH 7.4 with 5 mM HEPES [Agilent technologies, Santa Clara, CA]) containing 1% 200 mM glutamine and 1% 100 mM sodium pyruvate was added to each well (including blank wells A and H). Note: for experiments with mTOR targeted treatments, equivalents of 100 ng/mL of rapamycin or 2 µm of MHY1485 was added to seahorse media described above. After addition of seahorse media to the mini culture plates, mini plates were incubated at 37℃ in a non-CO_2 incubator for 30 minutes to an hour.

During this time, the Seahorse XFp machine was turned on, the assay was setup and saved using the seahorse software, and the calibration plate was removed from non-CO_2 incubator and put into the Seahorse XFp to calibrate the machine. After the machine was fully calibrated, bacteria was added to the designated wells of the mini culture plate. The cartridge plate was then replaced by the mini culture plate with the infected cells to start assay. During data analysis, ANOVA and Tukey Kramer statistical analyses were performed on readings 15 and 24 for the 30 minutes and 2 hours post infection time points.

3.8 Western Blot

After infection of HD11 cells with *Salmonella* (see protocol above), trypsin was added to each well and the cells were harvested in 1.5 mL centrifuge tubes. The harvested cells were spun at 300 x g for 5 minutes. After centrifugation, the cells were washed in ice cold PBS and centrifugation was repeated. The cells were then lysed in 100 µl of water for approximately 10 seconds and kept on ice for 5 minutes.

The lysed cell mixture containing target proteins were then centrifuged at 800g for 7 minutes. After centrifugation of lysis mixture, cell debris settled at the bottom, 50 µl of the supernatant per tube which contained 25 to 40 µg of protein was mixed with 50 µl of 2x laemmli buffer (Bio-Rad Laboratories, Hercules, CA). Sample -laemmli mix was placed in a water bath at 75 ℃ for 5 minutes and vortexed. 20 µl of heated sample-laemmli mix was added to each well of Mini-PROTEAN TGX precast 7.5% polyacrylamide gel (Bio-Rad Laboratories, Hercules, CA). HiMark pre-stained protein standards (Invitrogen, Carlsbad, CA) were loaded into two wells. Using Bio-Rad Laboratories (Hercules, CA) western blot kit, gel electrophoresis was performed in Tris/Glycine/SDS running buffer at 150 V for 1 to 1.5 hours. After electrophoresis, the gel cassette was disassembled to remove the polyacrylamide gel. The gel was placed in Tris/Glycine transfer buffer along with presoaked sponges, filter papers and PVDF membrane. The PVDF membrane was presoaked in methanol (Sigma-Aldrich, St Louis, MO) for 1 minute. The gel was sandwiched with the PVDF membrane in the following order; sponge, filter paper, gel, PVDF membrane, filter paper and sponge, in a sandwich cassette with the membrane placed closer to the positive electrode. Transfer was performed overnight at 22 volts in a cold room with cassette completely submerged in the buffer. After transfer, the membrane was immediately transferred to washing buffer (0.01M PBS and 0.05% triton X 100). After wash, the membrane was incubated for 1 hour at room temperature with agitation in blocking buffer (washing buffer with 3% BSA). After blocking, the membrane was rinsed in washing buffer 3 times for 5 minutes with agitation. Phospho-mTOR (Ser2448)

polyclonal primary antibody (Invitrogen, Carlsbad, CA) was prepared at a 1:1000 dilution in blocking buffer. The membrane was incubated in primary antibody in a cold room overnight. A goat anti-rabbit IgG horseradish peroxidase conjugated secondary antibody (Invitrogen, Carlsbad CA) was prepared at a 1:5000 dilution in blocking buffer. After incubation in primary antibody, the wash process was repeated and the membrane was incubated in secondary antibody at room temperature for up to 2 hours or in a cold room for at least 6 hours. Another wash was repeated after secondary antibody incubation. The membrane was incubated in an enhanced chemiluminescence (ECL) substrate that reacts with the horseradish peroxidase conjugate of the secondary antibody for 5 minutes. After 5 minutes substrate incubation, blots were viewed on a gel doc using chemiluminescence blot settings at optimum exposure. The images of the blots were analyzed using ImageJ software (version 1.5).

3.9 Flow Cytometry

2 million cells per well in a 24-well plate were plated in antibiotic free cell culture media and left to incubate in 5% CO_2 incubator for 2 hours. After incubation, the cells were infected with *S*. Enteritidis or *S*. Heidelberg for 1 hour at an MOI of 1:100. After infection, the cells were treated with 100 µg/ml of gentamicin for 30 minutes. After gentamicin treatment, the incubation media was removed and the cells were trypsinized for 3 minutes at 37 ℃. After trypsinization, the cells were transferred into a 1.5 mL centrifuge tube and rinsed with equal volume of antibiotic free cell

culture media. The cells were then centrifuged at 800 x g for 7 minutes. After centrifugation, the cells were resuspended in antibiotic free cell culture media and incubated for 20 minutes at room temperature. After 20 minutes, 0.01M PBS was added to the cell suspension and the mix was centrifuged at 1000 x g for 7 minutes. After centrifugation, the cells were fixed in 100 µl 3.7% formaldehyde (1 mL of 37% formaldehyde (Sigma-Aldrich, St Louis, MO) in 9 mL PBS) for 15 minutes at room temperature. After fixation, 100 µl of ice cold PBS was added into the cell formaldehyde mix. This mix was then centrifuged at 800 x g for 7 minutes. The supernatant was then discarded and cells were prepared for flow cytometry using FITC Annexin V/Dead Cell Apoptosis Kit with FITC annexin V and PI for Flow Cytometry (96) (Invitrogen, Carlsbad CA). The samples were ran in duplicates on a BD Accuri C6 cytometer (GE Healthcare, Piscataway, NJ). After the runs, samples were gated and analyzed using De Novo Software (111).

3.10 Statistics

Statistical analysis used in this study included analysis of variance (ANOVA) and Tukey-Kramer post hoc tests for all control (ctrl), infected or treated (rapamycin or MHY1485) cells in seahorse metabolic flux assay and gentamicin protection assay data to compare within and amongst groups using JMP pro 14.0.0. For the kinome peptide array, a one-sided paired t-test between infected/treated and control values was performed for each peptide via PIIKA2 (91).

Chapter 4

RESULTS

4.1 *Salmonella* alters host (HD11 cells) immunometabolism

Results of kinome peptide array in chicken macrophage-like cells infected with *S.* Enteritidis and *S.* Heidelberg showed changes in host immunity and metabolism at different time points post-infection with significant p-value less than or equal to 0.05. Figure 1 shows a few of the significant proteins changed in the immune and metabolic signals of HD11 cells after *Salmonella* infections over the different time points.

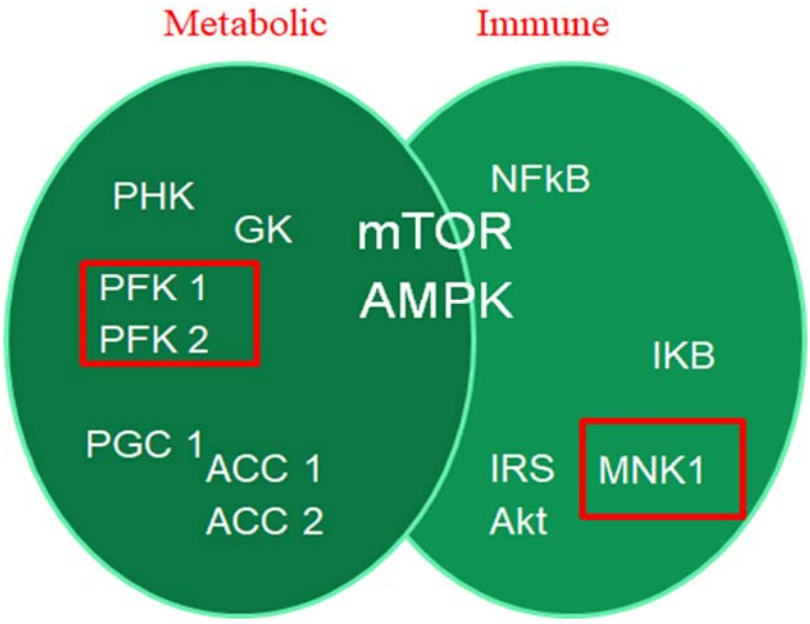

Figure 1: Proteins common to metabolic and immune pathway. This venn diagram illustrates metabolic and immune related proteins and a link between some metabolic and immune pathways discovered in the kinome peptide array data. The proteins highlighted in red boxes are involved in important regulatory functions.

Enzymes involved in immune responses common to the 5' adenosine monophosphate-activated protein kinase (AMPK), insulin and mammalian target of rapamycin (mTOR) signaling pathway were analyzed because these pathways were shown to be highly significant in the kinome peptide array results. Insulin receptor substrate (IRS), Phosphoinositide 3-kinase (PI3K), Phosphoinositide-dependent Kinase (PDK), Protein kinase B (Akt), tuberous sclerosis (TSC), mTOR, cAMP response element binding protein (CREB), nuclear factor kappa-light-chain-enhancer of activated B cells (NFkB) and AMPK are important in the signaling cascade of immune related peptides (Figure 1, Table 1). Ligands of immune receptors activate downstream kinases which leads to a phosphorylation cascade that results in the activation or deactivation of respective proteins and changes in cellular response. For example, kinome data analysis showed an increased activity of Tumor Necrosis Factor (TNF) receptor associated factor and proteins downstream of the receptor including Jun N-terminal kinase 1 (JNK1) and Mitogen-activated Protein Kinase (MAPK)-interacting Kinase 1 (MNK1) at *S*. Enteritidis 30 minutes post infection and *S*. Heidelberg at 2 hours post infection. Thus indicating a TNF-alpha related immune response and changes in cell survival via apoptosis for each serovar at different times. As observed in kinome peptide array results, the phosphorylation cascade for *S*. Enteritidis and *S*. Heidelberg at the different time points significantly altered host immune signaling (Figure 1, Table 1). In detail, JNK1 was phosphorylated at site T183 (Table 2), which is known to induce apoptosis (158, 159), thus stimulating cell death early on. MNK, which is also downstream of TNF-alpha-MAPK signaling was

significantly less phosphorylated (Table 2) than control for *S*. Enteritidis 30 minutes and *S*. Heidelberg 2 hours infected cells on the site T255, responsible for the inhibition of apoptosis (159). To add on, the NFkB inhibitor IkB-alpha was also significantly more phosphorylated on its active site (Y42) in *S*. Heidelberg 30 minutes post infection (Table 2). Y42 also plays a role in the inhibition of apoptosis (108).

Table 1: **Highly significant immunometabolic pathways** showing the number of changes (increased or decreased phosphorylation) in peptides common to both *S*. Enteritidis and *S*. Heidelberg infected HD11 extracted from the kinome peptide array data as illustrated by STRING database's biological signal transduction pathway table.

Signal Transduction Pathways	**30 minutes**	**2 hours**	**6 hours**
Insulin signaling	17	23	24
AMPK signaling	21	19	22
mTOR signaling	13	15	12
HIF-1a signaling	16	21	33

4.1.1 Kinome Peptide Array *S*. Enteritidis 30 minutes post infection.

In *S*. Enteritidis 30 minutes, enzymes involved in glycolysis showed predominantly increased phosphorylation (Table 2,3, Figure 2), i.e PFK1 and PFK2, which are involved in one of the most important steps of glycolysis were both phosphorylated [PFK1 (T211) (less phosphorylated S386), PFK2 (S461, Y366)]. PhK and HK were (Table 2,3) also phosphorylated at *S*. Enteritidis 30 minutes. In the literature, the activation of Sirt1, leads to the phosphorylation and activation of PDK

(S241, Y376) and Akt (T479, T305) (114). Sirt1 is responsible for enhancing Akt and PDK binding (114). One Sirt1 site (T530) was less phosphorylated (Table 3), it is responsible for acetylation of downstream proteins (115) including p53, SREBP1, NFkB, PGC1-a, etc. known to affect metabolism, inflammation and apoptosis. However, since T530 was less phosphorylated, it is expected that acetylation of Sirt1's downstream targets did not occur. Both Akt and PDK suspected to be indirectly involved with Sirt1 signaling are phosphorylated, suggesting a potential function of Sirt1's phosphosite S661 (Table 2). Two PDK sites were phosphorylated in the data set (S241 and Y376) (Table 2, Figure 2); both induce cell growth and alter apoptosis (114, 116, 128). PDK also phosphorylates and activates Akt and p70s6k (116, 128). Akt was phosphorylated on two sites (T479, T305) and less phosphorylated on 1 site (T308) (Table 2, 3). T479 (mTOR activated) and T308 (PDK activated) have the same function, however, they must be dual phosphorylated to be activated (89). When activated, they inhibit apoptosis and induce cell growth, yet only T479 is activated, thus the complex is inactive (89, 137). This leaves T305 which is suspected to be involved in the balance of survival and apoptosis (137). CREB which is also known for its regulatory role in cell survival, growth and differentiation was activated by phosphorylation of S133 (Table 3), which is known for its inhibitory effects on apoptosis (117). For IRS, Y896 was phosphorylated and S616 was less phosphorylated (Table 2). The function of phosphorylated S616 is to inhibit its enzymatic activity (119) while Y896 is involved in cell cycle regulation (118). IRS also serves as a docking site for PI3K. PI3K is important in cell cycle regulation,

indicating that Y896 might be an active docking site for PI3K (138). There were more dephosphorylated sites in the data set then there were phosphorylated for PI3K (Table 2). Although two (Y425, Y556) of the three known phosphorylation sites were determined by high throughput methods, site Y556 function is to induce enzymatic activity (142). Akt also plays a role in mTOR activation by inhibiting TSC2 (120) which functions as an mTOR inhibitor by targeting or inactivating Rheb. TSC2 was phosphorylated at S1418, thus inhibited (Table 2). One mTOR site (S863) was phosphorylated and another phosphorylation site S2448 (Table 2, 3), which is known to be the key determinant of mTOR activation (121, 122) was significantly less phosphorylated in the data set. Both sites induced enzymatic activity when phosphorylated (122,123). mTORC1 activates S6K and inactivates 4EBP1 to up regulate protein synthesis (69-71,121-123). mTORC1 activates transcription and translation through its interactions with S6K and 4EBP1 (69,70). An activated mTORC1 will phosphorylate 4EBP1 to inhibit its binding to the translation initiation factor (69, 70), leaving it free for translation to occur. mTORC1 phosphorylates S6K on at least two sites (usually threonine sites), this stimulates further phosphorylation by PDK. This will stimulate transcription and the initiation of protein synthesis. However, all S6K sites that had significant p-values in *S*. Enteritidis 30 minutes were less phosphorylated (Table 2). PP2a, phosphorylated on S60 and less phosphorylated on S75 (Table 2) is known as a S6K inhibitor (124). 4EBP1 was less phosphorylated on T37 (Table 2) and thus inhibited (145, 146). ACC1 (S1263, S80) and ACC2 (Y1560) responsible for catalyzing acetyl-CoA to malonyl-CoA used in fatty acid

synthesis (125) were more phosphorylated (Table 2,3), therefore inhibited indicating that fatty acid synthesis was being suppressed. SREBP1, which plays an important role in the inhibition of fatty acids genes (139) was inhibited via phosphorylation on S338 (Table 3). EEF2k which becomes phosphorylated when the cell is in a low energy state (89) had two sites (S78 enzyme activity inhibited/induced, S366) phosphorylated (Table 2). Although EEF2K activity was unclear, AMPK was significantly more phosphorylated on three sites (Table 2), one of which is an active site (Table 3), indicating an increase in energy demands (140). Since glucose transport was needed, the phosphorylation of Rab (S199, T136) (Table 2) suggests the activation of Glut4 to translocate to the cells membrane (141).

Table 2: **Changes in immunometabolic peptides of *S*. Enteritidis and *S*. Heidelberg infected HD11.**

Protein/Peptide	**30 Minutes**		**2 hours**		**6 hours**	
	S. Enteritidis	*S*. Heidelberg	*S*. Enteritidis	*S*. Heidelberg	*S*. Enteritidis	*S*. Heidelberg
PFK1	↑ ↓	↓	↑↑↑↓↓	↑ ↑ ↑ ↓	↓↓↓	↓↓
PFK2	↑↑	∅	↑↑	↑ ↑	↑	↑
PhK	↑↓	↑	↓↓↓	↑↓	↑↓	↓
ACC1	↑↑	↑↑	↑ ↓	↓	↑ ↓	↑ ↑
ACC2	↑	↑	↑ ↓	↑	↑ ↑	∅

CPT1	∅	∅	∅	∅	∅	↑
SREBP1	↑	↑	↓	↓	↑	↑
AMPK	↑↑↑ ↓↓	↑↑↑ ↓↓↓	↓↓	↑ ↑ ↑ ↑ ↓↓	↑↑↑ ↓↓	↑↑↑↑ ↓↓
AMPK-related peptide	↓	↓	↑	∅	↑ ↓	↑ ↓
CAMKK-B	↑	↑	∅	↑	↑	∅
EEF2K	↑ ↑	↑	∅	∅	↑ ↑↑	↑↑↑
Cyclin D1	↑	↑	∅	↑	↑↓	∅
CREB	↑	↑	↓↓	∅	↓	∅
HUR	∅	∅	↓↓	↑↓	↑	∅
LKB1	↓↓	↑↓	↓	∅	↓	↑
PP2A	↑↓	↓↓	↑↑	↑	↓↓	↓↓↓↑
mTORC1 (S2448)	↓	↓	↑	↑	↑	↑
mTORC1 (S863)	↑	∅	↓	↓	↑	↑
S6K	↓↓	↓	↑↓	↑	↑↓↓	↓↓
4EBP1	↑	↓↓	↓↓↓	↓↓		↓
PDK	↑ ↑	∅	↓	↑ ↓	↑ ↑	↑↑
AKT	↑↑↓	↑ ↓	↓	↓	↑ ↑↓	↑↑↑
TSC2	↑	↑	∅	∅	↑ ↑	↑(S939)
PGC1	↑	↑↑ ↓	↓	↑	↑ ↑ ↑	↑↑
IRS	↑ ↓	↑	↓↓	∅	↑	↑

PI3K	↑↑ ↓↓↓↓↓	↑↑ ↓↓↓↓	↑↑ ↓↓↓↓↓	↑↑ ↓↓↓↓	↑↑↑ ↓↓↓↓↓↓	↑↑ ↓↓↓↓↓
SIRT1	↑↓	↓	ø	↑	↑↑↓	↑↓
GSK	↓	↑	↑	↑	↑↑↓↓↓	↑↑
PYG	↓↓	↓	↑↓	↑↑↑	↓↓↓	↓↓
RAB	↑↑↓	ø	↓	ø	↓	ø
TAK-1	↓↓	↓↓	↓↓	ø	ø	ø
TRAF and TRAF related peptides	ø	↑	↑↓	↑↓	↑↑↑	↑↑
TNF-receptors	↑↓	↓	↑	↑↓	↑↓	↑↓
JNK (T183)	↑	ø	ø	↑	ø	ø
AP-1/c-Jun	↑↓	↓	↓	↓	↑↓	↑↓
MNK	↑	↓	ø	↑↓	↑	↑
Caspase-1	↑	ø	↓	ø	↑	↑
Caspase-3	↓	↓	ø	ø	↓	↓
NFkB	↑↑	↑↑	↓↓↓	↓	ø	↓
NFkB inhibitor	ø	↑	↓	ø	ø	ø
Inhibitor of NFkB inhibitor	↑	↑	↓	↓	ø	ø
PPAR-Gamma	ø	ø	↑	↑	ø	ø

This table shows the changes in the phosphorylation states of immune and metabolic related peptides adapted from AMPK, mTOR, insulin pathways amongst others as shown in the kinome peptide array data. The arrows represent significant sites for each peptide. ↑; significantly more phosphorylated, ↑; significantly more phosphorylated on an active site, ↑; significantly more phosphorylated on an inhibitory site, ↓: significantly less

phosphorylated, ↓: significantly less phosphorylated on an active site, ↓; significantly less phosphorylated on an inhibitory site.

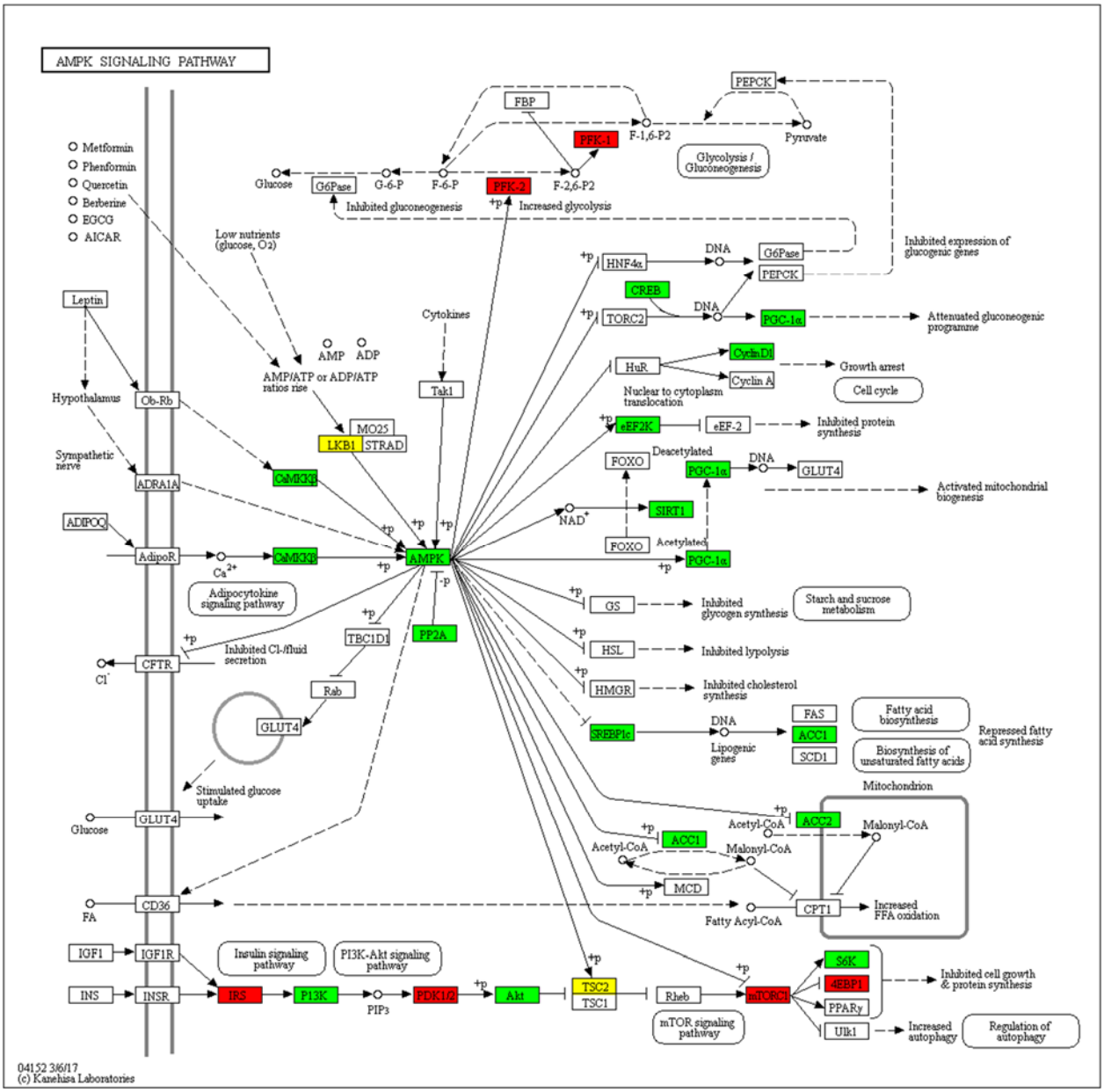

Figure 2: **Changes in AMPK signaling peptides at 30 minutes post *Salmonella* infections.** Kinome peptide array analysis revealed significant changes in the AMPK signaling pathway unique to *S.* Enteritidis infected HD11 cells indicated by red compared to *S.* Heidelberg infected HD11 cells indicated by yellow. Changes common to both *S.* Enteritidis and *S.* Heidelberg are indicated in green.

4.1.2 Kinome Peptide Array Analysis *S*. Heidelberg 30 minutes Post Infection

AMPK related peptides had three sites (S108, T165, T211) less phosphorylated (Table 2), including T211 which is involved in the inhibition of the energy consumption processes during glucose starvation (140, 150). AMPK also had three other sites phosphorylated (Table 2), which are important for cell cycle arrest, autophagy and energy stabilization (150). The AMPK site T183 known to induce enzyme activity (140) was phosphorylated (Table 6) however, an inhibitory site S496 (156) was also phosphorylated (Table 6), thus the enzyme activity was inhibited. The AMPK regulated protein Sirt1 was less phosphorylated at T530 (Table 6). Interestingly, PGC-1 alpha sites (T299, S266) and EEF2K at S78 (induces enzymes activity and inhibits calmodulin interaction (89, 140, 153)) were phosphorylated (Table 2). These proteins are phosphorylated and activated by AMPK. This raises questions about the energetic state of the cells and the regulatory role of S496. The peptide array data also showed the phosphorylation of ACC1 at two sites (S1263, Y1370) (Table 2), which indicates that it was inhibited. SREBP1 at S338, responsible for inhibition of transcription of fatty acid genes, was also phosphorylated (Table 6). Moreover, PI3K which is involved in cell growth and survival (138, 142) had four less phosphorylated sites (T1024, T607, S1070, S1039) and two sites (Y425, Y605) phosphorylated (Table 2). The IRS docking site for PI3K was phosphorylated on site Y896 (Table 2) which is responsible for phosphorylation and other molecular regulations (118). TSC2, which is an inhibitor of mTORC1 (160) was phosphorylated (Table 2) at S939 (essential for apoptosis inhibition and transcription alteration (161)).

Akt which also inhibits TSC2 is partially inactive because it has one of its dual phosphorylated activation sites (T308) less phosphorylated (Table 6) leaving only T479 phosphorylated (Table 2) (89, 137, 160). mTORC1 was not phosphorylated in *S.* Heidelberg 30 minutes post infection (Table 2) and S6K T444, S360, S380 were all less phosphorylated (Table 2). This is unusual because PP2A (S60, S75) was also less phosphorylated (Table 2). PP2A when phosphorylated, inhibits Akt and increases TSC activity (160). mTOR, a TSC target deactivates 4EBP1 (Table 6) (69, 121). 4EBP1 inhibits translation by binding to elF4E (145, 146), which is also less phosphorylated on two inhibitory sites (Table 2). C/EBP alpha, which is indirectly regulated by mTORC1 (143), was phosphorylated at T222 (Table 2) to inhibit transcription and regulate cell cycle arrest and differentiation.

4.1.2.1 S. Heidelberg infection at 30 minutes in HD11 cells does not induce the phosphorylation of three major glycolytic enzymes

Both PFK1 and PFK2 are important enzymes in glycolysis therefore the presence of their kinases and state of these enzymes in infected cells is a significant indication of the metabolism of the cells. The changes in the phosphorylation of PFK1 and PFK2 in *S.* Enteritidis 30 minutes post-infection suggest the induction of glycolysis early on during infection by *S.* Enteritidis (63). While the inactivation of PFK1 and the inactivity of PFK2 kinases in *S.* Heidelberg at 30 minutes post infection could mean one of two things (i) *S.* Heidelberg infection led to the inhibition of these

enzymes and thus glycolysis or (ii) *S*. Heidelberg infection led to the inhibition of PFK1, PFK2 and their kinases but induced an alternative pathway for glycolysis to occur. Upon analysis of KEGG mapper's glycolysis pathway, phosphorylase kinase (PhK) whose main function is to activate glycogen phosphorylase (by phosphorylation) (134) was significantly more phosphorylated than control for both *S*. Enteritidis and *S*. Heidelberg infected cells at the 30 minutes time point (Table 2). Also, analysis of the glycolysis pathway showed that kinases did not significantly influence the activities of three major enzymes important in the early step of glycolysis in *S*. Heidelberg infected cells at 30 minutes post-infection (Figure 3).

These enzymes without significantly detectable kinase activities included (i) phosphoglucose isomerase which converts glucose 1-phosphate to fructose 6-phosphate (135), (ii) PFK1 which converts fructose-6-phosphate to fructose-1,6-bisphosphate (135) and (iii) aldolase, which is important for the formation of glyceraldehyde-3-phosphate (135). However, the data revealed that the kinases that phosphorylate the enzymes in the later steps of glycolysis were present and active. This suggest that the enzymes whose kinase activities were not detected were bypassed by some other mechanism. The result from comparing *S*. Enteritidis and *S*. Heidelberg at 30 minutes post-infection provides evidence, which supports the hypothesis that *S*. Enteritidis and *S*. Heidelberg infections induce differences in the

immunometabolism of host cells.

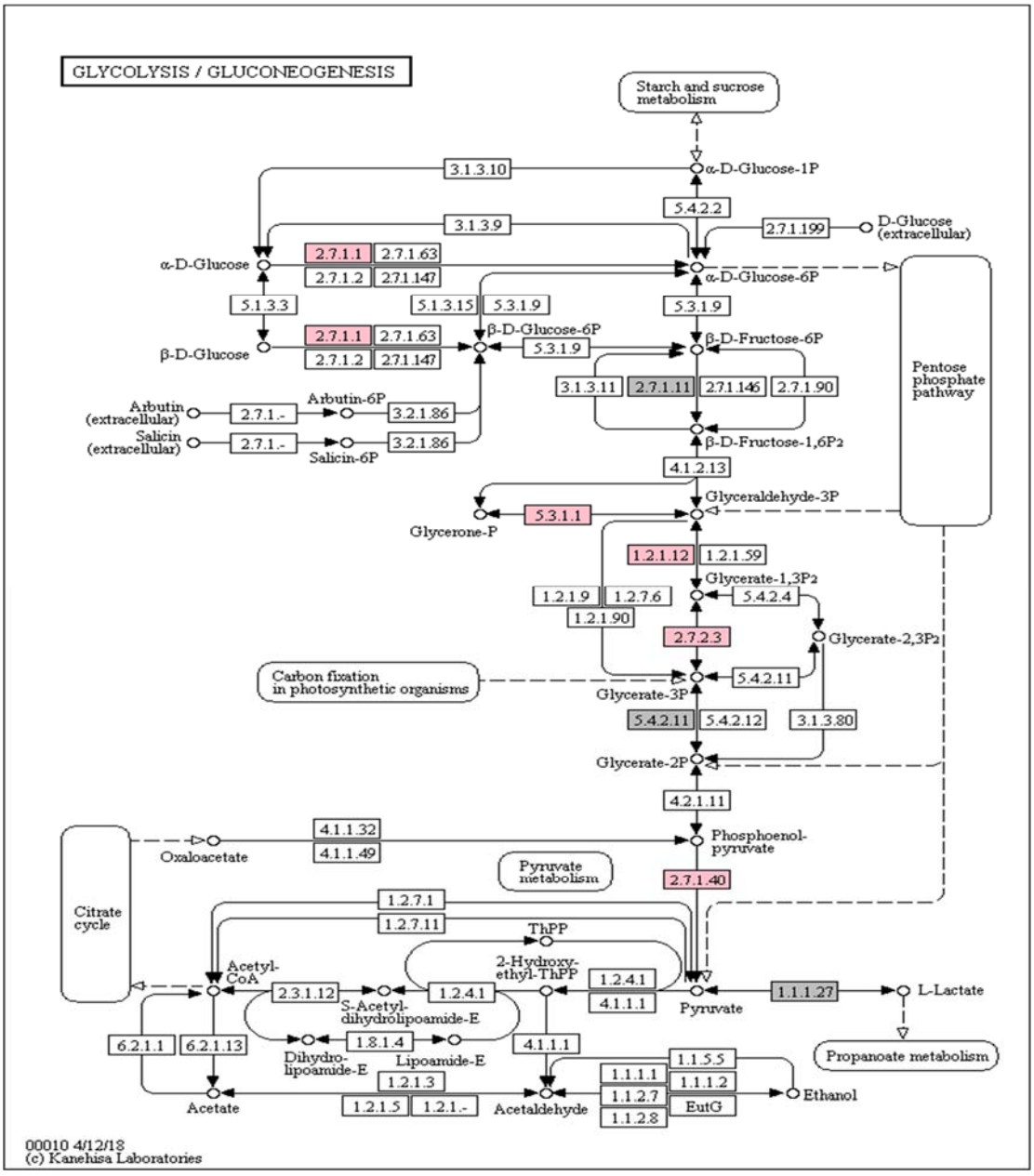

Figure 3: Changes in phosphorylation of glycolytic enzymes in 30 minutes post *S.* Heidelberg infection. This Figure illustrates the increased phosphorylation (pink) and decreased phosphorylation (grey) of glycolytic enzymes respective to *S.* Heidelberg infected HD11 cells at 30 minutes post infection.

4.1.3 Kinome Peptide Array Analysis *S*. Enteritidis 2 hours post infection.

Unlike the 30 minute time point, at 2 hours post-infection, PFK1 and PFK2 were activated (phosphorylated at their activating phosphosite) in *S*. Enteritidis. Also hexokinase was phosphorylated for all time points except *S*. Enteritidis at 2 hours post infection (Table 2, 4). CREB, an essential survival protein was less phosphorylated at S133 (Table 4) which when phosphorylated inhibits apoptosis and induces cell growth (117). PGC-1, a CREB regulator activated by AMPK was substantially less phosphorylated (Table 4). This indicates that AMPK was also less phosphorylated. As seen in the data set, two sites (S182, S108) of AMPK peptides were also less phosphorylated in *S*. Enteritidis 2 hours post infection (Table 2). Only one site (T211, inhibits growth and induces enzymatic activity (150)) of the AMPK related protein Nuak1 was phosphorylated (Table 4). LKB1, an AMPK phosphorylase was also less phosphorylated at an active site T363 (Table 2, 4). Rab was also less phosphorylated at Y14 (Table 2) whose function remains unknown. The ACC1 site, S80 responsible for inhibition of apoptosis was less phosphorylated (Table 4) and Y1370 phosphorylated (125, 144). ACC2 (Y1489, Y1560) remained completely phosphorylated (Table 2). IRS, which serves as a docking site for PI3K was substantially less phosphorylated on both sites (Y896, T340) (Table 2) (118, 138). PI3K was less phosphorylated on five sites (Y556, S1039, Y962, T607, T1024) and phosphorylated on two sites (S1070, S582) (Table 2). Only one Akt site (S476) was phosphorylated (Table 4). It's generally known function is to help balance apoptosis and survival (89, 137). Both S6K (T444 induces activity) and C/EBP alpha (T222,

transcription induced) were phosphorylated (Table 2) which are expected to initiate transcription and translation of apoptotic proteins (143). 4EBP1 was less phosphorylated on site T37 known to enhance the initiation of translation (Table 4) (145, 146). PDK's active site S241 responsible for inducing cell growth was significantly less phosphorylated than control (Table 2) (114, 116, 128). mTORC1 was phosphorylated on one site (S2448) (Table 4) and less phosphorylated on three sites (S2481, S863, T706) (Table 2). PPAR-gamma, which is known for its role in fatty acid storage, lipid uptake and glucose metabolism (148) is phosphorylated on S112 (Table 2). When activated, S112 degrades proteins and alters/inhibits transcription (147). SREBP1 S338, which inhibits transcription of fatty acid genes (139) was less phosphorylated (Table 4). Two sites on HuR, important in the translation (126) of cFOS, were also less phosphorylated in *S.* Enteritidis 2 hours. cFOS is known to play an important role in the regulation of cell growth, proliferation and survival (127).

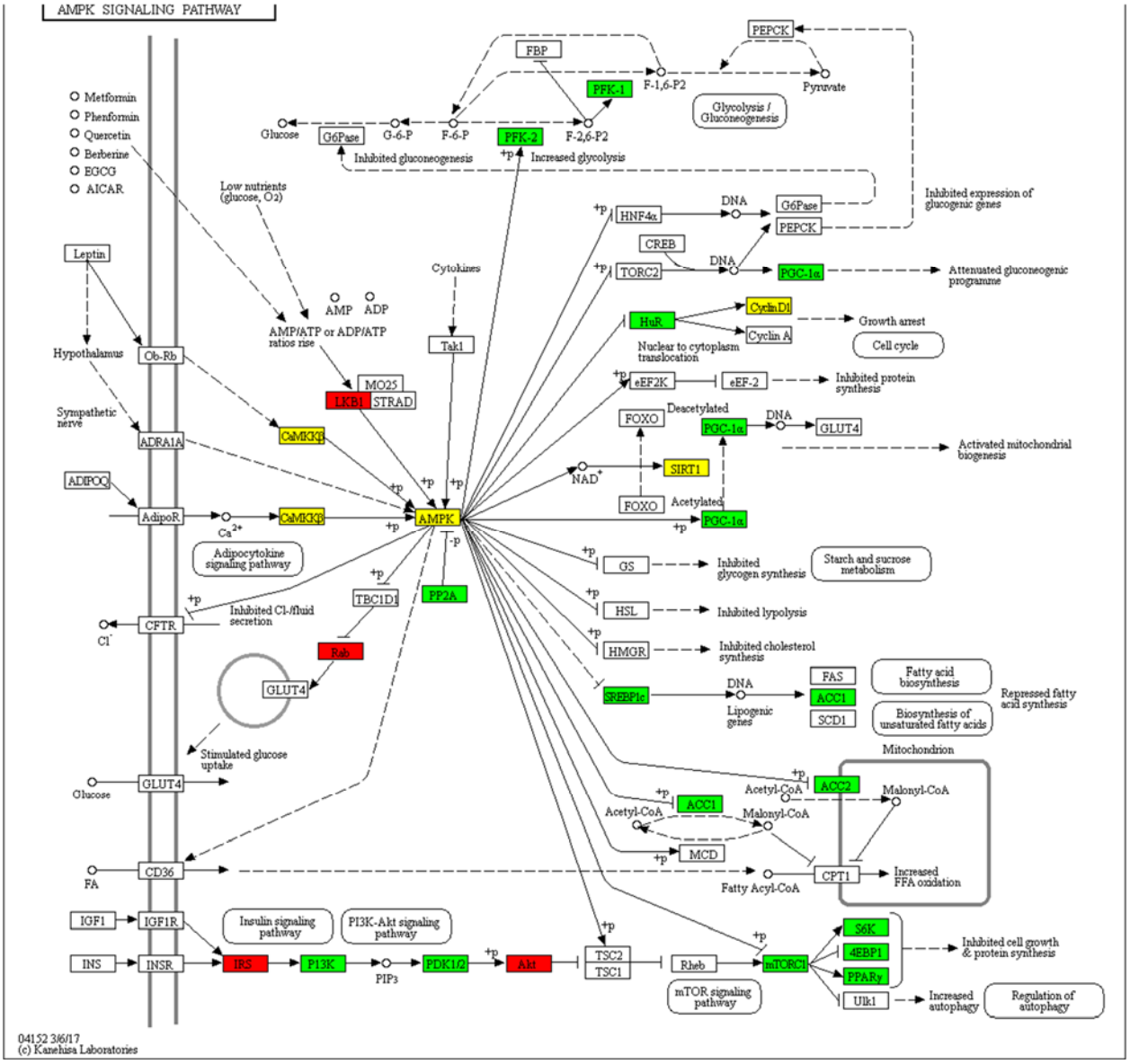

Figure 4: **Changes in AMPK signaling peptides at 2 hours post *Salmonella* infections.** Kinome peptide array analysis revealed significant changes in the AMPK signaling pathway unique to *S.* Enteritidis infected HD11 cells indicated by red compared to *S.* Heidelberg infected HD11 cells indicated by yellow. Changes common to both *S.* Enteritidis and *S.* Heidelberg are indicated in green.

4.1.4 Kinome Peptide Array Analysis *S*. Heidelberg 2 hours Post Infection.

Unlike the 30 minute time point, at 2 hours post-infection, PFK1 and PFK2 were activated (phosphorylated at their activating phosphosite) in *S*. Heidelberg infected cells, indicating a switch to glycolysis. AMPK was phosphorylated at an inhibition site. Sirt1 was phosphorylated on S27 (Table 7) (known to be involved in intracellular localization and enzymatic activities during oxidative stress (114, 115, 162)). The decreased phosphorylation of SREBP1 (Table 7) suggested that transcription of fatty acid genes were not being inhibited. A slight induction of fatty acid synthesis occurred as ACC1 inhibition was reduced via the decreased phosphorylation of S80 (Table 7) (144) but ACC2 was completely phosphorylated. This is supported by the metabolic data showing the sustained OCR readings past 2 hours *S*. Heidelberg infections (Figure 10). Because ACC1&2 also play a role in cell survival, the change in phosphorylation of these proteins could also highlight the viability of the cells at this time. PI3K had four sites (T607, Y962, S1039, Y556) less phosphorylated (Table 2) and two (Y425, Y605) phosphorylated (Table 2). PDK had one site (Y376) phosphorylated and one site (S241) less phosphorylated (Table 2). Akt (T479) was less phosphorylated (Table 7). With TSC2 (T268) less phosphorylated (Table 2) and Akt less phosphorylated, mTORC1 which would presumably be inhibited by AMPK, was phosphorylated on the most commonly recognized active site S2448 (Table 7) (70, 71, 128). An mTOR inhibited protein, 4EBP1 was less phosphorylated on an inhibitory site (Table 2, 7) (145, 146). One S6K site (T412) was phosphorylated along with PPAR-gamma (downstream of mTORC1)

(Table 2, 7). This implies that the one phosphorylated site (S2448) of mTORC1 regulates S6k and PPAR gamma but not 4EBP1. The regulation of 4EBP1 may be due to the activity of one of mTORC1's four less phosphorylated sites (S2441, S2446, T706, S863) (Table 2) or another regulator of 4EBP1 (155). HUR (S221) and cyclin D1 (T286) are both phosphorylated (Table 2, 7) which may lead to cell growth arrest.

4.1.5 Kinome Peptide Array Analysis *S*. Enteritidis 6 Hours Post Infection.

PFK1 was considerably less phosphorylated on the four sites (S386, T211, S33, Y674) that were previously phosphorylated (Table 2). When PFK1 is turned off, the cell falls back into a low ATP high AMP state (149). This corresponds with the phosphorylation of AMPK and its related peptides on four sites (S182, S172, S600, S184) and less phosphorylated on three sites (S108, T211, S108) (Table 2, 5). Of the phosphorylated AMPK and AMPK related peptides, only S600's functions to induce enzyme activity for the suppression of apoptosis was known (150, 151). Of the less phosphorylated sites, S108 induces AMPK activity and T211 inhibits cell growth. CAMKK-beta, a calcium dependent protein kinase that phosphorylates and activates AMPK was also phosphorylated at S511 (Table 2) (152). Peptides of EEF2K were also phosphorylated and activated by AMPK on three sites (S78, S366, S398) (Table 2), to inhibit protein synthesis, further highlighting the energetic state of the cell (153). The AMPK activated PGC-1 alpha was completely activated, with four sites (S62, T299, S266, T263 (Table 5)) phosphorylated (Table 2). Sirt1 T530 was less phosphorylated and S27 and S661 were both phosphorylated (Table 2, 5) to induce

activation of PGC-1 alpha (115). Since the data indicates AMPK and AMPK related peptides are activated, sites S182, S172 and S184 may be catalytic inducers of AMPK activity. PP2a known to have inhibitory effects on AMPK had two sites (Y307, S75) (124, 154) less phosphorylated (Table 2), one of which is an inhibitory site (154). The function of S75 remains unknown therefore PP2a activity on AMPK cannot be determined. PI3K, which is responsible for the production of PIP3 to activate Akt (138, 142), had six less phosphorylated sites and three more phosphorylated sites (Table 2). The validity of these sites is yet to be established due to high-throughput sequence-based discovery methods. Also the functions of the less phosphorylated sites are unknown and two of the phosphorylated sites function is to induce enzymatic activity (142). Akt in *S*. Enteritidis 6 hours had two site phosphorylated (Table 2) however, one of the dual phosphorylation sites remain less phosphorylated. TSC2, the mTORC1 inhibitor had two sites phosphorylated (Table 2), thus inhibited presumably by Akt. Without TSC2 acting upon Rheb, mTOR is phosphorylated thus activated on four sites (S2448, S2481, S2446, S863) and less phosphorylated on one site (T706) (Table 2, 5). S6k had one site phosphorylated and two less phosphorylated (Table 2), even though the validity of these sites has not been proven by low throughput methods, researchers speculate that mTOR sites S2446 and S2448 are involved in the phosphorylation of S6K (128, 155). PDK might have further phosphorylated the S6K site as a result of its two phosphorylated sites (Y376, S241) (Table 2) that inhibits apoptosis (114, 116). Unlike *S*. Enteritidis 2 hours, SREBP1, the fatty acid gene transcription inhibitor was phosphorylated (Table 5) (139). HUR was phosphorylated

at S221 (Table 2) to activate Cyclin D1 via T286 (ubiquitous site) phosphorylation (Table 2). The T14 site of Cyclin D1, which inhibits enzymatic activity and helps regulate the cell cycle was less phosphorylated (164) (Table 5) indicating cell cycle progression.

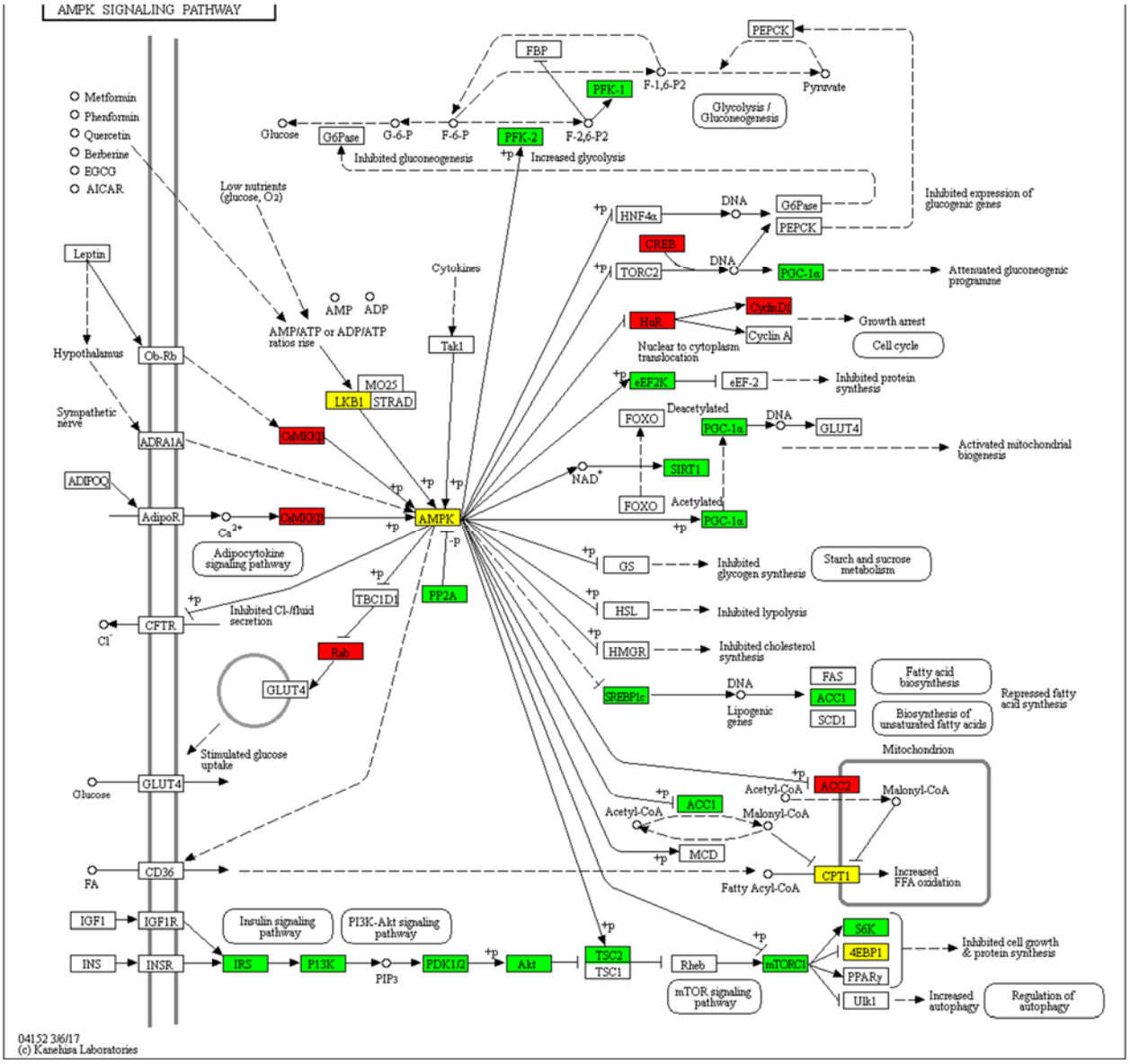

Figure 5: **Changes in AMPK signaling peptides at 6 hours post *Salmonella* infections.** Kinome peptide array analysis revealed significant changes in the AMPK signaling pathway unique to *S.* Enteritidis infected HD11 cells indicated by red compared to *S.* Heidelberg infected HD11 cells indicated by yellow. Changes common to both *S.* Enteritidis and *S.* Heidelberg are indicated in green.

4.1.6 Kinome Peptide Array Analysis *S*. Heidelberg 6 hours Post Infection.

At 6 hours post-infection PFK1 was significantly less phosphorylated in both *S*. Enteritidis and *S*. Heidelberg infected cells compared to their controls, indicating less activation (Table 2, Figure 5). Peptides of PFK2 were phosphorylated due to *S*. Heidelberg infection at 6 hours only (Table 2, Figure 5). This was an indication of an increase in energy production by the cells, that is, glycolysis, fatty acid oxidation and more. This interpretation was based on the phosphorylation of PGC-1, EEF2K, ACC1 (S1263, S80), PDK (S241, Y376), Akt, TSC2, mTORc1 (S2448, S2446, S2481, S863), S6K (S221, Y707, S369) and the decreased phosphorylation of PFK1 (table 2). PP2A had three less phosphorylated sites (S75, S60, Y307) and one phosphorylated site (S573) (Table 2). The activities of these PP2A sites is yet to be understood because there were more AMPK and AMPK related peptides less phosphorylated (T165,T211, S108, S496) then there were more phosphorylated (S182, S600) (Table 2). However, the activation state of AMPK remains unknown due to the phosphorylation of AMPK regulated peptides including PFK2, SIRT1, PGC-1 alpha, SREBP1 and ACC1. The kinome peptide array data suggested that *S*. Heidelberg infected cells at 6 hours post-infection induced fatty acid oxidation per the activation of CPT1, an important rate-limiting enzyme in the initiation of fatty acid oxidation in the mitochondria of a cell (64). CPT1 is inhibited by malonyl-CoA (64, 65). ACC1 and ACC2, which are important for malonyl-CoA production (a precursor for fatty acid synthesis) (64, 65) were both phosphorylated on their active sites in *S*. Heidelberg infected cells at 30 minutes post-infection. While at 2 hours post-infection there was

less phosphorylation of ACC1 on a site responsible for intracellular localization (Table 2). According to the literature, phosphorylation of ACC1 and ACC2 inhibits their function in the conversion of acetyl CoA to malonyl-CoA (89) which was also an indication of the change in energy demand of the infected cells compared to control.

4.2 *S.* Enteritidis and *S.* Heidelberg induce differential metabolic states.

To determine changes in the metabolic states of HD11 cells during *S.* Enteritidis or *S.* Heidelberg infections, a 2-hour seahorse metabolic flux assay was performed on *S.* Enteritidis and *S.* Heidelberg infected HD11 cells with gentamicin treatments. The assay showed differences in ECAR measurements for *S.* Enteritidis and *S.* Heidelberg infected cells from 20 minutes to 2 hours (Figure 6). OCR measurements were also noticeably different for *S.* Enteritidis and *S.* Heidelberg infected HD11 cells (Figure 6). These results indicate a differential metabolic response of HD11 cells to *S.* Enteritidis and *S.* Heidelberg infections.

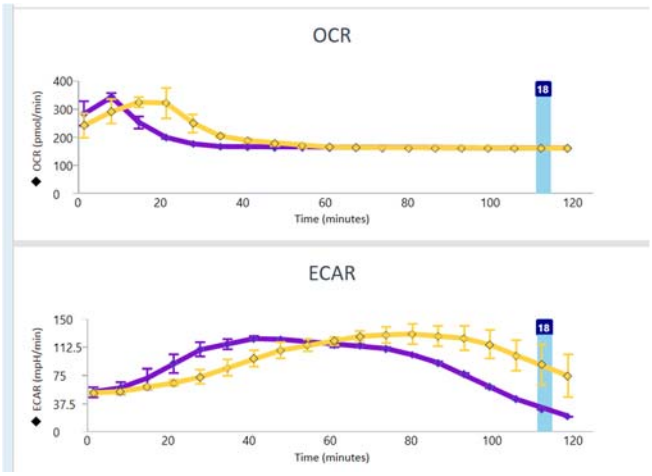

Figure 6: Metabolic differences between *S*. Enteritidis and *S*. Heidelberg infected HD11 cells. This graph shows the difference in OCR readings (top) and ECAR readings (bottom) between *S*. Enteritidis infected HD11 cells (purple lines) compared with *S*. Heidelberg infected HD11 cells (yellow lines) from the seahorse metabolic flux analysis. The cells were infected with the respective serovars of *Salmonella* and then treated with gentamicin in the seahorse media containing glucose.

4.2.1 *S*. Enteritidis infection induces an early increase in glucose metabolism

To determine the magnitude of metabolic differentiation *S*. Enteritidis induces in host cells at 30 minutes and 2 hours post-infection, a gentamicin free seahorse metabolic flux assay was performed on *S*. Enteritidis infected HD11 cells compared to control over 6 hours. *S*. Enteritidis infected cells at 30 minutes post-infection showed an increase in ECAR (15.365 mpH/min) followed by a drastic decrease (3.5 mpH/min) at 2 hours post-infection (Figure 7). There was also an increase in ECAR in cells infected with *S*. Enteritidis at 30 minutes compared to control (5.77 mpH/min). ECAR measurements indicated the rate of glycolysis, thus *S*. Enteritidis at 30 minutes post-infection increases glucose metabolism.

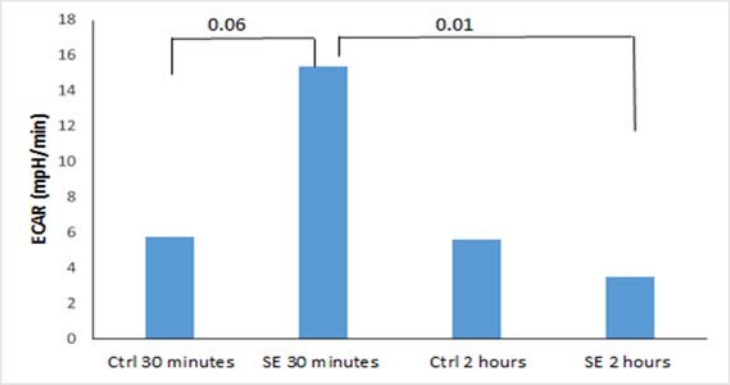

Figure 7: Difference in glucose metabolism in *S.* Enteritidis infected HD11 cells and uninfected HD11 cells. This graph shows the difference in ECAR readings between *S.* Enteritidis (SE) infected HD11 cells compared to uninfected HD11 cells from the seahorse metabolic flux analysis. Before running the assay, the cells plated in a mini culture plate were incubated in a CO_2 free incubator for at least 30 minutes upon the addition of glucose free media. After incubation, *S.* Enteritidis was added to the respective wells and the assay was started. An ANOVA significance of $P \leq 0.05$ was observed. Group comparisons were performed using the Tukey-Kramer test, p-values are shown at the top of the Figure.

4.2.2 Early *S.* Heidelberg infection reduces glucose metabolism.

To determine the magnitude of differentiation *S.* Heidelberg induced in host cells at 30 minutes and 2 hours post-infection, a seahorse metabolic flux assay without gentamicin was performed on *S.* Heidelberg infected HD11 cells compared to control over 6 hours. Results showed a decrease in ECAR of *S.* Heidelberg infected cells at 30 minutes post infection (-4.41 mpH/min) compared to control (5.77 mpH/min), p-value of 0.02 (Figure 8). At 2 hours post-infection, although not significant per Tukey-Kramer analysis, there was a numerical increase in ECAR readings of *S.* Heidelberg infected cells (4.31 mpH/min) compared to the 30 minutes results (Figure 8). Thus, *S.*

Heidelberg at 30 minutes post-infection induces a decrease in glucose metabolism in HD11 cells.

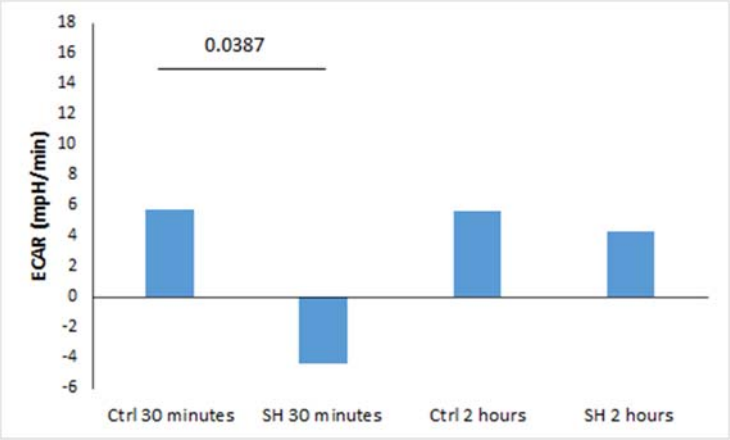

Figure 8: Difference in glucose metabolism in *S.* Heidelberg infected HD11 cells and uninfected HD11 cells. ECAR readings of *S.* Heidelberg (SH) infected HD11 cells compared to uninfected HD11 cells from the seahorse metabolic flux analysis. Before running the assay, the cells plated in a mini culture plate were incubated in a CO_2 free incubator for at least 30 minutes upon the addition of glucose free media. After incubation, *S.* Heidelberg was added to the respective wells and the assay was started. Significant P-values are indicated at the top of each bar. $P \leq 0.05$ observed using Tukey-Kramer statistical tests following ANOVA.

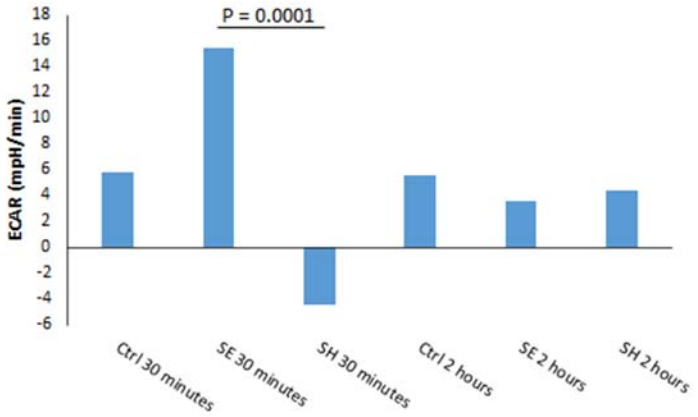

Figure 9: Difference in glucose metabolism between *S.* Enteritidis infected, *S.* Heidelberg infected and uninfected HD11 cells. ECAR readings of *S.* Enteritidis and *S.* Heidelberg infected HD11 cells compared to uninfected HD11 cells from the seahorse metabolic flux analysis. Before running the assay, the cells plated in a mini culture plate were incubated in a CO_2 free incubator for at least 30 minutes upon the addition of glucose free media. After incubation, *S.* Enteritidis or *S.* Heidelberg was added to the respective wells and the assay was started. Significant P-values are indicated at the top of each bar. $P \leq 0.05$ observed using Tukey-Kramer statistical tests following ANOVA.

4.2.3 *Salmonella* infections induce increased oxygen metabolism in HD11 cells

OCR measurements indicating the oxygen consumption of the HD11 cells showed an increase in OCR in cells infected with *S.* Enteritidis (164.525 pmol/min) or *S.* Heidelberg (164.19 pmol/min) at 30 minutes compared to control (56.44 pmol/min) (Figure 10). This increase in OCR was sustained passed the 2 hour time points with *S.* Enteritidis infected cells OCR being 165 pmol/min and *S.* Heidelberg infected cells being 165 pmol/min and control cells remaining relatively low at 51.83 pmol/min (Figure 10). These measurements comparing OCR of infected cells to control showed statistical significance at both time points ($p \leq 0.0001$).

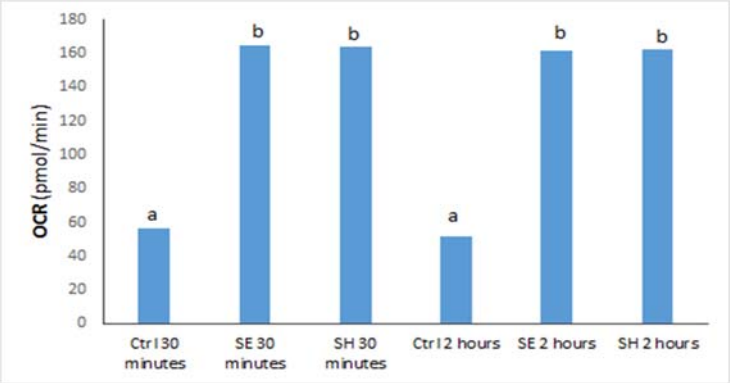

Figure 10: Oxygen consumption in HD11 cells infected with *S*. Enteritidis, *S*. Heidelberg, or cells alone. Before running the assay, the cells plated in a mini culture plate were incubated in a CO_2 free incubator for at least 30 minutes upon the addition of glucose free media. After incubation, *S*. Enteritidis and *S*. Heidelberg were added to the respective wells and the assay was started. Bars with the same letters on the top are not significantly different from each other. Tukey-Kramer significance; P ≤0.0001.

4.3 Rapamycin inhibits mTOR and MHY1485 indirectly activates mTOR in HD11 cells

The kinome peptide array data showed changes in mTORC1 activity in HD11 cells infection with both strains at different time points (Figure 2, Figure 4). To determine the role of mTOR in *Salmonella* infections, the mTOR inhibitor rapamycin and the mTOR activator MHY1485 were used. To test the effect of rapamycin treatment, HD11 cells were treated with 100 ng/mL of rapamycin and a kinome peptide array analysis was performed. The kinome peptide array results showed that mTOR was significantly less phosphorylated in rapamycin treated groups compared to control (Figure 11). This is evidence that rapamycin actively inhibits mTOR. To test

the effect of MHY1485, HD11 cells were treated with 2 µm of the MHY1485 compound and plated in 12 well plates including control and rapamycin treated groups. 5 hours later, the cells were harvested and counted using a hemocytometer. The results of the count showed that MHY1485 treated cells had a significant increased (with p-value less than 0.005) cell number compared to control and rapamycin treated cells (Figure 12). This was evidence that the activation of mTOR by increased cell growth and viability (129).

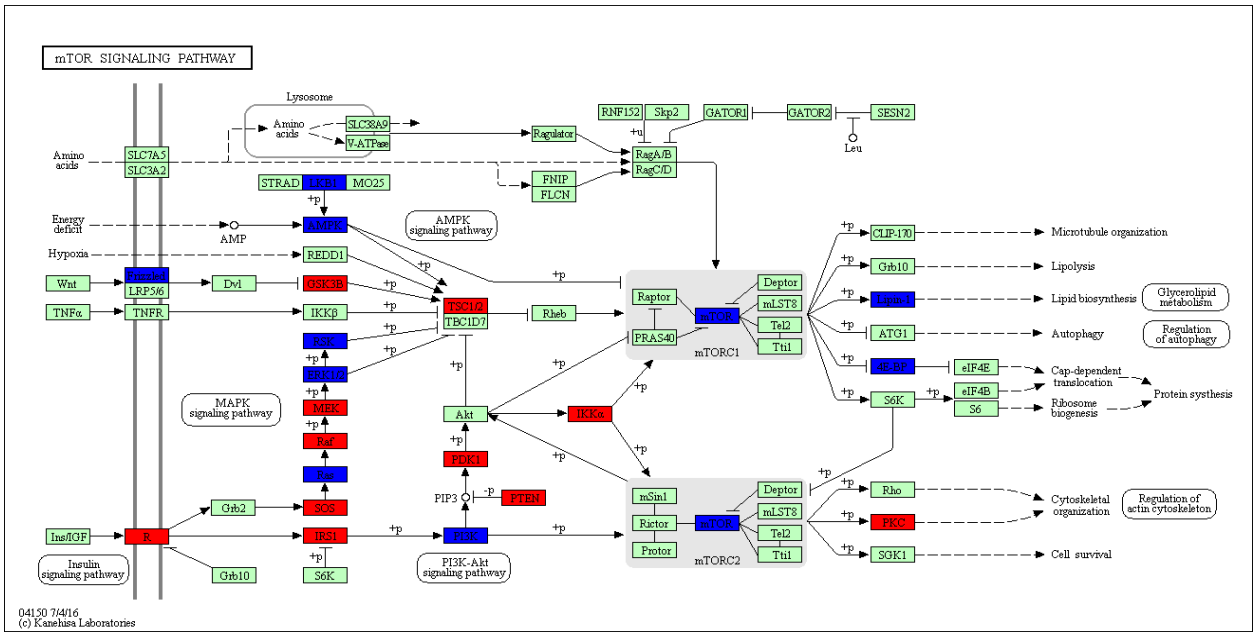

Figure 11: Decreased phosphorylation of mTOR due to rapamycin. Kinome peptide array analysis was performed on HD11 cells treated with rapamycin. The Figure shows proteins of the mTOR signaling pathway. Peptides more phosphorylated than control are highlighted in red boxes (TSC1/2), peptides less phosphorylated than control are highlighted in blue boxes (e.g mTOR)

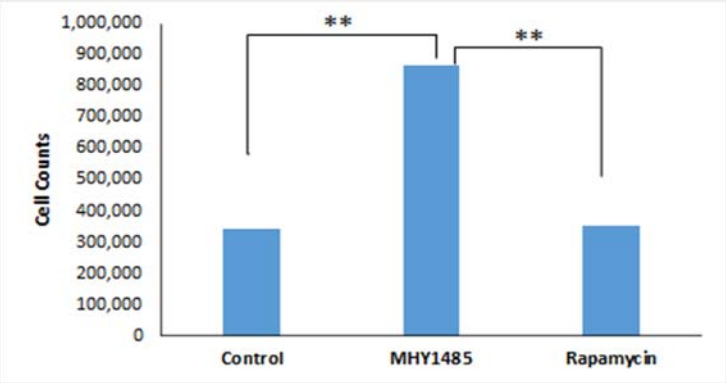

Figure 12: Increase cell growth due to MHY1485 activity. Half a million HD11 cells were treated with MHY1485 or rapamycin along with a control group. After 10 hours of incubation in treatments, the cells were counted. Statistical significance observed using student's T-tests. P-value ≤0.005 represented by **.

4.4 The action of mTOR in *Salmonella* infected cells is not glycolysis dependent.

To examine the metabolic effects of rapamycin and MHY1485 treatments on *Salmonella* infected HD11 cells, uninfected cells were plated in seahorse media containing the mTOR targeted treatments respectively before infection with *S.* Enteritidis or *S.* Heidelberg. ECAR results showed that there were no statistically significant difference between treated and untreated infections (Figure 13).

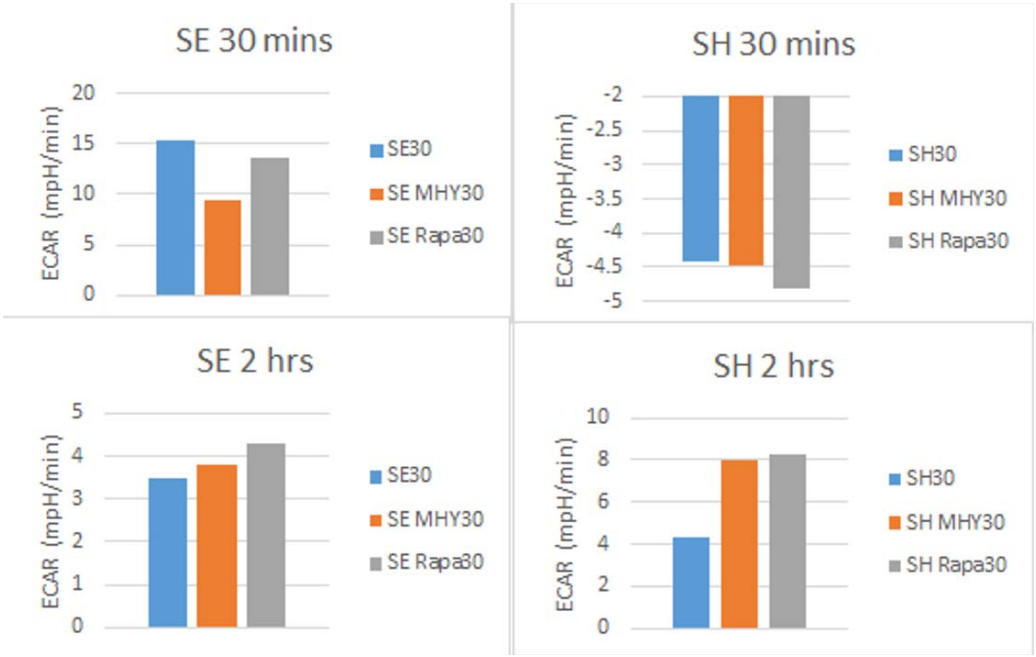

Figure 13: Difference in glucose metabolism between *S.* Enteritidis and *S.* Heidelberg infected HD11 cells treated with MHY1485 or rapamycin treatment. ECAR readings between MHY1485 and rapamycin treated HD11 cells with *S.* Enteritidis (SE) or *S.* Heidelberg (SH) infection. Before running the assay, the cells plated in a mini culture plate were incubated in a CO_2 free incubator for at least 30 minutes upon the addition of glucose free media containing rapamycin or MHY1485. After incubation, *S.* Enteritidis or *S.* Heidelberg was added to the respective wells and the assay was started. No statistical significance was found between treated and untreated at a p-value ≤0.05.

4.5 *S.* Enteritidis is more invasive than *S.* Heidelberg.

Gentamicin protection assays were performed to quantify *S.* Enteritidis' and *S.* Heidelberg's ability to invade HD11 cells respectively at 30 minutes and 2 hours post infection. Results of the gentamicin protection assays showed that there was a significant increase in *S.* Enteritidis compared to *S.* Heidelberg at 30 minutes post infection (Figure 14). While at 2 hours post infection, *S.* Enteritidis plate counts were

higher than *S*. Heidelberg with a p-value of 0.053 (Figure 15). The overnight colony counts for *S*. Enteritidis at 30 minutes was $37.44x10^4$ while *S*. Heidelberg at 30 minutes was $17.44x10^4$, with a p-value of 0.0081. Thus, *S*. Enteritidis is exceptional at invading HD11 cells than *S*. Heidelberg at 30 minutes post infection. There was a trend observed at 2 hours post *S*. Enteritidis infection only ($19x10^4$), showing an increase in plate counts in *S*. Enteritidis infection with rapamycin treatment ($24x10^4$) and a decrease in *S*. Enteritidis with MHY1485 treatment ($12x10^4$) (Figure 15), the statistical analysis for these plate counts showed no significant difference between *S*. Enteritidis and treatment groups at 2 hours post infection.

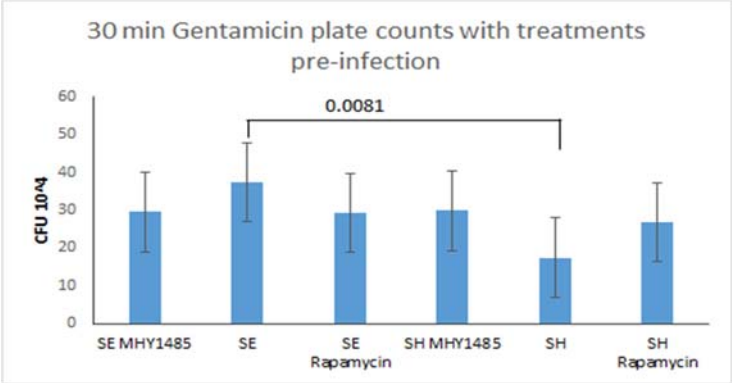

Figure 14: Invasiveness of *S*. Enteritidis (SE) and *S*. Heidelberg (SH) in HD11 macrophages at 30 minutes post-infection. Each bar in this graph represents the average colony count of respective strains of *Salmonella* that infected HD11 cells treated with or without MHY1485 or rapamycin before 30 minute gentamicin protection assay. P-value indicated on graph. $P \leq 0.05$ observed using ANOVA and Tukey Kramer statistical tests.

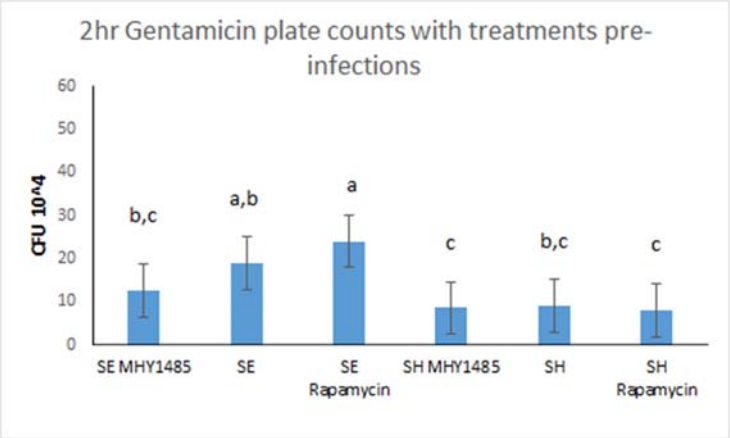

Figure 15: Invasiveness of *S.* Enteritidis (SE) and *S.* Heidelberg (SH) in HD11 macrophages at 2 hours post-infection. Each bar in this graph represents the average colony count of respective strains of *Salmonella* that infected HD11 cells treated with or without MHY1485 or rapamycin before 1 hour gentamicin protection assay. Bars not connected by the same letter are significantly different. $P \leq 0.05$ observed using ANOVA and Tukey Kramer statistical tests. Note p-value between SE and SH is 0.053.

4.6 Validation of Kinome peptide array via western blot.

A Western blot of phosphorylated mTOR at site S2448 was performed on HD11 cells with 30 minutes post-*S.* Enteritidis and *S.* Heidelberg infections to further validate our interpretation of the kinome peptide array results. The results of the Western blot showed an increase in band intensity of HD11 cells without infection (ctrl) compared to the band intensity from *S.* Enteritidis or *S.* Heidelberg infected cells.

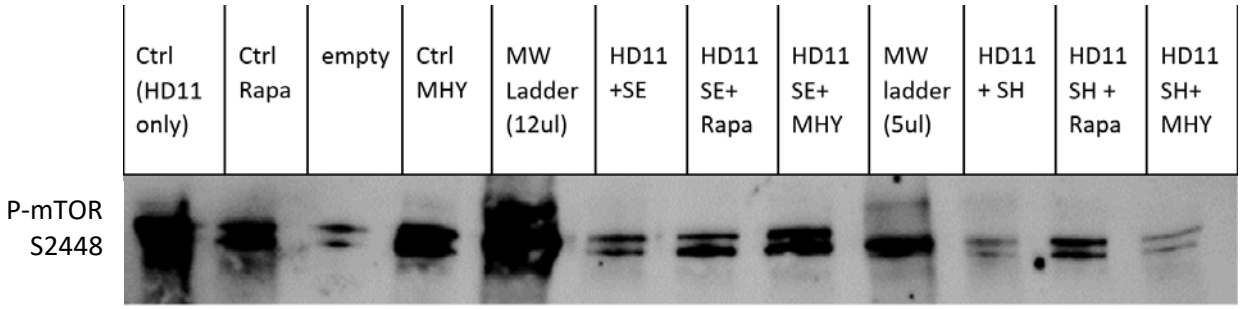

Figure 16: Western blot analysis of mTOR S2448 in HD11 macrophages. Each band denotes P-mTOR S2448. 25-40 µg of protein isolated from HD11 macrophages pre-treated with MHY1485 and rapamycin before 30 minutes *S*. Enteritidis (SE) or *S*. Heidelberg (SH) infection followed by a 1 hour gentamicin treatment was loaded onto gel. Note: Double bands indicate post translation modification of the proteins in the sample. P: phosphorylated

4.7 Early *S*. Enteritidis Infection Induces Increased Cell Death

The kinome peptide array results showed significant changes in the phosphorylation of apoptotic, cell death and cell survival proteins at 30 minutes and 2 hours post-*Salmonella* infections in HD11 cells. To validate the changes observed in the phosphorylation and signaling of these proteins at 30 minutes post-*S*. Enteritidis and *S*. Heidelberg infections, flow cytometry of HD11 cells was performed using a dead cell apoptosis kit with annexin V and propidium iodide (PI) stains. Annexin V binds to phosphatidylserine on the outer leaflet of cells undergoing apoptosis (108) while PI stains nucleic acid within permeated cells (109). Together these two mark apoptotic cells, necrotic cells, or both thus, they are used to measure cell death (96, 110). Analysis of the flow cytometry data using De Novo Software (111), revealed the averaged population of dead cells primarily due to apoptosis, that is, with higher

fluorescence intensity for both annexin V and PI was 38.69% for *S*. Enteritidis and 17.18% for *S*. Heidelberg after 1.5 hours of infection. On the other hand, 80.44% of *S*. Heidelberg and 58.64% of *S*. Enteritidis infected cells were live indicated by lower uptake of PI and annexin. Together, the results indicate that early *S*. Enteritidis infection induces increased cell death compared to *S*. Heidelberg.

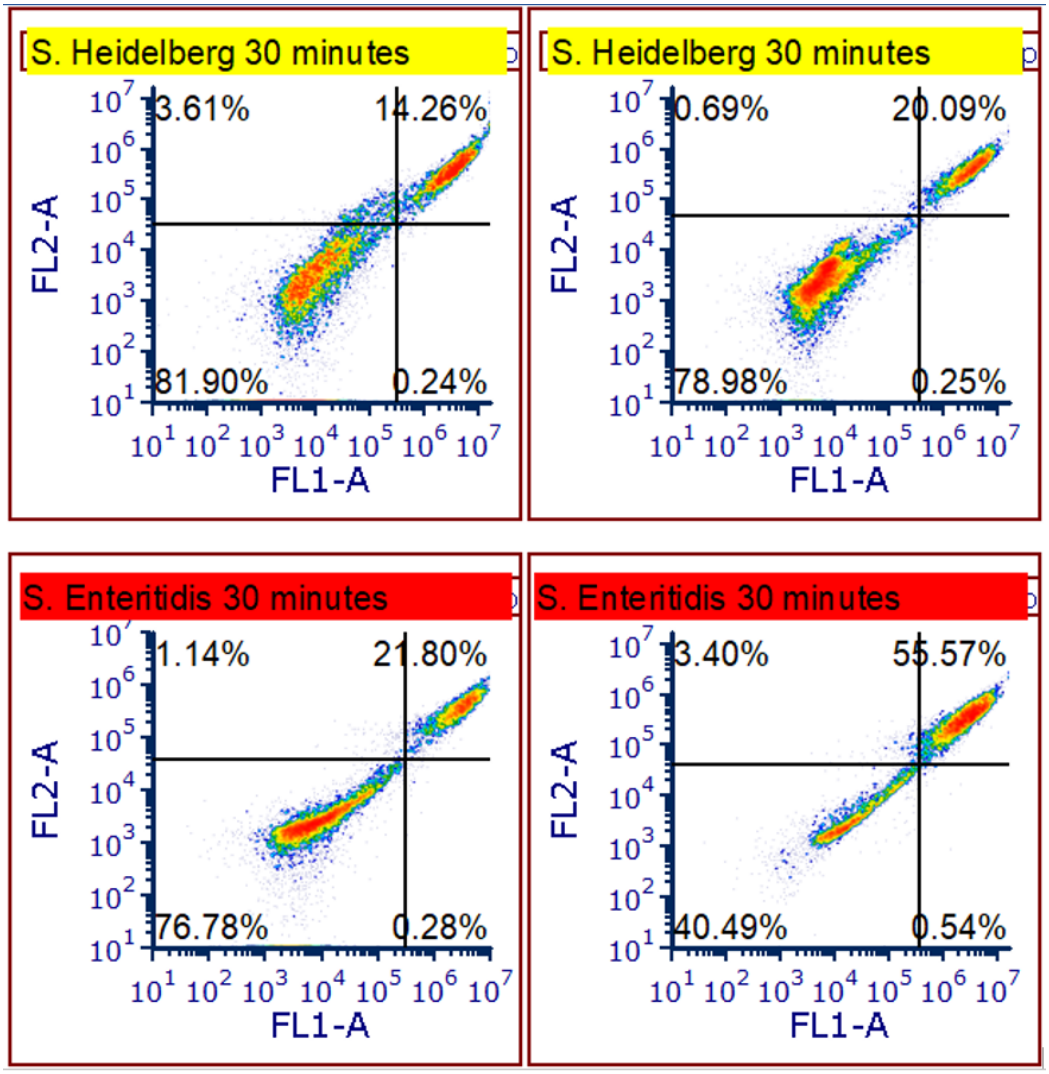

Figure 17: Flow cytometry of *S.* Heidelberg and *S.* Enteritidis infected HD11 cells 30 minutes post infection. Each plot represents the fluorescence intensity of annexin V (FL1-A) against PI (FL2-A) to characterize cell populations as dead or apoptotic in each sample. The plots are further divided into four main quadrants, live (lower left), necrotic only (upper left), apoptotic only (lower right) and dead/apoptotic (upper right) to determine the population of cells.

Chapter 5

DISCUSSION

S. Enteritidis and *S*. Heidelberg were chosen for this study because of their high prevalence and isolation rates in poultry (4, 28, 29, 130). These bacteria along with many other *Salmonella* serotypes are capable of surviving in host macrophages and can manipulate the host innate defenses to promote its survival (40, 76). In chickens, they infect host cells without eliciting any obvious symptoms of disease. This is a major public health concern because *Salmonellae* bacteria can be transmitted from animals to humans and because infected livestock do not show symptoms of infection (77), these infections can go undetected. In many countries including the US, the use of antibiotics in livestock production has stopped due to restrictions on antibiotic use or consumer preferences and concerns (78). Also, many *Salmonella* strains have developed resistance to major drugs used to combat S*almonella* infections (77, 78). These factors have made the production of healthy food animals more difficult. Hence, there is a need to understand the infectious mechanisms of *Salmonella*.

Using the HD11 chicken macrophage-like cell line, we aimed to determine the intracellular changes *Salmonella* induces in host cells, by focusing on how *S*. Enteritidis and *S*. Heidelberg affect the immunometabolic status of phosphorylated peptides. A kinome peptide array analysis was performed on *S*. Enteritidis and *S*. Heidelberg infected HD11 cells to determine the activities of kinases in the cell.

5.1 Overview of the kinome peptide array data of HD11 cells

The chicken-specific kinome peptide arrays were designed by using orthologous sequences found in human proteome databases (57, 58, 70). For data analysis, the human identifiers were used as inputs so they would be recognized in online databases and we could take advantage of the substantial functional annotation available from human sources. The peptides discussed here are from human and mouse sequences orthologous to chickens, and are inferred to have similar function in these species based on genomic and proteomic sequence similarities. Appendix 1 shows the UniProt numbers and phosphorylation sites of many immunometabolic peptides in human/mouse and their orthologs in chickens. In addition, the chicken site for some important peptides in the discussion are available in Table 3-8.

From a list of immunometabolic pathways obtained from STRING (90), the AMPK, mTOR complex 1 and insulin signaling pathways appeared most significant. Therefore, the phosphorylation sites of human peptides orthologous to chicken sites involved in the above mentioned pathways were further analyzed using KEGG mapper color and search pathway (90), Uniprot (93-95) and PhosphoSitePlus (89). Using these databases and the fold changes from PIIKA2 (91) the activating phosphosites of most of the proteins in the above mentioned pathways were determined with a central focus on the AMPK-mTORC1 signaling pathway. A negative fold change and p-value less than 0.05 indicated the peptides were significantly less phosphorylated than in control cells while a positive fold change with a significant p-value indicated that the peptides

of the infected cells were more phosphorylated than control. Using the information made available on different databases and in the literature (89-91, 93-95), the activation states of the many peptides in the data set was determined. Analysis of the kinome peptide array data using the process described above provided a better understanding of phosphorylation events at the three time points for both strains (Table 1, Appendix). Note that the peptides discussed in this section has been referenced in the results.

5.1.1 *S.* Enteritidis at 30 minutes post infection alters host AMPK-mTORC1 signaling cascade

The kinome peptide array results of HD11 cells at 30 minutes *S.* Enteritidis infections showed the increase phosphorylation of AMPK on its active site, indicating increased activity of AMPK. This increased activity of AMPK indicates a decrease in energy availability or decrease in the ratio of ATP to ADP/AMP (99). Since the HD11 cells were in a low energy state due to *S.* Enteritidis infection, increased glucose metabolism was being used to restore the energy level. This is supported by the phosphorylation of key glycolytic enzymes, hexokinase and PFK2, on their activity inducing sites (Table 3). The phosphorylation of SREBP1 and ACC1 to inhibit fatty acid synthesis and the increased phosphorylation of CREB on its activity inducing site supports that energy metabolism is being restored (Table 3). Results from the metabolic assays further supports that there is an increase in glycolytic activities and

oxygen metabolism of these cells (Figure 7, 10). With these supporting evidences, it was confirmed that *S*. Enteritidis infection induces increase in glycolytic activities common to M1 macrophages as early as 30 minutes post infection.

The kinome peptide array results also showed a decrease in the phosphorylation of mTOR S2448 (Table 3) consistent with the decrease in Akt phosphorylation. Since mTOR is involved in the regulation of immune proteins involved in immune responses (71), and the activity of mTOR was decreased via S2448, this suggests that *S*. Enteritidis infection lessens the activity of mTOR to decrease the synthesis of proteins that strengthens immune responses. However, there was another activity inducing site of mTOR that was significantly more phosphorylated than control. This site was S863 (Table 3). Active mTORc1 phosphorylates 4EBP1 to promote protein synthesis (69, 70). This is consistent with the kinome peptide array data as 4EBP1 was phosphorylated on an inhibitory phosphosite (Table 3). With this information, the action of mTORc1 during *S*. Enteritidis infection of HD11 cells cannot be predicted.

Table 3: Phosphorylation status of some important peptides in the *S*. Enteritidis 30 minutes post infection kinome array data along with their known functions.

Protein	**Chicken Site**	**Human Site**	**Site Function**	**Phosphorylation Status**
PFK2	S462	S466	Increase Glycolysis	Increased
Hexokinase	Y304	Y301	Glycolysis	Increase
ACC1	S80	S80	Inhibits apoptosis, Induce autophagy	Increased

Sirt1	T388	T530	activation/acetylation-oxidative stress	Decreased
CREB	S119	S133	Inhibits apoptosis, Induce cell growth	Increased
mTOR	S864	S863	Activates mTOR	Increased
mTORc1	S2352	S2448	Activates mTOR	Decreased
4EBP1	T38	T37	Inhibition of transcription	Increased
AMPK	T185	T183	Activates AMPK	Increased
SREBP1	S114	S338	Inhibit transcription of fatty acid genes	Increased
Akt	T74	T308	Inhibits apoptosis, promotes growth	Decreased

5.1.2 *S.* Enteritidis at 2 hours post infection alters host AMPK-mTORC1 signaling cascade

The state of the peptides in cells infected with *S*. Enteritidis for 2 hours suggested that cell survival was being challenged (Table 2, 4, Figure 4) due to the decrease in phosphorylation of inhibitors of apoptosis. The data also suggested a decrease in glycolytic activities. Despite the substantial phosphorylation of PFK1 (S386, Y651, Y674) and PFK2 (S461, Y366) (Table 2), hexokinase was significantly less phosphorylated than control at 2 hours post *S*. Enteritidis infection on a site that induces enzymatic activity (Table 4). Hexokinase is the first rate limiting enzyme of glycolysis (135). Therefore, a decrease in hexokinase activity indicates a decrease in glucose metabolism as indicated by the ECAR measurement at 2 hours post *S*. Enteritidis infection (Figure 7). To add on, proteins involved in the regulation of oxygen metabolism and inhibition of fatty acid synthesis were also significantly less phosphorylated than control. These proteins include CREB, SREBP1, ACC1 and PGC1-alpha (Table 4). Cells undergo fatty acid oxidation to produce energy (125),

increase in fatty acid synthesis suggests a decrease in fatty acid oxidation, thus decrease in energy production. The decreased phosphorylation of these metabolic proteins on their activity inducing sites indicates a decrease in energy production at 2 hours post *S*. Enteritidis infection. This reduced energy production could be as a result of a decline energy demands as suggested in the kinome peptide array by the inactivity of AMPK kinases to phosphorylate their target peptides at 2 hours post *S*. Enteritidis infection. However, an AMPK related peptide, NuaK1 which acts as an energy sensor is more phosphorylated on a site that activates its energy sensor function (150) (Table 4). Unlike 30 minutes post *S*. Enteritidis infection, HD11 cells at 2 hours post infection showed a significant increase in mTOR S2448 phosphorylation and a subsequent increase in its downstream effector S6K (Table 4) which also promotes of cell growth and survival (70).

Table 4: Phosphorylation status of some important peptides in the *S*. Enteritidis 2 hours post infection kinome array data along with their known functions.

Protein	**Chicken Site**	**Human Site**	**Site Function**	**Phosphorylation Status**
CREB	S119	S133	Inhibit Apoptosis, Induce Cell Growth	Decreased
NuaK1	T204	T211	Energy sensor, inhibits cell growth	Increased
ACC1	S80	S80	Inhibits apoptosis, induce autophagy	Decreased
SREBP1	S114	S338	Inhibit transcription of fatty acid genes	Decreased
PGC1-alpha	T261	T263	Protein stabilization, oxidative stress	Decreased
PFK2	S462	S466	Increase glycolysis	Increased
Hexokinase	Y304	Y301	Glycolysis	Decreased
mTORc1	S864	S863	Activates raptor	Decreased

mTORc1	S2352	S2448	Activates mTOR	Increased
S6k	T421	T444	Cell cycle regulation	Increased
4EBP1	T38	T37	Inhibition of translation	Decreased
Akt	S476	S476	phosphorylation	Decreased

5.1.3 *S.* Enteritidis at 6 hours post infection alters host AMPK-mTORC1 signaling cascade

In 6 hour *S*. Enteritidis infected cells, only a few proteins remained in the same states as in 2 hour *S*. Enteritidis infected cells. These proteins include CREB, Rab, ACC2 and LKB1 (Table 2, Figure 5). Although phosphorylation of AMPK peptides by kinases was not detected, there was an increased in the phosphorylation of metabolic regulations including ACC1, SREBP1, PGC1-alpha and sirt1 (Table 5), an indication of increased oxygen metabolism and promotion of cell survival. Evidence of increase in cell growth and survival activities were also seen in the phosphorylation of mTORc1 on multiple sites, the phosphorylation of S6K and the inhibition of cyclin D1 T14, which inhibits cells cycle progression (164) (Table 5). However, the glucose metabolism of HD11 cells at 6 hours post *S*. Enteritidis infection was predicted to remain the same as the 2 hour time point because phosphosites of PFK1 were significantly less phosphorylated than control despite the increased phosphorylation of hexokinase (Table 5).

Table 5: Phosphorylation status of some important peptides in the *S*. Enteritidis 6 hours post infection kinome array data along with their known functions.

Protein	Chicken Site	Human Site	Site Function	Phosphorylation Status
CREB	S119	S133	Inhibit Apoptosis, Induce Cell Growth	Decreased
NuaK1	S593	S600	Energy sensor, inhibits cell growth	Increased
ACC1	S80	S80	Inhibits apoptosis, Induce autophagy	Increased
SREBP1	S114	S338	Inhibit transcription of fatty acid genes	Increased
PGC1-alpha	T261	T263	Protein stabilization, oxidative stress	Increased
Sirt1	S53	S27	Activate enzyme, oxidative stress	Increased
Hexokinase	Y304	Y301	Glycolysis	Increased
Cyclin D1	T14	T14	Inhibitory, cell cycle regulator	Decreased
mTORc1	S2352	S2448	Activates mTOR	Increased
S6k	S424	S447	Cell cycle regulation	Increased
Akt	T74	T308	Inhibits apoptosis	Decreased

5.1.4 *S.* Heidelberg at 30 minutes post infection alters host AMPK-mTORC1 signaling cascade

Unlike *S*. Enteritidis 30 minutes, *S*. Heidelberg infected cells at 30 minutes energy demand was not clearly revealed in the kinome peptide array analysis (Figure 2). Two important phosphosites of AMPK were significantly more phosphorylated than control. AMPK T183 functions to induce enzymatic activity (140) was significantly phosphorylated (Table 6) and AMPK S496 an inhibition site (156) was also significantly phosphorylated (Table 6). Usually, the phosphorylation of a protein on a site that has inhibitory effects on that protein indicates the inhibition of the entire

protein (165, 166). However, the phosphorylation of AMPK downstream effectors was not consistent with this interpretation (Table 2, Figure 2). For example, the AMPK activated PGC1-alpha (Table 6) and EEF2K (Table 2) were significantly phosphorylated on their active sites, suggesting that AMPK might be active. Furthermore, some enzymes involved in the regulation of energy metabolism were significantly less phosphorylated (PFK1 and Sirt1) while others were significantly more phosphorylated (CREB, SREBP1 and hexokinase). Therefore, the active state of AMPK and the energetic state of the cells cannot be predicted based of the kinome peptide array data alone. Fortunately, the energetic demands of *S*. Heidelberg infected cells were reflected in the ECAR results, which was lower than control at 30 minutes post infection (Figure 8). This suggests that phosphorylation of AMPK T183 did activate the enzyme's activity and that S496 may not regulate the entire protein function. Nonetheless, more evidence is needed to consider *S*. Heidelberg infected HD11 cells at 30 minutes post infection M1 macrophages based on these results. The kinome peptide array data indicated changes in phosphorylation and signaling events in infected cells compared to uninfected cells (Figure 2, Table 2), and the phosphorylation of CREB and cyclin D1 indicate inhibition of apoptosis (Table 6). Therefore *S*. Heidelberg at 30 minutes post infection induces major alterations in HD11 cells survival upon initial infection.

Table 6: Phosphorylation status of some important peptides in the *S*. Heidelberg 30 minutes post infection kinome array data along with their known functions.

Protein	Chicken Site	Human Site	Site Function	Phosphorylation Status
CREB	S119	S133	Inhibit Apoptosis, Induce Cell Growth	Increased
AMPK	T185	T183	Energy sensor, AMPK activator	Increased
AMPK	S496	S496	Inhibitory site	Increased
Sirt1	T388	T530	activation/acetylation-oxidative stress	Decreased
SREBP1	S114	S338	Inhibit transcription of fatty acid genes	Increased
4EBP1	T47	T46	Translation regulator	Decreased
Hexokinase	Y304	Y301	Glycolysis	Increased
PGC-1alpha	T272	T266	Protein stabilization, oxidative stress	Increased
Cyclin D1	T283	T286	cell cycle regulator	Increased
Akt	T74	T308	Inhibits apoptosis	Decreased

5.1.4.1 *S*. Heidelberg Relies on the Pentose Phosphate Shunt for Initial Invasion

In *S*. Heidelberg 30 minutes, one PFK1 site was shown to be significant, yet, this site was less phosphorylated than control while all PFK2 sites were non-significant in the data set (Table 2, Figure 2). In *S*. Heidelberg at 2 hours infection, both PFK1 and PFK2 were significantly more phosphorylated than control at multiple sites, however, only one phosphosite on PFK2 (site S466) was known to induce enzymatic activity. This led to the comparison of the *S*. Heidelberg 30 minutes and *S*. Heidelberg 2 hours glycolytic pathways. The comparison showed that glycolysis did occur at both time points, however, there were key glycolytic enzymes whose kinase activities were not detected by the kinome peptide array in *S*. Heidelberg 30 minutes

post infections (Figure 3). These enzymes included phosphoglucose isomerase, PFK and aldolase (Figure 3). However, the enzymes downstream were phosphorylated and activated, we hypothesize that the products of these enzymes (whose kinase activities were not detected) were made available via an alternative substrate provider. The pentose phosphate pathway is an alternative substrate provider for glycolysis. Specifically, undergoing the pentose phosphate pathway makes available fructose-6 phosphate and glyceraldehyde-3 phosphate (79), end products of the missing enzymes (Figure 3). Undergoing the pentose phosphate pathway also makes available NADPH, which serves as a cofactor for inducible nitric oxide synthase for the production of nitric oxide (NO) (79, 80). This hypothesis is supported in a publication by Haiqi et al. 2018, where there is a significant decrease in iNOS (Table 2) phosphorylation on its inhibitory site thus inducing its activity (45). The researchers also performed a nitrite assay and the results showed a gradual increase in nitrite concentration which is comparable to NO concentration in *S*. Heidelberg infected HD11 cells (45). NO plays an important role in the killing of pathogens in macrophages, therefore, it is an important component of HD11 cells immune response to *Salmonella*. It is known to induce the transcription of proinflammatory proteins and cytokines thus promoting inflammatory death of infected cells (81). On the other hand, nitrite can quickly isomerize to nitrate, which is produced by the immune system in response to *Salmonella* infection and can promote bacterial growth (40). Therefore, the bacteria benefits from this immune response.

5.1.5 *S.* Heidelberg at 2 hours post infection alters host AMPK-mTORC1 signaling cascade

S. Heidelberg at 2 hours post infection alters host AMPK-mTORC1 signaling cascade. Unlike *S.* Heidelberg 30 minutes, *S.* Heidelberg 2 hours post infection showed increased phosphorylation of PFK1 and PFK2 on their suspected active sites (Table 2, Table 7), along with the phosphorylation of hexokinase (Table 7), suggesting that glucose metabolism increased in the cell at 2 hours after *S.* Heidelberg infection. However, the significant increase in phosphorylation of AMPK S496 (Table 7) suggested the inhibition of AMPK, but as seen previously (Table 6), S496 may not regulate the entire protein. AMPK was phosphorylated on at least three other sites whose functions are unknown (Table 2). These three sites might be indicators of energy demand. This is supported by the ECAR results for *S.* Heidelberg at 2 hours post infection (Figure 8). Also, Camkk-beta (S511) that acts on AMPK positively was also phosphorylated (Table 2, Figure 4) (152). Moreover, ACC1 and SREBP1 which are negatively regulated by AMPK were significantly less phosphorylated and Sirt1 and PGC1-alpha which are positively regulated by AMPK were significantly more phosphorylated at 2 hours post *S.* Heidelberg infection. This strongly suggests that AMPK was active during this infection. mTOR S2448 was significantly more phosphorylated than control, so was its downstream counterpart S6K. The cascade of mTOR signaling along with the phosphorylation of an activity inducing peptide of cyclin D1 indicate increased protein synthesis and cell growth despite the decreased

phosphorylation of the apoptotic inhibitor ACC1 at *S*. Heidelberg 2 hours post infection.

Table 7: Phosphorylation status of some important peptides in the *S*. Heidelberg 2 hours post infection kinome array data along with their known functions.

Protein	Chicken Site	Human Site	Site Function	Phosphorylation Status
PFK2	S461	S466	Inhibit Apoptosis, Induce Cell Growth	Increased
ACC1	S80	S80	Inhibits apoptosis, Induce autophagy	Decreased
AMPK	S496	S496	Inhibitory site	Increased
Sirt1	S53	S27	activation/acetylation-oxidative stress	Increased
SREBP1	S114	S338	Inhibit transcription of fatty acid genes	Decreased
Hexokinase	Y304	Y301	Glycolysis	Increased
PGC-1alpha	T297	T299	Protein stabilization, oxidative stress	Increased
Cyclin D1	T283	T286	cell cycle regulator	Increased
Akt	T74	T308	Inhibits apoptosis	Decreased
S6K	T389	T412	Active, cell cycle and adhesion	Increased
4EBP1	T47	T46	Translation regulator	Decreased
mTORc1	S2352	S2448	Activates mTOR	Increased

5.1.6 *S.* Heidelberg at 6 hours post infection alters host AMPK-mTORC1 signaling cascade

The kinome peptide array data showed that *S*. Heidelberg infected cells at 6 hours were undergoing an increase in mitochondrial biogenesis; by increasing glycolytic activities (hexokinase and PFK2), fatty acid metabolism (ACC1, SREBP1 and PGC1-alpha as seen in table 8), and inhibiting protein synthesis by the decreased

the activity of S6K and the increased activity of 4EBP1 via decreased phosphorylation (Table 8, Figure 5). It was presumed that AMPK was active although it was significantly phosphorylated on its inhibitory site S496. The kinome peptide array data further suggested that *S*. Heidelberg infected cells at 6 hours post-infection induced fatty acid oxidation per the activation of CPT1, an important rate-limiting enzyme in the initiation of fatty acid oxidation (64). Nonetheless, this data indicates that the energy level of HD11 cells was being restored at 6 hours *S*. Heidelberg infection via increase in metabolic processes to produce ATP.

Table 8: Phosphorylation status of some important peptides in the *S*. Heidelberg 6 hours post infection kinome array data along with their known functions.

Protein	Chicken Site	Human Site	Site Function	Phosphorylation Status
ACC1	S80	S80	Inhibits apoptosis, Induce autophagy	Increased
AMPK	S496	S496	Inhibitory site	Decreased
Sirt1	T388	T530	activation/acetylation-oxidative stress	Decreased
SREBP1	S114	S338	Inhibit transcription of fatty acid genes	Increased
PGC-1alpha	T272	T266	Protein stabilization, oxidative stress	Increased
Akt	S476	S476	phosphorylation	Increased
S6K	T389	T412	Active, cell cycle and adhesion	Decreased
4EBP1	T38	T37	Blocks inhibition of translation	Decreased
mTORc1	S2352	S2448	Activates mTOR	Increased

5.2 TNF-alpha induced cell death validation via flow cytometry

The changes observed in the kinome array data was not limited to metabolism. There were also major changes in signaling of immune related peptides (Table 2).

Amongst these immune peptides were TNF-alpha and JNK1 activity. The presence of TNF-alpha in chickens has been recently confirmed (82) and TNF-alpha signaling during *Salmonella* infection has being validated in other species (107) Therefore, TNF-alpha signaling is anticipated in the kinome peptide array results of *Salmonella* infected chicken macrophage like cells. JNK1, which is activated by MAPK activities via the TNF alpha receptors was significantly more phosphorylated than control for *S*. Enteritidis at 30 minutes and *S*. Heidelberg at 2 hours post infection. All in all, the kinome peptide array suggests that due to the decrease in phosphorylation of key phosphorylation sites and inhibition of cell death inducing factors at 30 minutes post *S*. Heidelberg infections and an increased phosphorylation and activation of these factors in 30 minutes post *S*. Enteritidis infections, *S*. Enteritidis infection induced increased cell death compared to *S*. Heidelberg at 30 minutes post infection.

To validate these results, flow cytometry was carried out on HD11 cells at 30 minutes post infection with *S*. Enteritidis or *S*. Heidelberg using a dead cell apoptosis kit that contained FITC annexin V and PI as cell markers (96). Annexin V is a protein that binds phospholipids (96, 109). In flow cytometry, annexin is used for its high affinity with phosphatidylserine, a phospholipid found on the outer membrane of the cell during apoptosis (109). PI is a dye that binds to nucleic acids within a cell (108, 110). However, PI is not membrane permeable therefore, it should not stain live cells (109,110). Using De Novo Software (111), the flow cytometry data was gated to exclude debris and analyzed for dead and live cell populations. As expected, the flow

cytometry data showed an increased number of dead cells due to apoptosis in *S*. Enteritidis compared *S*. Heidelberg (Figure 17, Table 9).

The kinome data indicated a decrease in signaling via apoptotic peptides at 30 minutes post *S*. Heidelberg infection and an increase in *S*. Enteritidis 30 minutes post infection, and the flow cytometry supported these results by showing more cell death via dual (PI and annexin V) staining in *S*. Enteritidis at 30 minutes post infection compared to *S*. Heidelberg. In the flow cytometry results we did not observe annexin V stained cells that were not positive for PI. One possible reasons for this is that: Macrophages are known to phagocytose other macrophages, because HD11 are macrophages, they are capable of such. According to Bendall, L. J. and Green, D. R., when macrophages phagocytose other macrophages during early apoptosis, they cannot be detected by annexin V (109). This would explain the low/absence of apoptotic population (annexin V stain only). Despite the variable described above, we do see an increase in annexin V and PI binding in *S*. Enteritidis as compared to *S* Heidelberg at 30 minutes, in agreement with the peptide array kinome data.

Table 9: Average percentage of live cells compared to apoptotic/dead cells in a *S*. Enteritidis or *S*. Heidelberg infection at 30 minutes post infection.

	Live cells	**Dead/apoptotic cell population**
***S*. Enteritidis**	58.64%	38.69%

S. Heidelberg	80.44%	17.18%

5.3 The metabolic states of HD11 cells during *Salmonella* infection

Based on the changes in the phosphorylation states of glycolytic proteins (e.g PhK, HK, PFK1 and PFK2) Seahorse Xfp metabolic flux assays were performed to determine the metabolic effect of the two strains of *Salmonella* on HD11 macrophages by measuring the OCR and ECAR. Initially, a seahorse flux assay was performed on infected HD11 cells treated with gentamicin. This experiment was used as a baseline to determine noticeable immunometabolic differences between *S*. Enteritidis and *S*. Heidelberg infected cells, and between infected and control cells (Figure 6). The results showed that there were metabolic difference between *S*. Enteritidis and *S*. Heidelberg infected cells throughout the two-hour experiment. There were also significant differences between control cells and cells infected with *S*. Enteritidis or *S*. Heidelberg.

Based on this initial experiment, subsequent seahorse metabolic flux assays without gentamicin were performed to compare the metabolism of infected and controls cells at 30 minutes and 2 hours post infection. Comparing the metabolic states of the cells without gentamicin was important because it revealed the metabolic changes that occurred in HD11 cells during invasion at 30 minutes and 2 hours post infection to compliment the kinome peptide array data. Although the metabolic assay measures both ECAR and OCR, the majority of the analyses for this project focus on

ECAR measurements. Partly because OCR measure oxygen consumption due to oxidative phosphorylation; pyruvate and glutamine are substrates that promote oxidative phosphorylation. Therefore, cells are likely to consume more oxygen due to the presence of those substrates in the media. ECAR is the amount of hydrogen ions in the media due to the process of glycolysis (66), therefore, ECAR measurements represent glucose metabolism in the cell. Many studies have reported that increased glucose metabolism in the cell is indicative of stress and inflammation (51-54). Immunologists have also developed a system of distinguishing pro-inflammatory macrophages from anti-inflammatory macrophages (67, 68). Pro-inflammatory macrophages are identified as M1 macrophages and increased glucose metabolism is a key characteristic of these cells (54). Therefore, comparing the ECAR measurements of infected cells and to control is important to provide a better understanding of macrophage polarization and the immunometabolic effects of *S*. Enteritidis and *S*. Heidelberg *in vitro*.

After ANOVA and Tukey Kramer analyses, the results showed that *S*. Enteritidis infected cells at 30 minutes had an ECAR of 15.365 mpH/min with a dramatic decrease to 3.5 mpH/min at 2 hours (Figure 7). *S*. Enteritidis infected cells' ECAR at 30 minutes was significantly higher than ECAR at 2 hours meaning there was a significant decrease in glucose metabolism from 30 minutes to 2 hours (p-value of 0.01 Figure 7). These results were in agreement with the kinome peptide array data at 30 minutes, which indicated phosphorylation of AMPK, PhK and PFK 1 & 2,

further supporting that *S*. Enteritidis 30 minutes post infection increases glycolytic activity in HD11 macrophages.

On the other hand, *S*. Heidelberg infected cells ECAR at 30 minutes was -4.41 mpH/min with an increase to 4.31 mpH/min at 2 hours (Figure 8). The low ECAR readings at 30 minutes post *S*. Heidelberg infection agrees with the kinome peptide array data that showed a deactivation of PFK1 and the absence of PFK2 during *S*. Heidelberg infections (30 minutes post infection). However, the Tukey Kramer tests did not show a significant difference between *S*. Heidelberg 30 minutes post infection and *S*. Heidelberg 2 hours post infection. This, in conjunction with the kinome peptide array results, agree with the occurrence of glycolysis at 30 minutes post *S*. Heidelberg infection (without the activity of PFK1 and PFK2) is less than *S*. Heidelberg at 2 hours post infection (with the activity of PFK1 and PFK2).

Upon the comparison of *S*. Enteritidis and *S*. Heidelberg infected cells at both time points, the results showed that ECAR for *S*. Enteritidis at 30 minutes was significantly higher than *S*. Heidelberg at 30 minutes with a p-value less than 0.0001. Meanwhile, at 2 hours there was no statistical significant difference between control and infected cells or infected cells compared to each other (Figure 9). This is consistent with the activity of PFK1 and PFK2 as seen in the peptide array results. ECAR reading were statistically significant for *S*. Heidelberg at 30 minutes post infection compared to control with a p-value of 0.0387. *S*. Enteritidis at 30 minutes compared to control had a p-value of 0.0604. These results imply that there are

statistically significant differences between infected cells and uninfected cells at 30 minutes post infection at an alpha of 0.07. All infections at 2 hours were not statistically significant from control.

It is important to note that OCR measurements for both *S*. Enteritidis and *S*. Heidelberg remained fairly consistent between the 30 minute and 2 hour time points. Interestingly, the control showed a significant decrease OCR during the 30 minute and 2 hour time points (Figure 10). The increase in OCR of infected cells compared to control was possibly due to the production of ROS. There were also many changes in oxidative stress regulators including Sirt1, NFkB, PGC 1alpha, CREB, NADPH oxidase and more seen in the kinome peptide array data. However, more metabolic experiments are required to conclude that *Salmonella* induces oxidative stress in host cells.

Based on the difference in the ECAR measurements observed between *S*. Enteritidis and *S*. Heidelberg infected cells at the two time points and their synchronicity with glycolytic proteins found in the AMPK-mTOR signaling cascade, analysis of other proteins in this cascade was imperative for further determination of how these two strains of bacteria affect immunometabolism. The kinome peptide array results showed a decrease in mTOR activation at site S2448 at 30 minutes post infection and an increase in mTOR activity at site S2448 at 2 hours post infection. Also, because of mTOR's role in the regulation of immune functions and metabolism, mTOR was chosen as a protein of interest. mTOR is a regulator of cellular growth,

survival and metabolism by sensing amino acids and ATP availability (69). mTOR is a serine/threonine kinase that phosphorylates S6K and EIF4EBP1 to promote protein synthesis and cell growth (69,70). Research suggests that *Salmonella* infections alter the activities of mTOR complex 1(70). Also, inhibition of mTOR complex leads to immunosuppressive effects (71). Therefore, examining the mTOR complex 1 was necessary to determine whether the changes in the immunometabolism and macrophage polarization of host cells during *Salmonella* infections were due to manipulation of mTOR functions.

To understand the role of mTOR in *Salmonella* infections, cells were treated with the mTOR activator MHY1485 and the mTOR inhibitor rapamycin. MHY1485 is a cell permeable chemical compound derived from triazine (72). MHY1485 is known to have inhibitory effects on autophagy in rat liver cells by reducing fusion of autophagosomes to lysosomes (73, 129)). More interestingly, by some unknown mechanism MHY1485 has been shown to increase cellular levels of phosphorylated mTOR serine 2448 (73). In opposition to MHY1485, rapamycin is a drug known to inhibit mTOR activity (74). Although rapamycin actions on mTOR is not fully understood, it is known to have immunosuppressive effects on T-cell activation and cytokine production *in vitro* (71, 74, 75). These treatments were used to monitor the metabolic effects of activating or inhibiting mTOR during an infection. Before performing seahorse metabolic flux assays, positive controls experiments were used to test the activity of both MHY1485 and rapamycin as seen in the results. The kinome

peptide array confirmed the deactivation of mTOR as there was a decrease in the phosphorylation of mTOR and an increase in the phosphorylation of the mTOR inhibitor TSC1/2 (Figure 11). The MHY1485 treatment significantly increased cell growth compared to control and rapamycin treatment (Figure 12).

Upon analysis of the metabolic assays with mTOR targeted treatments, no significant difference was found between groups (Figure 13). One conclusion from these results is that the mechanism by which mTOR signaling is altered by *Salmonella* is not dependent on glycolysis or energy metabolism measured by the seahorse. This is because mTOR does not directly affect glucose metabolism and the proteins downstream of mTOR are not effectors or regulators of glycolysis. Also, glycolysis is an energy generating process that affects AMPK and AMPK regulates mTOR. However, mTOR does not regulate glycolysis or AMPK activity, therefore switching mTOR on or off will have no effect on glycolysis but the activation of AMPK by reduced glycolysis might affect mTOR's status.

5.4 The gentamicin protection assays are reflective of the inflammatory profile of HD11 during *Salmonella* infections.

The gentamicin protection assays showed a significant difference between the invasiveness of HD11 macrophages by *S*. Enteritidis and *S*. Heidelberg at 30 minutes post infection. At 2 hours post infection, *S*. Enteritidis plate counts were higher than *S*. Heidelberg with a p-value of 0.053. The high number of intracellular *S*. Enteritidis in

HD11 macrophages highlights its ability to invade and form a suitable niche in the host. *S*. Enteritidis invades cells causing a change to the M1 profile, this induces the proinflammatory response (51). The ability of *S*. Enteritidis to invade more host cells then increases due to this increase in proinflammation. This increased inflammation can ultimately lead to cell death and rupture, enabling the bacteria to invade neighboring healthy cells. Although apoptosis is a naturally occurring non-inflammatory process carried out in a cell, it is also a mechanism to clear out infected cells. However, *Salmonella* uses this to its advantage. When apoptotic bodies form from infected cells, those bodies contain vacuoles of *Salmonella*, those bodies are ingested by phagocytic cells resulting in the infection of those phagocytic cells (37, 50). Thus induction of apoptosis early on will enable *S*. Enteritidis to carry out such a process for better invasion, hence, its known prevalence and invasiveness in farm animals. *Salmonella* also induces inflammatory cell death (98), this is evident in the *S*. Enteritidis 30 minutes kinome peptide array data via the phosphorylation of the pyroptosis marker, caspase-1.

The colony plate count for *S*. Heidelberg remained low throughout both time points, yet *S*. Heidelberg is still capable of inducing extreme changes in the immune and metabolic signaling of host cells. This implies that *S*. Heidelberg does not require a vast number of bacteria to survive and create a suitable niche in host cells. Thus, may explain its high isolation rates in farm animals.

To determine whether inhibition or activation of mTOR would increase or decrease *Salmonella* invasiveness respectively, HD11 cells were treated with 100 g/mL of rapamycin or 2 μM of MHY1485 before infection. Based on the results of the treatment groups of the gentamicin protection assay, there is no difference in invasiveness of HD11 macrophages by *S*. Enteritidis or *S*. Heidelberg at 30 minutes or 2 hours post infections (Figure 14, 15). Although MHY1485 showed a decrease in *S*. Enteritidis count at 2 hours and rapamycin showed an increase in *S*. Enteritidis count at 2 hours, statistical analysis showed no significant difference between the groups and *S*. Enteritidis infections alone therefore the hypothesis that inhibition of mTOR potentiates *S*. Enteritidis infections cannot be accepted.

Moreover, a study done by Schmutz et al. in Hela human epithelial cell lines showed that rapamycin did not increase the invasiveness of the bacteria *Shigella flexneri* (83). However, the study by Schmutz et al. did show a decrease in S6K activity due to rapamycin treatment. S6K is a kinase that when activated can suppress pro apoptotic proteins and promote cell survival. The results of the 30 minutes post infection gentamicin protection assay show that *Salmonella* had successfully invaded and established a niche in host cells, therefore its goal at 2 hours post infection was to invade neighboring cells. In order to do this, the bacteria induces death of the occupied host cells. Treatment with rapamycin decreases the activity of cell survival promoter S6K and its downstream substrates. Thus, *Salmonella* can trigger the induction of

apoptosis via the TNF-alpha JNK signaling cascade without much resistance, hence invading more cells.

5.5 Presence of mTOR S2448 in *Salmonella* Infected HD11 Cells

A western blot of mTOR at site S2448 was performed on HD11 cells 30 minutes post-infection with *S*. Enteritidis and *S*. Heidelberg to further validate our interpretation of the kinome peptide array results. The 30 minutes post-infection blot showed a reduction of phospho mTOR S2448 signal in *S*. Enteritidis and *S*. Heidelberg infected cells compared to control (Figure 16). Thus, further validating the changes in the state of phosphospecific peptides as denoted by the peptide array.

Although the infections alone compared to control were more consistent with the kinome peptide array data than the 30 minutes post infection with treatments. The western blot also included treatment of infected and uninfected HD11 cells with rapamycin and MHY1485. The results for the 30 minutes post infection Western blot showed a small increase in band size of MHY1485 treated HD11 cells compared to rapamycin. However, the bands from cells treated with rapamycin before infection were slightly more intense than infection alone. This could be due to the differences in technique specificity. Western blots can be used as a qualitative assay that measures the presence, absence or abundance of the proteins of interest, the kinome peptide array measures the activity of different kinases within a biological sample; not the presence or absence of proteins. Studies have also reported that the *Salmonella* type 3 secretion system can co-regulate certain host pathways via kinase activities including

those involved in the signal transduction of pro and anti-apoptotic proteins including mTOR (83). Thus, the discrepancies seen in the western blot could be the result of long term effects of treatments on bacteria kinase activity on mTOR.

Chapter 6

CONCLUSION

Salmonella exploits hosts innate immune responses for its benefit and survival, i.e. the mechanisms hosts employ to limit the spread of bacteria are used by *Salmonella* to increase its replication and infection (40). For example, apoptosis is a mechanism used by the innate immune system to rid itself of infected cells; however, *Salmonella* can survive after apoptosis and uses that opportunity to invade other surrounding cells (40). Understanding the mechanisms by which different serovars of *Salmonella* invade and establish an infection in host cells is crucial in identifying a target for the treatment and prevention of *Salmonella* infections. According to the kinome peptide array analysis, *S*. Enteritidis and *S*. Heidelberg induce differential changes in kinase activities in metabolic and immune related peptides. The AMPK-mTOR signaling cascade was analyzed because of its significance within the kinome dataset and its involvement in the regulation of cells immunometabolic status. The kinome peptide array data showed differential changes in phosphorylation of the energy sensor AMPK and glycolytic enzymes PFK1 and PFK2. At 30 minutes post *S*. Enteritidis infection, there was a significant increase in AMPK-PFK2 activity, which is an indication of increased glycolysis and as seen in the seahorse metabolic flux assay, there was an increase in glucose metabolism. High glucose metabolism is an indication of pro-inflammation, a characteristic common to M1 macrophages. There was a decrease in AMPK-PFK2 activity at 30 minutes post *S*. Heidelberg infection, thus a decrease in glucose metabolism as indicated by the metabolism assay.

Interestingly, *S*. Heidelberg bacteria induced activation of the pentose phosphate pathway in infected cells to produce nitric oxide during invasion. To add on, there was an increase in the dead cell population in *S*. Enteritidis infected cells compared to *S*. Heidelberg after 1.5 hours of initial infection. Lastly, the gentamicin protection assay followed by plate counts also showed an increase in invasiveness of *S*. Enteritidis compared to *S*. Heidelberg at 30 minutes and 2 hours post infection. With these results we conclude that macrophages have different immunometabolic responses to *S*. Enteritidis and *S*. Heidelberg. *S*. Enteritidis induces the classic proinflammatory macrophage profile during infection which leads to cell death to enhance its invasion of and replication in host cells. While *S*. Heidelberg avoids the increased induction of proinflammatory factors during infection to avoid clearance by the host immune system, except the induction of NO which promotes its growth.

Common to both *S*. Enteritidis and *S*. Heidelberg, the metabolic assay showed a significant increase in oxygen consumption compared to control. The kinome peptide array also showed a similar trend in the activity of fatty acid regulators. Another common trend seen between *S*. Enteritidis and *S*. Heidelberg at 30 minutes and 2 hours post infection is the activity of mTORC1 site S2448 per the kinome peptide array analysis and Western blot analysis. This indicated an essential role for mTORC1 in *Salmonella* invasion and infection of host cells. However, plate counts and the metabolic flux data showed no significant change in macrophage response to *Salmonella* infections after inhibition or activation of mTOR. Per these validation

assays, direct targeting of mTOR does not ameliorate *Salmonella* infections. Thus, we conclude that the changes seen in mTOR phosphorylation are an effect of bacteria activity but not a target for the treatment or clearance of *Salmonella* infections.

Overall, this research demonstrates the difference between the invasiveness and persistence of *S*. Enteritidis and *S*. Heidelberg. That is, the immunometabolic responses that *S*. Enteritidis exploits in host for increased invasion only presents short term benefits to the bacteria. While the host delayed immunometabolic response to *S*. Heidelberg at the cost of decreased invasiveness poses long term benefits to the bacteria because this increases its persistence. The tradeoff for *S*. Enteritidis increasing its invasiveness is the increased immune response produced by the host to clear the infection, hence the decrease in *S*. Enteritidis prevalence. The persistence of *S*. Heidelberg infection is evident in the increasing isolation and prevalence of the bacteria in poultry over *S*. Enteritidis in the past decade. This project reveals the difficulty associated with the efficient treatment of *Salmonellla* infections because the different serovars of *Salmonella* induce different immunometabolic responses in host therefore, an immune or metabolic target for the treatment of one serovar may benefit another serovar. Lastly, this supports the theory that although chickens do not show any physical symptoms to *Salmonella* infections, their immune systems respond to *Salmonella* invasion to clear the pathogen. As seen in this study, HD11 chicken macrophage like cells can fight off *S*. Enteritidis infections better than *S*. Heidelberg. Thus, the persistence of *S*. Heidelberg poses a greater risk to poultry producers and public health as it is more likely to reach consumers than *S*. Enteritidis.

Chapter 7

FUTURE DIRECTIONS

Now that we have validated the changes in the immunometabolic response of cells to *Salmonella* infections, a number of experiments can be carried out to further examine the effects of *S*. Enteritidis and *S*. Heidelberg infections on the AMPK-mTORC1 signaling cascade. Since we were unsuccessful in showing that the direct inhibition or activation mTORC1 affects the invasiveness of *Salmonella*, using an upstream target of the AMPK-mTORc1 cascade will confirm the significance of this pathway in host cells immunometabolic response. That is, treating infected and uninfected cells with the AMPK activator metformin which would lead to the downstream inhibition of mTOR. A gentamicin protection assay and flow cytometry will reveal if mTOR inhibition would increase *Salmonella* invasiveness and cell death. Another future experiment for the full understanding of the effects of *Salmonella* infections over a longer period of time will be to validate the 6 hour kinome peptide array data with the methods used to validate the 30 minutes and 2 hours post infection kinome peptide array data.

To understand the extent to which *Salmonella* induces these effects in host cells, the design and objectives of this study should be applied to a study carried out in human macrophages. Thus, an understanding of how *Salmonella* affects the immunometabolic responses of human macrophages *in vitro* at different times of infection.

REFERENCES

1. Andino A, Hanning I. Salmonella enterica: Survival, Colonization, and Virulence Differences among Serovars. Sci World J [Internet]. 2015 [cited 2018 Dec 3];2015. Available from: https://www.ncbi.nlm.nih.gov/pmc/articles/PMC4310208/
2. Swaggerty CL, Kogut MH, He H, Genovese KJ, Johnson C, Arsenault RJ. Differential Levels of Cecal Colonization by Salmonella Enteritidis in Chickens Triggers Distinct Immune Kinome Profiles. Front Vet Sci [Internet]. 2017 [cited 2019 Feb 14];4. Available from: https://www.frontiersin.org/articles/10.3389/fvets.2017.00214/full
3. Majowicz SE, Musto J, Scallan E, Angulo FJ, Kirk M, O'Brien SJ, et al. The Global Burden of Nontyphoidal Salmonella Gastroenteritis. Clin Infect Dis. 2010 Mar 15;50(6):882–9.
4. V. T. Nair D, Venkitanarayanan K, Kollanoor Johny A. Antibiotic-Resistant Salmonella in the Food Supply and the Potential Role of Antibiotic Alternatives for Control. Foods [Internet]. 2018 Oct 11 [cited 2018 Dec 3];7(10). Available from: https://www.ncbi.nlm.nih.gov/pmc/articles/PMC6210005/
5. Gal-Mor O, Boyle EC, Grassl GA. Same species, different diseases: how and why typhoidal and non-typhoidal Salmonella enterica serovars differ. Front Microbiol [Internet]. 2014 Aug 4 [cited 2018 Dec 5];5. Available from: https://www.ncbi.nlm.nih.gov/pmc/articles/PMC4120697/
6. Porwollik S. Salmonella: From Genome to Function. Horizon Scientific Press; 2011. 315 p.
7. Bäumler AJ, Tsolis RM, Ficht TA, Adams LG. Evolution of Host Adaptation inSalmonella enterica. Infect Immun. 1998 Oct 1;66(10):4579–87.
8. Fookes M, Schroeder GN, Langridge GC, Blondel CJ, Mammina C, Connor TR, et al. Salmonella bongori Provides Insights into the Evolution of the Salmonellae. PLOS Pathog. 2011 Aug 18;7(8):e1002191.
9. Feasey NA, Dougan G, Kingsley RA, Heyderman RS, Gordon MA. Invasive non-typhoidal salmonella disease: an emerging and neglected tropical disease in Africa. The Lancet. 2012 Jun 30;379(9835):2489–99.
10. Porwollik S, Boyd EF, Choy C, Cheng P, Florea L, Proctor E, et al. Characterization of Salmonella enterica Subspecies I Genovars by Use of Microarrays. J Bacteriol. 2004 Sep 1;186(17):5883–98.
11. Demczuk W, Soule G, Clark C, Ackermann H-W, Easy R, Khakhria R, et al. Phage-Based Typing Scheme for Salmonella enterica Serovar Heidelberg, a Causative Agent of Food Poisonings in Canada. J Clin Microbiol. 2003 Sep 1;41(9):4279–84.
12. Haeusler GM, Curtis N. Non-typhoidal Salmonella in Children: Microbiology, Epidemiology and Treatment. In: Curtis N, Finn A, Pollard AJ, editors. Hot Topics in Infection and Immunity in Children IX [Internet]. New York, NY: Springer New York; 2013 [cited 2019 Feb 14]. p. 13–26. (Advances in Experimental Medicine and Biology). Available from: https://doi.org/10.1007/978-1-4614-4726-9_2

13. Jackson BR, Griffin PM, Cole D, Walsh KA, Chai SJ. Outbreak-associated Salmonella enterica Serotypes and Food Commodities, United States, 1998–2008. Emerg Infect Dis. 2013 Aug;19(8):1239–44.
14. Finstad S, O'Bryan CA, Marcy JA, Crandall PG, Ricke SC. Salmonella and broiler processing in the United States: Relationship to foodborne salmonellosis. Food Res Int. 2012 Mar 1;45(2):789–94.
15. Carrasco E, Morales-Rueda A, García-Gimeno RM. Cross-contamination and recontamination by Salmonella in foods: A review. Food Res Int. 2012 Mar 1;45(2):545–56.
16. Nidaullah H, Abirami N, Shamila-Syuhada AK, Chuah L-O, Nurul H, Tan TP, et al. Prevalence of Salmonella in poultry processing environments in wet markets in Penang and Perlis, Malaysia. Vet World. 2017 Mar;10(3):286–92.
17. Salmonella Homepage | CDC [Internet]. 2019 [cited 2019 Feb 14]. Available from: https://www.cdc.gov/salmonella/index.html
18. D'Aoust J-Y, Maurer J. Salmonella Species. Food Microbiol Fundam Front Third Ed. 2007 Jan 1;187–236.
19. Dhanani AS, Block G, Dewar K, Forgetta V, Topp E, Beiko RG, et al. Genomic Comparison of Non-Typhoidal Salmonella enterica Serovars Typhimurium, Enteritidis, Heidelberg, Hadar and Kentucky Isolates from Broiler Chickens. PLOS ONE. 2015 Jun 17;10(6):e0128773.
20. Gordon MA. Salmonella infections in immunocompromised adults. J Infect. 2008 Jun 1;56(6):413–22.
21. Epidemiology, Clinical Presentation, Laboratory Diagnosis, Antimicrobial Resistance, and Antimicrobial Management of Invasive Salmonella Infections | Clinical Microbiology Reviews [Internet]. [cited 2019 Feb 14]. Available from: https://cmr.asm.org/content/28/4/901
22. Arpaia N, Godec J, Lau L, Sivick KE, McLaughlin LM, Jones MB, et al. TLR Signaling Is Required for Salmonella typhimurium Virulence. Cell. 2011 Mar 4;144(5):675–88.
23. MacLennan C. Interleukin (IL)-12 and IL-23 Are Key Cytokines for Immunity against Salmonella in Humans | The Journal of Infectious Diseases | Oxford Academic [Internet]. 2004 [cited 2019 Feb 14]. Available from: https://academic.oup.com/jid/article/190/10/1755/2191509
24. Shimoni Z, Pitlik S, Leibovici L, Samra Z, Konigsberger H, Drucker M, et al. Nontyphoid Salmonella Bacteremia: Age-Related Differences in Clinical Presentation, Bacteriology, and Outcome. Clin Infect Dis. 1999 Apr 1;28(4):822–7.
25. Zhao X, Gao Y, Ye C, Yang L, Wang T, Chang W. Prevalence and Characteristics of Salmonella Isolated from Free-Range Chickens in Shandong Province, China. BioMed Res Int [Internet]. 2016 [cited 2019 Feb 14];2016. Available from: https://www.ncbi.nlm.nih.gov/pmc/articles/PMC5075293/
26. Fan S, Zheng J, Duan Z, Yang N, Xu G. The influences of SE infection on layers' production performance, egg quality and blood biochemical indicators. J Anim Sci Biotechnol. 2014 Jan 9;5(1):4.

27. Thomson NR, Clayton DJ, Windhorst D, Vernikos G, Davidson S, Churcher C, et al. Comparative genome analysis of Salmonella Enteritidis PT4 and Salmonella Gallinarum 287/91 provides insights into evolutionary and host adaptation pathways. Genome Res [Internet]. 2008 Sep 1 [cited 2019 Feb 14]; Available from: http://genome.cshlp.org/content/early/2008/09/17/gr.077404.108
28. Andres VM, Davies RH. Biosecurity Measures to Control Salmonella and Other Infectious Agents in Pig Farms: A Review. Compr Rev Food Sci Food Saf. 2015;14(4):317–35.
29. Shah DH, Paul NC, Sischo WC, Crespo R, Guard J. Population dynamics and antimicrobial resistance of the most prevalent poultry-associated Salmonella serotypes. Poult Sci. 2017 Mar 1;96(3):687–702.
30. de Jong B, Ekdahl K. The comparative burden of salmonellosis in the European Union member states, associated and candidate countries. BMC Public Health. 2006 Jan 10;6:4.
31. Chang Q, Wang W, Regev-Yochay G, Lipsitch M, Hanage WP. Antibiotics in agriculture and the risk to human health: how worried should we be? Evol Appl. 2015 Mar;8(3):240–7.
32. Phillips I, Casewell M, Cox T, De Groot B, Friis C, Jones R, et al. Does the use of antibiotics in food animals pose a risk to human health? A critical review of published data. J Antimicrob Chemother. 2004 Jan 1;53(1):28–52.
33. Sadeyen J-R, Trotereau J, Velge P, Marly J, Beaumont C, Barrow PA, et al. Salmonella carrier state in chicken: comparison of expression of immune response genes between susceptible and resistant animals. Microbes Infect. 2004 Nov;6(14):1278–86.
34. Student Competition: Animal Well-Being and Behavior. Poult Sci. :6.
35. Ahmer BM, Gunn JS. Interaction of Salmonella spp. with the Intestinal Microbiota. Front Microbiol [Internet]. 2011 [cited 2019 Feb 15];2. Available from: https://www.frontiersin.org/articles/10.3389/fmicb.2011.00101/full
36. Imlay JA. Where in the world do bacteria experience oxidative stress? Environ Microbiol [Internet]. [cited 2018 Dec 3];0(0). Available from: https://onlinelibrary.wiley.com/doi/abs/10.1111/1462-2920.14445
37. Vazquez-Torres A, Fang FC. Salmonella evasion of the NADPH phagocyte oxidase. Microbes Infect. 2001 Nov 1;3(14):1313–20.
38. Gorbach SL. Microbiology of the Gastrointestinal Tract. In: Baron S, editor. Medical Microbiology [Internet]. 4th ed. Galveston (TX): University of Texas Medical Branch at Galveston; 1996 [cited 2018 Dec 19]. Available from: http://www.ncbi.nlm.nih.gov/books/NBK7670/
39. Bratburd JR, Keller C, Vivas E, Gemperline E, Li L, Rey FE, et al. Gut Microbial and Metabolic Responses to Salmonella enterica Serovar Typhimurium and Candida albicans. mBio. 2018 Dec 21;9(6):e02032-18.
40. Behnsen J, Perez-Lopez A, Nuccio S-P, Raffatellu M. Exploiting host immunity: the Salmonella paradigm. Trends Immunol. 2015 Feb;36(2):112–20.

41. Bäumler AJ, Sperandio V. Interactions between the microbiota and pathogenic bacteria in the gut. Nature. 2016 Jul 6;535(7610):85–93.
42. Crhanova M, Hradecka H, Faldynova M, Matulova M, Havlickova H, Sisak F, et al. Immune Response of Chicken Gut to Natural Colonization by Gut Microflora and to Salmonella enterica Serovar Enteritidis Infection ▿. Infect Immun. 2011 Jul;79(7):2755–63.
43. Cascales E. Inside the Chamber of Secrets of the Type III Secretion System. Cell. 2017 Mar 9;168(6):949–51.
44. Jennings E, Thurston TLM, Holden DW. Salmonella SPI-2 Type III Secretion System Effectors: Molecular Mechanisms And Physiological Consequences. Cell Host Microbe. 2017 Aug 9;22(2):217–31.
45. He H, Arsenault RJ, Genovese KJ, Johnson C, Kogut MH. Chicken macrophages infected with Salmonella (S.) Enteritidis or S. Heidelberg produce differential responses in immune and metabolic signaling pathways. Vet Immunol Immunopathol. 2018 Jan 1;195:46–55.
46. Shi Z, Cai Z, Yu J, Zhang T, Zhao S, Smeds E, et al. Toll-like Receptor 11 (TLR11) Prevents Salmonella Penetration into the Murine Peyer Patches. J Biol Chem. 2012 Dec 21;287(52):43417–23.
47. Tellez G. Probiotics/direct fed microbials for Salmonella control in poultry - ScienceDirect [Internet]. 2012 [cited 2019 Feb 17]. Available from: https://www.sciencedirect.com/science/article/pii/S0963996911002067?via%3Dihub
48. Kaljee LM, Pach A, Garrett D, Bajracharya D, Karki K, Khan I. Social and Economic Burden Associated With Typhoid Fever in Kathmandu and Surrounding Areas: A Qualitative Study. J Infect Dis. 2018 Nov 10;218(suppl_4):S243–9.
49. Roberts JA, Sockett PN, Gill ON. Economic impact of a nationwide outbreak of salmonellosis: cost-benefit of early intervention. BMJ. 1989 May 6;298(6682):1227–30.
50. Hirayama D, Iida T, Nakase H. The Phagocytic Function of Macrophage-Enforcing Innate Immunity and Tissue Homeostasis. Int J Mol Sci [Internet]. 2017 Dec 29 [cited 2019 Feb 17];19(1). Available from: https://www.ncbi.nlm.nih.gov/pmc/articles/PMC5796042/
51. Langston PK, Shibata M, Horng T. Metabolism Supports Macrophage Activation. Front Immunol [Internet]. 2017 Jan 31 [cited 2019 Feb 17];8. Available from: https://www.ncbi.nlm.nih.gov/pmc/articles/PMC5281575/
52. Gog JR, Murcia A, Osterman N, Restif O, McKinley TJ, Sheppard M, et al. Dynamics of Salmonella infection of macrophages at the single cell level. J R Soc Interface. 2012 Oct 7;9(75):2696–707.
53. Yang M, Xu J, Wang Q, Zhang A-Q, Wang K. An obligatory anaerobic Salmonella typhimurium strain redirects M2 macrophages to the M1 phenotype. Oncol Lett. 2018 Mar;15(3):3918–22.
54. Brundu S FA. Polarization and Repolarization of Macrophages. J Clin Cell Immunol [Internet]. 2015 [cited 2019 Feb 17];06(02). Available from:

https://www.omicsonline.org/open-access/polarization-and-repolarization-of-macrophages-2155-9899-1000319.php?aid=52357
55. Arsenault RJ, Kogut MH. Immunometabolism and the Kinome Peptide Array: A New Perspective and Tool for the Study of Gut Health. Front Vet Sci [Internet]. 2015 Oct 13 [cited 2019 Feb 18];2. Available from: https://www.ncbi.nlm.nih.gov/pmc/articles/PMC4672240/
56. Li Y, Arsenault RJ, Trost B, Slind J, Griebel PJ, Napper S, et al. A Systematic Approach for Analysis of Peptide Array Kinome Data. Sci Signal. 2012 Apr 17;5(220):pl2–pl2.
57. Arsenault RJ, Kogut MH. Chicken-specific peptide arrays for kinome analysis: Flight for the flightless. :11.
58. Jalal S, Arsenault R, Potter AA, Babiuk LA, Griebel PJ, Napper S. Genome to Kinome: Species-Specific Peptide Arrays for Kinome Analysis. Sci Signal. 2009 Jan 20;2(54):pl1–pl1.
59. Parikh K, Peppelenbosch MP, Ritsema T. Kinome Profiling Using Peptide Arrays in Eukaryotic Cells. In: Graauw M de, editor. Phospho-Proteomics: Methods and Protocols [Internet]. Totowa, NJ: Humana Press; 2009 [cited 2019 Feb 18]. p. 269–80. (Methods in Molecular Biology™). Available from: https://doi.org/10.1007/978-1-60327-834-8_20
60. Ferrante AW. Macrophages, fat, and the emergence of immunometabolism. J Clin Invest. 2013 Dec 2;123(12):4992–3.
61. Mathis D, Shoelson SE. Immunometabolism: an emerging frontier. Nat Rev Immunol. 2011 Feb;11(2):81.
62. Wu J, Pugh R, Laughlin RC, Andrews-Polymenis H, McClelland M, Bäumler AJ, et al. High-throughput Assay to Phenotype Salmonella enterica Typhimurium Association, Invasion, and Replication in Macrophages. J Vis Exp JoVE [Internet]. 2014 Aug 11 [cited 2019 Feb 18];(90). Available from: https://www.ncbi.nlm.nih.gov/pmc/articles/PMC4500590/
63. Larade K, Storey KB. Chapter 3 - A Profile of the Metabolic Responses to Anoxia in Marine Invertebrates. In: Storey KB, Storey JM, editors. Cell and Molecular Response to Stress [Internet]. Elsevier; 2002 [cited 2019 Feb 28]. p. 27–46. (Sensing, Signaling and Cell Adaptation; vol. 3). Available from: http://www.sciencedirect.com/science/article/pii/S1568125402800055
64. Sharma R. Chapter 41 - Biochemical Mechanisms of Fatty Liver and Bioactive Foods: Fatty Liver, Diagnosis, Nutrition Therapy. In: Watson RR, Preedy VR, editors. Bioactive Food as Dietary Interventions for Liver and Gastrointestinal Disease [Internet]. San Diego: Academic Press; 2013 [cited 2019 Feb 28]. p. 623–55. Available from: http://www.sciencedirect.com/science/article/pii/B9780123971548001810
65. Planavila A, van Bilsen M. Chapter 11 - PPARs as Modulators of Cardiac Metabolism and Inflammation. In: Blankesteijn WM, Altara R, editors. Inflammation in Heart Failure [Internet]. Boston: Academic Press; 2015 [cited 2019 Feb 28]. p. 155–

67. Available from:
http://www.sciencedirect.com/science/article/pii/B9780128000397000116
66. Seahorse XFp Analyzer | Agilent [Internet]. [cited 2019 Feb 28]. Available from: https://www.agilent.com/en/products/cell-analysis/seahorse-analyzers/seahorse-xfp-analyzer
67. Mantovani A, Sica A, Sozzani S, Allavena P, Vecchi A, Locati M. The chemokine system in diverse forms of macrophage activation and polarization. Trends Immunol. 2004 Dec 1;25(12):677–86.
68. Sica A, Larghi P, Mancino A, Rubino L, Porta C, Totaro MG, et al. Macrophage polarization in tumour progression. Semin Cancer Biol. 2008 Oct 1;18(5):349–55.
69. Saxton RA, Sabatini DM. mTOR Signaling in Growth, Metabolism, and Disease. Cell. 2017 Mar 9;168(6):960–76.
70. Kogut MH, Genovese KJ, He H, Arsenault RJ. AMPK and mTOR: sensors and regulators of immunometabolic changes during Salmonella infection in the chicken. Poult Sci. 2016 Feb 1;95(2):345–53.
71. Buerger C, Shirsath N, Lang V, Berard A, Diehl S, Kaufmann R, et al. Inflammation dependent mTORC1 signaling interferes with the switch from keratinocyte proliferation to differentiation. Blumenberg M, editor. PLOS ONE. 2017 Jul 10;12(7):e0180853.
72. mTOR Activator, MHY1485 - Calbiochem | 500554 [Internet]. [cited 2019 Feb 18]. Available from: http://www.emdmillipore.com/US/en/product/mTOR-Activator-MHY1485-Calbiochem,EMD_BIO-500554#anchor_MSD
73. Choi YJ, Park YJ, Park JY, Jeong HO, Kim DH, Ha YM, et al. Inhibitory Effect of mTOR Activator MHY1485 on Autophagy: Suppression of Lysosomal Fusion. PLoS ONE [Internet]. 2012 Aug 22 [cited 2019 Feb 18];7(8). Available from: https://www.ncbi.nlm.nih.gov/pmc/articles/PMC3425474/
74. Li J, Kim SG, Blenis J. Rapamycin: one drug, many effects. Cell Metab. 2014 Mar 4;19(3):373–9.
75. Ballou LM, Lin RZ. Rapamycin and mTOR kinase inhibitors. J Chem Biol. 2008 Nov;1(1–4):27–36.
76. Foley SL, Johnson TJ, Ricke SC, Nayak R, Danzeisen J. Salmonella Pathogenicity and Host Adaptation in Chicken-Associated Serovars. Microbiol Mol Biol Rev MMBR. 2013 Dec;77(4):582–607.
77. Meerburg BG, Kijlstra A. Role of rodents in transmission of Salmonella and Campylobacter. J Sci Food Agric. 2007;87(15):2774–81.
78. Cohen ML, Tauxe RV. Drug-resistant Salmonella in the United States: an epidemiologic perspective. Science. 1986 Nov 21;234(4779):964–9.
79. Berg JM, Tymoczko JL, Stryer L. 20.3 the Pentose Phosphate Pathway Generates NADPH and Synthesizes Five-Carbon Sugars. Biochem 5th Ed [Internet]. 2002 [cited 2019 Mar 1]; Available from:
https://www.ncbi.nlm.nih.gov/books/NBK22416/

80. Poulsen BR, Nøhr J, Douthwaite S, Hansen LV, Iversen JJL, Visser J, et al. Increased NADPH concentration obtained by metabolic engineering of the pentose phosphate pathway in Aspergillus niger. FEBS J. 2005;272(6):1313–25.
81. Mogensen TH, Paludan SR. Molecular Pathways in Virus-Induced Cytokine Production. Microbiol Mol Biol Rev. 2001 Mar;65(1):131–50.
82. Rohde F, Schusser B, Hron T, Farkašová H, Plachý J, Härtle S, et al. Characterization of Chicken Tumor Necrosis Factor-α, a Long Missed Cytokine in Birds. Front Immunol [Internet]. 2018 [cited 2019 Mar 1];9. Available from: https://www.frontiersin.org/articles/10.3389/fimmu.2018.00605/full
83. Christoph Schmutz, Erik Ahrné, Christoph A. Kasper, Therese Tschon, Isabel Sorg, Roland F. Dreier, Alexander Schmidt, Cécile Arrieumerlou
Molecular & Cellular Proteomics October 1, 2013, First published on July 4, 2013, 12 (10) 2952-2968; DOI: 10.1074/mcp.M113.029918
84. Ciraci, C., Tuggle, C. K., Wannemuehler, M. J., Nettleton, D. & Lamont, S. J. Unique genome-wide transcriptome profiles of chicken macrophages exposed to Salmonella-derived endotoxin. BMC Genomics 11, 545 (2010).
85. Beug, H., von Kirchbach, A., Döderlein, G., Conscience, J. F. & Graf, T. Chicken hematopoietic cells transformed by seven strains of defective avian leukemia viruses display three distinct phenotypes of differentiation. Cell 18, 375–390 (1979).
86. Jarvis, N. A., Donaldson, J. R., O'Bryan, C. A., Ricke, S. C. & Crandall, P. G. Listeria monocytogenes infection of HD11, chicken macrophage-like cells. Poultry Science pew358 (2016). doi:10.3382/ps/pew358
87. Wisner, A. L. S., Potter, A. A. & Köster, W. Effect of the Salmonella Pathogenicity Island 2 Type III Secretion System on Salmonella Survival in Activated Chicken Macrophage-Like HD11 Cells. PLoS One 6, (2011).
88. Kannan V. Balan, Uma S. Babu, Comparative responses of chicken macrophages to infection with Salmonella enterica serovars, Poultry Science, Volume 96, Issue 6, June 2017, Pages 1849–1854, https://doi.org/10.3382/ps/pew477
89. Hornbeck PV, Zhang B, Murray B, Kornhauser JM, Latham V, Skrzypek E PhosphoSitePlus, 2014: mutations, PTMs and recalibrations. Nucleic Acids Res. 2015 43:D512-20
90. Szklarczyk D, Morris JH, Cook H, Kuhn M, Wyder S, Simonovic M, Santos A, Doncheva NT, Roth A, Bork P, Jensen LJ, von Mering C. The STRING database in 2017: quality-controlled protein-protein association networks, made broadly accessible. Nucleic Acids Res. 2017 Jan; 45:D362-68.PubMed
91. Trost B, Kindrachuk J, Määttänen P, Napper S, Kusalik A. PIIKA 2: an expanded, web-based platform for analysis of kinome microarray data. PLoS One. 2013;8(11):e80837. Published 2013 Nov 29. doi:10.1371/journal.pone.0080837
92. Minoru Kanehisa, Yoko Sato, Masayuki Kawashima, Miho Furumichi, Mao Tanabe, KEGG as a reference resource for gene and protein annotation, Nucleic Acids Research, Volume 44, Issue D1, 04 January 2016, Pages D457–D462, https://doi.org/10.1093/nar/gkv1070

93. Boutet E, Lieberherr D, Tognolli M, Schneider M, Bansal P, Bridge AJ, Poux S, Bougueleret L, Xenarios I. UniProtKB/Swiss-Prot, the Manually Annotated Section of the UniProt KnowledgeBase: How to Use the Entry View Methods Mol. Biol. 1374:23-54 (2016)
94. Zaru R, Magrane M, O'Donovan C, UniProt Consortium From the research laboratory to the database: the Caenorhabditis elegans kinome in UniProtKB Biochem J. 474(4):493-515 (2017)
95. Pundir S, Martin MJ, O'Donovan C. UniProt Protein Knowledgebase Methods Mol. Biol. 1558:41-55 (2017)
96. Galindo CL, Fadl AA, Sha J, Gutierrez C, Popov VL, Boldogh I, Aggarwal BB, Chopra AK J Biol Chem (2004) 279:37597-37612
97. Lopez, C. A. et al. Phage-Mediated Acquisition of a Type III Secreted Effector Protein Boosts Growth of Salmonella by Nitrate Respiration. mBio 3, (2012).
98. Ardito, F., Giuliani, M., Perrone, D., Troiano, G. & Muzio, L. L. The crucial role of protein phosphorylation in cell signaling and its use as targeted therapy (Review). Int J Mol Med 40, 271–280 (2017).
99. Hardie, D. G. AMP-activated protein kinase—an energy sensor that regulates all aspects of cell function. Genes Dev. 25, 1895–1908 (2011).
100. Bugarel, M., Tudor, A., Loneragan, G. H. & Nightingale, K. K. Molecular detection assay of five Salmonella serotypes of public interest: Typhimurium, Enteritidis, Newport, Heidelberg, and Hadar. Journal of Microbiological Methods 134, 14–20 (2017).
101.Hong, Y. et al. Rapid screening of Salmonella enterica serovars Enteritidis, Hadar, Heidelberg and Typhimurium using a serologically-correlative allelotyping PCR targeting the O and H antigen alleles. BMC Microbiol 8, 178 (2008).
102. Borsoi, A. et al. Behavior Of Salmonella Heidelberg and Salmonella Enteritidis Strains Following Broiler Chick Inoculation: Evaluation Of Cecal Morphometry, Liver And Cecum Bacterial Counts And Fecal Excretion Patterns. Braz J Microbiol 42, 266–273 (2011).
103. Müller, A. J. et al. The S. Typhimurium Effector SopE Induces Caspase-1 Activation in Stromal Cells to Initiate Gut Inflammation. Cell Host & Microbe 6, 125–136 (2009).
104. Müller, A. J. et al. The S. Typhimurium Effector SopE Induces Caspase-1 Activation in Stromal Cells to Initiate Gut Inflammation. Cell Host & Microbe 6, 125–136 (2009).
105. Dysbiosis-Associated Change in Host Metabolism Generates Lactate to Support Salmonella Growth - ScienceDirect. Available at: https://www.sciencedirect.com/science/article/pii/S1931312817305000.
106. Anderson, C. J. & Kendall, M. M. Salmonella enterica Serovar Typhimurium Strategies for Host Adaptation. Front. Microbiol. 8, (2017).
107. Hehlgans, T. & Pfeffer, K. The intriguing biology of the tumour necrosis factor/tumour necrosis factor receptor superfamily: players, rules and the games. Immunology 115, 1–20 (2005).

108. Fan, C., Yang, J. & Engelhardt, J. F. Temporal pattern of NFκB activation influences apoptotic cell fate in a stimuli-dependent fashion. Journal of Cell Science 115, 4843–4853 (2002).
109. Bendall, L. J. & Green, D. R. Autopsy of a cell. Leukemia 28, 1341–1343 (2014).
110. Stiefel, P., Schmidt-Emrich, S., Maniura-Weber, K. & Ren, Q. Critical aspects of using bacterial cell viability assays with the fluorophores SYTO9 and propidium iodide. BMC Microbiology 15, 36 (2015).
111. Novo D, Grégori G, Rajwa B. (2013) Generalized unmixing model for multispectral flow cytometry utilizing nonsquare compensation matrices.Cytometry Part A. 83(5): 508-20.
112. Gewirtz, A. T. et al. Salmonella typhimurium induces epithelial IL-8 expression via Ca^{2+}-mediated activation of the NF-κB pathway. J Clin Invest 105, 79–92 (2000).
113. Suzuki, J., Umeda, M., Sims, P. J. & Nagata, S. Calcium-dependent phospholipid scrambling by TMEM16F. Nature 468, 834–838 (2010).
114. Sundaresan, N. R. et al. The Deacetylase SIRT1 Promotes Membrane Localization and Activation of Akt and PDK1 During Tumorigenesis and Cardiac Hypertrophy. Sci. Signal. 4, ra46–ra46 (2011).
115. Sasaki, T. et al. Phosphorylation regulates SIRT1 function. PLoS ONE 3, e4020 (2008).
116. Higuchi M, Onishi K, Kikuchi C, Gotoh Y (2008) Scaffolding function of PAK in the PDK1-Akt pathway. Nat Cell Biol 10, 1356-64
117. Bonni A, et al. (1999) Cell survival promoted by the Ras-MAPK signaling pathway by transcription-dependent and -independent mechanisms. Science 286, 1358-62
118. Association of insulin receptor substrate 1 (IRS-1) y895 with Grb-2 mediates the insulin signaling involved in IRS-1-deficient brown adipocyte mitogenesis. Mol Cell Biol 21, 2269-80
119. Protein kinase C modulation of insulin receptor substrate-1 tyrosine phosphorylation requires serine 612. Biochemistry 36, 12939-47
120. Hahn-Windgassen, A. et al. Akt activates the mammalian target of rapamycin by regulating cellular ATP level and AMPK activity. J. Biol. Chem. 280, 32081–32089 (2005).
121. Morphoproteomic Evidence of Constitutively Activated and Overexpressed mTOR Pathway in Cervical Squamous Carcinoma and High Grade Squamous Intraepithelial Lesions. Int J Clin Exp Pathol 2, 249-60
122. Kristof AS, Marks-Konczalik J, Billings E, Moss J (2003) Stimulation of signal transducer and activator of transcription-1 (STAT1)-dependent gene transcription by lipopolysaccharide and interferon-gamma is regulated by mammalian target of rapamycin. J Biol Chem 278, 33637-44
123. Wu XN, et al. (2011) Phosphorylation of Raptor by p38beta participates in arsenite-induced mammalian target of rapamycin complex 1 (mTORC1) activation. J Biol Chem 286, 31501-11

124. Hahn, K. et al. PP2A Regulatory Subunit PP2A-B′ Counteracts S6K Phosphorylation. Cell Metabolism 11, 438–444 (2010).
125. Wakil, S. J. & Abu-Elheiga, L. A. Fatty acid metabolism: target for metabolic syndrome. J Lipid Res 50, S138–S143 (2009).
126. Protein kinase C alpha-dependent phosphorylation of the mRNA-stabilizing factor HuR: implications for posttranscriptional regulation of cyclooxygenase-2. Mol Biol Cell 18, 2137-48
127. Xiao, G., Deng, A., Liu, H., Ge, G. & Liu, X. Activator protein 1 suppresses antitumor T-cell function via the induction of programmed death 1. Proc Natl Acad Sci U S A 109, 15419–15424 (2012).
128. Romanelli, A., Martin, K. A., Toker, A. & Blenis, J. p70 S6 kinase is regulated by protein kinase Czeta and participates in a phosphoinositide 3-kinase-regulated signalling complex. Mol. Cell. Biol. 19, 2921–2928 (1999).
129. Choi, Y. J. *et al.* Inhibitory effect of mTOR activator MHY1485 on autophagy: suppression of lysosomal fusion. *PLoS ONE* **7**, e43418 (2012).
130. Djeffal, S., Mamache, B., Elgroud, R., Hireche, S., & Bouaziz, O. (2018). Prevalence and risk factors for *Salmonella* spp. contamination in broiler chicken farms and slaughterhouses in the northeast of Algeria. *Veterinary world*, *11*(8), 1102–1108. doi:10.14202/vetworld.2018.1102-1108
131. Patrick, M. E., Adcock, P. M., Gomez, T. M., Altekruse, S. F., Holland, B. H., Tauxe, R. V....Swerdlow, D. L. (2004). Salmonella Enteritidis Infections, United States, 1985–1999. *Emerging Infectious Diseases*, *10*(1), 1-7. https://dx.doi.org/10.3201/eid1001.020572.
132. Sonja J. Olsen, Richard Bishop, Frances W. Brenner, Thierry H. Roels, Nancy Bean, Robert V. Tauxe, Laurence Slutsker, The Changing Epidemiology of *Salmonella:* Trends in Serotypes Isolated from Humans in the United States, 1987–1997, *The Journal of Infectious Diseases*, Volume 183, Issue 5, 1 March 2001, Pages 753–761, https://doi.org/10.1086/318832
133. Hunter T. (2012). Why nature chose phosphate to modify proteins. *Philosophical transactions of the Royal Society of London. Series B, Biological sciences*, *367*(1602), 2513–2516. doi:10.1098/rstb.2012.0013
134. Brushia, R. J. & Walsh, D. A. Phosphorylase kinase: the complexity of its regulation is reflected in the complexity of its structure. *Front. Biosci.* **4**, D618-641 (1999).

135. Werner, C., Doenst, T., Schwarzer, M. The scientist's guide to cardiac metabolism: Metabolic pathways and cycles. *Elsevier. Academic Press* 4, P39-55 (2016)

136. Blondel, C. J. *et al.* Contribution of the Type VI Secretion System Encoded in SPI-19 to Chicken Colonization by Salmonella enterica Serotypes Gallinarum and Enteritidis. *PLoS One* **5**, (2010).

137. JCI - MAPK4 overexpression promotes tumor progression via noncanonical activation of AKT/mTOR signaling. Available at:https://www.jci.org/articles/view/97712.

138. Xu B, Bird VG, Miller WT (1995) Substrate specificities of the insulin and insulin-like growth factor 1 receptor tyrosine kinase catalytic domains. *J Biol Chem* **270**, 29825-30

139. Lu M, Shyy JY (2006) Sterol regulatory element-binding protein 1 is negatively modulated by PKA phosphorylation. *Am J Physiol Cell Physiol***290**, C1477-86

140. Nielsen JN, et al. (2003) 5'-AMP-activated protein kinase activity and subunit expression in exercise-trained human skeletal muscle. *J Appl Physiol* **94**, 631-41

141. Sano, H. Insulin-stimulated phosphorylation of a Rab GTPase-activating protein regulates GLUT4 translocation. - PubMed - NCBI. Available at: https://www.ncbi.nlm.nih.gov/pubmed/12637568.

142. Kwon M, et al. (2006) Recruitment of the tyrosine phosphatase Src homology 2 domain tyrosine phosphatase-2 to the p85 subunit of phosphatidylinositol-3 (PI-3)

kinase is required for insulin-like growth factor-I-dependent PI-3 kinase activation in smooth muscle cells. *Endocrinology* **147**, 1458-65

143. Ross, S. & Wu, B. Phosphorylation of C/EBPα Inhibits Granulopoiesis | Molecular and Cellular Biology. Available at: https://mcb.asm.org/content/24/2/675.

144. Prakasam G, et al. (2017) Pyruvate kinase M knockdown-induced signaling via AMP-activated protein kinase promotes mitochondrial biogenesis, autophagy, and cancer cell survival. *J Biol Chem* **292**, 15561-15576

145. Lekmine F, et al. (2004) Interferon-gamma engages the p70 S6 kinase to regulate phosphorylation of the 40S S6 ribosomal protein. *Exp Cell Res* **295**, 173-82

146. Rose AJ, et al. (2009) Skeletal muscle eEF2 and 4EBP1 phosphorylation during endurance exercise is dependent on intensity and muscle fiber type. *Am J Physiol Regul Integr Comp Physiol* **296**, R326-33

147. Adams M, et al. (1997) Transcriptional activation by peroxisome proliferator-activated receptor gamma is inhibited by phosphorylation at a consensus mitogen-activated protein kinase site. *J Biol Chem* **272**, 5128-32

148. Wang, Y. PPARs: Diverse Regulators in Energy Metabolism and Metabolic Diseases. Available at: https://www.ncbi.nlm.nih.gov/pmc/articles/PMC4084607/.

149. Berg, J. & Tymoczko, J. L. Gluconeogenesis and Glycolysis Are Reciprocally Regulated - Biochemistry - NCBI Bookshelf. Available at: https://www.ncbi.nlm.nih.gov/books/NBK22423/.

150. Humbert N, et al. (2010) Regulation of ploidy and senescence by the AMPK-related kinase NUAK1. *EMBO J* **29**, 376-86

151. Suzuki A, et al. (2004) ARK5 is a tumor invasion-associated factor downstream of Akt signaling. *Mol Cell Biol* **24**, 3526-35

152. Blesbois, E. & Nyugen, T. mong. Ca2+/Calmodulin-Dependent Protein Kinase Kinases (CaMKKs) Effects on AMP-Activated Protein Kinase (AMPK) Regulation of Chicken Sperm Functions. Available at: https://journals.plos.org/plosone/article?id=10.1371/journal.pone.0147559.

153. Browne GJ, Proud CG (2004) A novel mTOR-regulated phosphorylation site in elongation factor 2 kinase modulates the activity of the kinase and its binding to calmodulin. *Mol Cell Biol* **24**, 2986-97

154. Zonta F, et al. (2015) Lyn sustains oncogenic signaling in chronic lymphocytic leukemia by strengthening SET-mediated inhibition of PP2A. *Blood* **125**, 3747-55

155. Holz MK, Blenis J (2005) Identification of S6 kinase 1 as a novel mammalian target of rapamycin (mTOR)-phosphorylating kinase. *J Biol Chem***280**, 26089-93

156. Heathcote HR, et al. (2016) Protein kinase C phosphorylates AMP-activated protein kinase α1 Ser487. *Biochem J* **473**, 4681-4697

157. Takeda K, et al. (2007) Apoptosis signal-regulating kinase (ASK) 2 functions as a mitogen-activated protein kinase kinase kinase in a heteromeric complex with ASK1. *J Biol Chem* **282**, 7522-31

158. Brint EK, et al. (2002) Characterization of signaling pathways activated by the interleukin 1 (IL-1) receptor homologue T1/ST2. A role for Jun N-terminal kinase in IL-4 induction. *J Biol Chem* **277**, 49205-11

159. Dolniak B, et al. (2008) Regulation of arsenic trioxide-induced cellular responses by Mnk1 and Mnk2. *J Biol Chem* **283**, 12034-42

160. Inoki, K., LI, Y. & Zhu, T. TSC2 is phosphorylated and inhibited by Akt and suppresses mTOR signalling. - PubMed - NCBI. Available at: https://www.ncbi.nlm.nih.gov/pubmed/12172553.

161. Roux PP, et al. (2004) Tumor-promoting phorbol esters and activated Ras inactivate the tuberous sclerosis tumor suppressor complex via p90 ribosomal S6 kinase. *Proc Natl Acad Sci U S A* **101**, 13489-94

162. Nasrin N, et al. (2009) JNK1 phosphorylates SIRT1 and promotes its enzymatic activity. *PLoS One* **4**, e8414

163. Tagore, V. S. G. and S. Kinomics. *Current Drug Metabolism* (2008). Available at: http://www.eurekaselect.com/66576/article.

164. Timofeev O, et al. (2010) Cdc25 phosphatases are required for timely assembly of CDK1-cyclin B at the G2/M transition. *J Biol Chem* 285, 16978-90

165. Lai, S. & Pelech, S. Regulatory roles of conserved phosphorylation sites in the activation T-loop of the MAP kinase ERK1. *Mol Biol Cell* **27**, 1040–1050 (2016).

166. Feng, J. *et al.* Inhibitory phosphorylation site for Rho-associated kinase on smooth muscle myosin phosphatase. *J. Biol. Chem.* **274**, 37385–37390 (1999).

Appendix

CHANGES IN IMMUNOMETABOLIC PEPTIDES AT THE DIFFERENT SITES ESSENTIAL TO THIS STUDY

PROTEIN/ PEPTIDE	Human Uniprot number	Human site	Phosphorylated	Dephosphorylated	Site function	Chicken site	Chicken Uniprot number
4EBP1	Q13541	T37	SE30	SE2, SH6	inhibitory site	T38	E1C115
4EBP1	Q13541	T46		SH30, SE2, SH2	inhibitory site	T47	E1C115
4EBP1	Q13541	S65		SH30, SE2, SH2	inhibitory site	S66	E1C115
ACC1	Q13085	S1263	SE30,SH30, SH6		??	S1263	F1NWT0
ACC1	Q13085	S80	SE6,SH6, SE30	SE2, SH2	??	S80	F1NWT0
ACC1	Q13085	Y1370	SH30, SE2	SE6		Y1347	P11029
ACC2	O00763	Y1560	SE30,SH30,SE2, SH2, SE6			Y1388	F1P1B5
ACC2	O00763	Y1489	SE6	SE2		Y1317	F1P1B5
AKT	P31749	T308		SH30,SE30, SE6	active site	T74	F1NQI8
AKT	P31749	T479	SH30, SE30, SH6	SH2		T245	F1NQI8
AKT	Q9Y243	S476	SE6,SH6	SE2		S476	F1NRC8
AKT	Q9Y243	T305	SE6,SH6, SE30			T305	F1NRC8
AMPK	O43741	S108		SE6,SH6, SH30, SH2,		S110	F1NV45
AMPK	O43741	S184	SH2, SE6			S186	F1NV45
AMPK	P54646	S377	SE30, SH2			S389	F1NLY6
AMPK	Q13131	T183	SE30, SH30,		active site	T185	F1NLY6
AMPK	Q13131	S172	SE6	SE30, SH2		S174	F1NLY6
AMPK	Q13131	S496	SH30, SH2,	SH6	inhibitory site	S496	E1C811
AMPK	Q9UGJ0	T165		SE30,SH30, SH6		T160	F1NXL4
AMPK	Q9y478	S182	SH2, SH30, SE30, SH6, SE6,	SE2,		S111	Q27IP4
AMPK	Q9y478	S108		SE2, SE6,	active site	S185	Q27IP4
AMPK-related protein kinase 5	O60285	T211	SE2	SE30,SH30, SE6,SH6	active site	T204	F1P356
AMPK-related protein kinase 5	O60285	S600	SE6,SH6		active site	S593	F1P356
CAMKK-B	Q96RR4	S511	SE30,SH30,SH2, SE6		phospho-site	S483	F1P326
Caspase-3	P42574	S150		SE30, SH30, SE6,SH6	inhibitory site	S158	O93417
CBL	P22681	Y774	SH2,SE6		phospho-site	Y636	F1NXW5
CBL	P22681	Y700		SE2	phospho-site	Y725	F1NXW5
CPT1	P50416	Y165	SH6,			Y166	E1BVX6

CREB	P15336	S69		SE2	active site	S72	G1K321
CREB	P16220	S133	SE30,SH30	SE2, SE6,	active site	S119	E1BSK3
CRK2	P46108	Y251	SE2,SH2		active site	Y252	Q04929
CRK2	P46108	Y221		SE6,SH6, SH2	??	Y222	Q04929
CRK2	P46108	Y239	SH30,SE2	SE6		Y240	Q04929
CRK2	P46109	Y207		SE30,SE6	inhibitory site	Y184	F1P241
CRK2	P46109	Y251		SE2	??	Y228	F1P241
CRK2	Q9NYV4	Y892		SE2,SH2, SH30,		Y602	F1NBD9
CYCLIN D1	P06493	T14		SE6,	Inhibitory site	T14	F1NBD7
CYCLIN D1	P24385	T286	SE30, SH30, SE6,SH2		??	T283	F1NS84
EEF2K	O00418	s78	SE30,SH30, SE6, SH6		??????	S78	E1C172
EEF2K	O00418	S398	SE6,SH6			S398	E1C172
EEF2K	O00418	S366	SE6,SH6, SE30			S366	E1C172
ERK	P28482	T185		SE2,SH2,SE6,SH6, SH30	active site	T146	F1P066
ERK	P31152	S186		SE2,SH2,SE6,SH6	??	S189	E1BRA1
ERK	Q16659	T698	SE6,SH6		??	T698	Q5F3W3
GRB	P62993	Y209		SE2,SE6	??	Y209	A3R0S3
GRB	Q13322	S476		SE2	inhibitory site	S476	F1NQ03
GSK	P49840	T338	SE6,SH6			T245	F1NPL8
GSK	P49840	S278		SE6		S185	F1NPL8
GSK	P49841	Y216	SH30,SE2	SE30,SE6	active site	Y186	F1NPL8
GSK	P49841	S219		SE6,SH6, SH30		S189	F1NPL8
GSK	P49841	S389	SE6,SH6, SH2			S359	F1NPL8
HK	P19367	S298		SE30,SH30,SE2,SH2		S299	F1NEF0
HK	P19367	S827	SH30	SE6,SH6, SH2		S828	F1NEF0
HK	P19367	T821	SE6,SH6,SH2			T822	F1NEF0
HK	P52789	Y301	SH2, SH30,SE30, SE6,SH6	SE2		Y304	H9L325
HK	P52789	T762		SE2,SH2		T763	F1NEF0
HK	P52789	Y461	SH30	SE6,SH6		Y462	F1NEF0
HK	Q2TB90	S772		SE6,SH6,SE30		S773	E1BRU7
HUR	Q15717	S221	SH2, SE6	SE2	??	S221	F1N9I5
HUR	Q15717	S158		SE2,SH2	??	S158	F1N9I5
Inhibitor of NFkB inhibitor	O15111	S180	SH30	SH2	active site	S194	F1NLD4

Inhibitor of NFkB inhibitor	O15111	T23	SE30	SE2	active site	T37	F1NLD4
iNOS	P35228	Y151		SH30, SH2, SE2, SE6, SH6	inhibitory site	Y148	F1N867
IRS	P35568	Y896	SH30, SE30, SH6,SE6,	SE2	??	Y409	F1P2R4
IRS	P35568	S616		SE30	inhibitory site	T175	F1P2R4
IRS	Q9UQB8	T340		SE2	??	T340	F1NIJ2
JNK	P45983	T183	SE30, SH2		active site	T183	E1C8C6
LAMP3	Q9UQV4	T268		SE2,SH2		T76	E1BU34
LKB1	Q15831	T185	SH30, SH6	SE30, SE6	active site	T187	F1NG57
LKB1	Q15831	T363		SE30, SH30, SE2, SH6	active site	T367	F1NG57
MEK	P36507	S222		SE6,SH6,SH30	active site	S220	F1NYZ2
MEK	P36507	S306	SH30,SH2,SE6			S304	F1NYZ2
MEK	P45985	T261		SE6,SH6	active site	T228	F1P3T1
MEK	P45985	S80		SE6,SH6,SH2	inhibitory site	S47	F1P3T1
MEK	P46734	S218		SE2,SH2	active site	S217	F1NMX4
MEK	P53349	T1381	SE2,SH2			T1236	F1N938
MEK	Q02750	S298	SE2,SH2, SE6,SH6		??	S300	Q5ZIF0
MEK	Q02750	S222		SE2,SH2, SH30, SE6	active site	S224	F1NYZ2
MEK	Q13163	T315		SE2, SH2, SE6,SH6	active site	T238	F1NU31
MEK	Q13163	S137		SH30		S60	F1NU31
MEK	Q13163	S311		SE6	active site	S234	F1NU31
MEK	Q13233	S292		SE6,SH6		S133	F1N938
MEK	Q99683	T838		SH2,SH30	active site	T693	F1NYS9
MEK	Q99759	S526	SE2,SH2	SE6	active site	S526	F1NLB9
MEK	Q99759	T294	SH30		??	T294	F1NLB9
MNK	Q9BUB5	T385	SE6,SH6, SE30,SH2			T344	F1N9J6
MNK	Q9BUB5	T255		SH30,SH2	active site	T199	F1NXQ3
MTOR	P42345	S2448	SE2,SH2, SE6,SH6		active site	S2387	F1NUX4
MTOR	P42345	S2441	SE6, SH6	SE2,SH2		T2350	F1NUX4
MTOR	P42345	S2446	SE6,SH6	SH2		S2352	F1NUX4
MTOR	Q8N122	T706	SE6	SE2,SH2		S864	E1C1B6
MTOR	Q8N122	S863	SE6,SH6, SE30	SE2,SH2	active site	T707	E1C1B6
MTOR	Q8N122	S877		SH30		S878	E1C1B6
NADPH ox activator 2	P19878	T233	SE30	SE2, SH2		T222	F1NIH3
NAPDH ox activator	P14598	S370	SE6	SH30, SE2, SH2	active site	S371	E1BSX6

NFkB inhibitor	P25963	Y42	SH30	SE2	active site	Y46	F1N8J4
NFkB-p100	Q00653	S866	SE30	SE2	??	S871	P98150
NFkB-p105	P19838	S932	SH30	SE2	??	S946	F1NBF4
NFkB-p105	P19838	S337	SE30, SH30	SE2, SH2, SH6	??	S345	F1NBF4
PDK	O15530	S241	SE6,SH6, SE30	SE2,SH2	active site	S245	E1BSA6
PDK	O15530	Y376	SE6,SH6, SE30, SH2		active site	Y380	E1BSA6
PFK-1	P17858	Y674	SE2,SH2			Y664	F1NW16
PFK-1	P17858	S775		SE2, SE6,		S765	F1NW16
PFK-1	P70266	S33		SE6		S31	Q91348
PFK-1	Q01813	S386	SE2,SH2,	SE30, SH30, SE6,SH6		S386	F1NHI9
PFK-1	Q01813	Y651	SE2,SH2,			Y651	F1NHI9
PFK-1	Q01813	T211	SE30	SE2,SH2, SE6,SH6		T192	F1NW16
PFK-2	O60825	Y366	SE2,SH2, SE6,SH6, SE30			Y364	E1BXR3
PFK-2	Q16875	S461	SE2,SH2, SE30,			S462	E1BUK2
PGC-1	Q9UBK2	T299	SE30,SH30,SE6, SH6, SH2		??	T297	F1NHI0
PGC-1	Q9UBK2	T266	SE6,SH6,SH30		??	S264	F1NHI0
PGC-1	Q9UBK2	T263	SE6	SH30,SE2	??	T261	F1NHI0
PHK	P46020	Y549	SH30,SE6	SE30		Y549	E1BQZ7
PHK	Q16816	Y338		SE2,SH2, SE6, SH6		Y337	F1P5T2
PHK	Q93100	S701	SH2, SE30,	SE2		S694	Q5ZME3
PI3K	O00329	S1039		SE2,SH2, SE6,SH6, SH30	inhibitory site	S1041	F1NHX1
PI3K	O00459	Y605	SE30,SH30,SH2			Y609	E1C2C5
PI3K	O00459	S365		SE30, SE6		Y369	E1C2C5
PI3K	P27986	Y556	SE6,SH6	SE2,SH2, SE30	active site	Y556	E1C8M4
PI3K	P27986	Y608	SE6		active site	S608	E1C8M4
PI3K	P42338	Y425	SE30, SH30, SE6,SH6, SH2			Y420	Q5F4A2
PI3K	P42338	Y962		SE2, SH2, SE30, SE6		Y958	Q5F4A2
PI3K	P42338	S1070	SE2	SE6, SH6, SH30		S1066	Q5F4A2
PI3K	P48736	T1024		SE30, SH30, SE6, SH6, SE2		T1027	E1C093
PI3K	P48736	T607		SE30, SH30, SE2, SH2, SE6, SH6		T610	E1C093
PI3K	P48736	S582	SE2	SE6, SH6		S585	E1C093
PKA	P17612	T198	SH30, SE2	SE30,SE6, SH6	active site	T245	E1BRS0
PKA	P17612	S140	SE2,SH2,SH30	SE6,SH6		S187	E1BRS0
PP2A	P67775	Y307	SE2,SH2,	SE6,SH6	inhibitory site	Y307	Q5ZM47
PP2A	Q14738	S60	SE30, SE2,	SH30, SH6	??	S17	F1P090

PP2A	Q14738	S75		SE30, SH30, SE6, SH6	??	S32	F1P090
PP2A	Q14738	S573	SH6,		??	S551	E1BRG5
PPAR-GAMA	P37231	S112	SE2,SH2		??	S82	Q9I878
PTP1B	P18031	Y152		SH2,SE6	??	Y79	E1BWI7
PYG	P06737	S15	SH2	SE2,SE6,SH6		S15	F1NAD9
PYG	P06737	Y733		SE30,SH30,SE6,SH6, SH2		Y732	F1NAD9
PYG	P06737	Y75	SE2,SH2	SE30, SE6		Y75	E1BSN7
PYG	P11217	Y186	SH2			Y187	E1BSN7
Pyk2	Q13489	T254	SE2,SH2,SE6,SH6			T115	F1NPV2
Pyk2	Q14289	Y402	SE6,SH6			Y405	E1BTC3
Pyk2	Q14289	Y580		SE6,SH6		Y584	E1BTC3
Pyk2	Q14289	Y881	SH30			Y846	E1BTC3
RAB	P20338	S199	SE30, SH2			S199	E1C8H0
RAB	P61106	Y14		SE30, SE2, SE6		Y14	Q5ZKU5
RAB	P62491	T136	SE30, SH2			T136	Q5F3R8
RAF	P04049	S259	SE30,SH30, SE6		inhibitory site	S259	P05625
RAF	P04049	S43		SH30,SE2,SE6	inhibitory site	S43	P05625
RAF	P04049	S338	SH30,SE2		active site	S338	P05625
RAF	P15056	S729		SE2,SH2, SE6	active site	S723	F1P1L9
RAF	P15056	S365		SE2,SH2, SH6	inhibitory site	S328	F1NJV6
RAF	P15056	S446		SE6,SH6	active site	S449	F1NJV6
RAS	P01112	T35	SH2		??	T35	E1BTS2
RAS	P51149	Y183	SH2		??	Y183	E1C0F3
RSK	O75582	S360		SE30,SH30, SE6	active site	S350	Q5F3L1
RSK	O75582	S376		SH6,SE6	active site	S366	Q5F3L1
RSK	O75582	T581		SE6,SH6, SE30	??	T571	Q5F3L1
RSK	P51812	Y707	SE6,SH6			Y664	F1NLJ3
RSK	P51812	S369	SE6,SH6	SE30	active site	S326	F1NLJ3
RSK	Q15418	S380	SE6	SE30,SH30		S398	E1C554
RSK	Q15418	S221	SE6,SH6			S239	E1C554
RSK	Q15418	S363	SE6		active site	S381	E1C554
S6K	P23443	S447	SE6,	SH6, SE30, SE2	active site	S424	F1P4J0
S6K	P23443	T444	SE2	SE30, SH30, SE6	active site	T421	F1P4J0
S6K	P23443	T412	SH2	SE6, SH6	active site	T389	F1P4J0
SHC	P29353	Y427	SH6		??	Y262	E1BSC1
SHC	Q92529	Y342	SH2	SE30		Y343	E1C4D4

SIRT1	Q96EB6	T530		SE30,SH30,SE6,SH6	active site	T388	F1N886
SIRT1	Q96EB6	S661	SE6,SH6, SE30,			S519	F1N886
SIRT1	Q96EB6	S27	SH2, SE6		active site	S53	Q5F3H4
SOCS	O14543	Y221		SE6,SH6,SE30,SH2	??	Y205	F1NBA9
SOCS	O14543	Y204	SE6		??	Y188	F1NBA9
SOS	Q07889	S1193	SE2,SH2, SE6,SH6		??	S1178	F1NMA4
SOS	Q07889	S1167	SE30,SH2		??	S1152	F1NMA4
SREBP1	P36956	S338	SE30,SH30, SH6,SE6	SE2,SH2	??	S114	F1NFU5
TAK-1	Q8N5C8	S60		SE30, SH30,SE2		S60	E1BU29
TAK-1	Q8N5C8	T404		SE30,SH30,SE2	??	T403	E1BU29
TGF-B	P36897	T200		SH30	active site	T200	Q06900
TNFRSF19	Q9NS68	Y122		SH2		Y121	F1P173
TRAF2	Q12933	S11	SE6		??	S11	E1BTY1
TRAF2 and NCK	Q9UKE5	S764	SE6,SH6		??	V730	F1P3F8
TRAF2 and NCK	Q9UKE5	S678	SH30			S644	F1P3F8
TRAF6	Q9Y4K3	Y353	SE2,SH2			Y379	E1C626
TRAF7	Q6Q0C0	S88	SE6,SH6	SE2,SH2		S88	F1NEH1
TSC2	P49815	S1418	SE30,SE6			S1374	F1P0G2
TSC2	P49815	S939	SH30, SH6		inhibitory site	S941	F1P0G2
TSC2	P49815	T1462	SE6		inhibitory site	T1423	F1P0G2

Sites whose only known functions are molecular regulation or phosphorylation are illustrated as ??